HOX11 FUNCTION IN REGION-SPECIFIC ADULT MESENCHYMAL STEM/STROMAL CELLS IS REQUIRED FOR FRACTURE REPAIR

By

Danielle Renae Rux

A dissertation submitted in partial fulfillment
of the requirements for the degree of
Doctor of Philosophy
(Cell and Developmental Biology)
in the University of Michigan
2016

Doctoral Committee:

Assistant Professor Benjamin L. Allen, Chair
Professor Renny T. Franceschi
Professor Karl J. Jepsen
Assistant Professor Daniel Lucas-Alcaraz
Professor Laurie K. McCauley
Professor Deneen M. Wellik

© Danielle Renae Rux

- - - - - - - - - - - - - - - - - - -

All rights reserved.
2016

To my mom and dad, whom have lovingly supported every decision I have made. To my sister, my life-long best friend. To my Aunt Janet, whose own passion for education and medicine influenced my career in science.

ACKNOWLEDGEMENTS

First, and foremost, I thank Deneen Wellik. The last five years have been a roller coaster of struggles and triumphs. Your enthusiasm for science is contagious and kept me motivated on the bad days. On the good days you celebrated along with me. I have grown as a scientist due directly to your guidance and support.

To the many members of the Wellik lab, thank you for the support. To Steve, for a daily dose of sarcastic humor. To Brian, for your thoughts on data and mellow attitude. To Jane, for your incredible hard work and contributions to my project. To Leilani, for keeping me grounded through my last months. To Ilea, for initial support in the adult *Hox11* project. And, finally, to Kyriel, for lending your thoughts and brainstorming new ideas with me. I am so thankful to have had the chance to work with you most directly these past few years. I wish you all of the best in your endeavors.

To the wonderful undergraduate and high school scientists I have had the pleasure to work directly with: Kayla, Kelsey and Aleesa; you all played critical roles in my research, and taught me how to be a good mentor.

To Sherry Taylor, thank you for your unending support throughout my Ph.D. training. Your willingness to solve any problem that I encountered was so valuable.

To the members of my thesis committee, you pushed me to be the best through my Ph.D training. Thank you for the constructive criticism and support along the way. I

am grateful to have had a group of committee members that took great interest, not only in my science, but also in my well being throughout my training.

To Daniel, thank you for the extensive amount of time that you have taken to help train me and to push my project forward. I am so grateful for everything that you have contributed to the project and to my scientific training.

To Steve Goldstein and Ken Kozloff, thank you for the invaluable support with our fracture models. The project demanded several new models of which needed a vast amount of testing. Thank you for taking the time!

To all of the researchers and staff in the orthopedic research labs at Michigan, thank you for the research support. To Kathy Sweet and Bonnie Nolan for superb technical assistance during fracture surgeries and post-operative care, John Baker for assistance with plastic processing and histologic staining, and Basma Khoury and Joseph Peroski for assistance with scanning of microCT specimens.

To the attendees of the developmental genetics meetings, thank you for asking difficult questions and forcing me to think more deeply about my data and my project. These were the most difficult presentations I gave during my Ph.D training, but they were also the ones that I learned the most from.

To Yuji Mishina, thank you for the advice and support. I always enjoyed discussing data and new questions with you.

To Scott Barolo and Kristen Verhey, for being fantastic mentors and taking the time to check-in.

To the CDB staff, your patience and willingness to help with anything is truly appreciated. Thank you for making sure that I was always paid, and that problems with registration were always solved!

To the Michigan research core facilities: the mouse facilities, the microscopy and image analysis core as well as the flow cytometry core. Without the equipment and staff that maintain these facilities, none of this research would have been possible. I used the cores to collect data for my research, but the support and care provided from the staff was absolutely wonderful.

To my funding sources, thank you for the support of my project research and of my professional growth. Thank you to the National Institues of Health RO1 AR 061402 awarded to Deneen Wellik. Thank you to the TEAM (Tissue Engineering At Michigan) training grant (T32 DE007057) and the training I received focused on tissue engineering. Thank you to ASBMR (American Society for Bone and Mineral Research) for awarding me with the opportunity to attend an ECTS (European Calcified Tissue Society) Ph.D. training course. This was a critical part of my training and expanded my professional network. Thank you, to the department of Cell and Developmental Biology at Michigan for support by the Bradley M. Patten fellowship.

To Michelina, Robert and Ismail, thank you for the continued friendship since our time at Minnesota. You have each played critical roles in developing my professional career, but I cherish the life-long friendships we have built even more.

To Jen and Briana, you truly are like sisters to me. We have shed so many tears of laughter and joy together. I can't imagine getting through graduate school with you!

To my many friends in Minnesota and Wisconsin, thank you for maintaining my sanity. I can't imagine my life without all of you in it.

To Carolyn and Phil, thank you for taking me in as a part of your family.

To Tony and Cheryl, thank you for supporting me as my own parents do.

To Ben, my graduate school years were some of the best of my life because of you. Thank you for making me laugh and for making me take the vacations that I would never have made time for on my own.

To my sister, thank you for the large doses of laughter and fun whether we were together or apart. You have grown into such a beautiful woman these past 5 years and I am so happy to call you my very best friend.

To my parents, words cannot express the kind of gratitude that I owe to you. My successes are the direct result of your unending support and the example that you have set for me.

TABLE OF CONTENTS

DEDICATION……ii

ACKNOWLEDGEMENTS……..……..iii

LIST OF FIGURES……..……..ix

ABSTRACT……..…… xi

CHAPTER 1: INTRODUCTION ……1

Hox Genes ……..……1

Hox genes and limb development ……...…….6

Hox genes beyond embryonic patterning: dissecting current literature……12

Adult Mesenchymal Stem/Stromal Cells (MSCs) ……..……..…15

Adult fracture repair……23

CHAPTER 2: REGIONALLY RESTRICTED HOX11 FUNCTION IN ADULT BONE MARROW MULTI-POTENT MESENCHYMAL STEM/STROMAL CELLS……...….27

Summary……27

Introduction ……..……28

Results ……..……30

Discussion ……48

Supplemental Figures……...……..…… 51

Materials and Methods ..……57

CHAPTER 3: *HOX11* GENES ARE REQUIRED FOR REGION-SPECIFIC FRACTURE REPAIR.……68

Summary……68

Introduction ……..……69

Results ……..…..……71

Discussion ……..85

Supplemental Figures ……...……..……88

Materials and Methods ……90

CHAPTER 4: CONCLUSION..……94

Summary of findings ……..94

Contributions to the field ……..……..……...96

Future Directions ……..…..…98

APPENDIX: PUBLICATIONS AND MANUSCRIPTS.……...……..….104

REFERENCES…….……...……105

LIST OF FIGURES

Figure 1.1. *Hox* mutations in *Drosophila Melanogaster* result in homeotic Transformations……..2

Figure 1.2. The mammalian *Hox* complex and axial skeleton transformations……4

Figure 1.3. Loss of Hox function results in region-specific limb malformations……..8

Figure 1.4. Expression of *Hoxa11eGFP* through embryonic limb development ……11

Figure 1.5. The stages of fracture healing…..……24

Figure 2.1. *Hoxa11eGFP* surrounds the zeugopod skeletal elements of the developing limbs……..……31

Figure 2.2. *Hoxa11eGFP* is maintained regionally through postnatal and adult stages ……..……....32

Figure 2.3. *Hoxa11eGFP* is not expressed in differentiated cell types……..…34

Figure 2.4. *Hoxa11eGFP*-expressing cells are a subset of bone marrow mesenchymal stem/stromal cells (BM-MSCs) ……36

Figure 2.5. *Hoxa11eGFP*-expressing cells expand following injury and do not overlap with differentiated cell types…….39

Figure 2.6. *Hoxa11eGFP*-expressing cells in the fracture callus are progenitors that give rise to differentiated cell types…….....41

Figure 2.7. Loss of Hox11 function impairs fracture healing *in vivo* and results in *in vitro* differentiation defects……...43

Figure 2.8. *Hox* expression and function is regionally restricted……..…47

Figure S2.1. *Hoxa11eGFP* is regionally expressed through postnatal and adult stages in hindlimbs and forelimbs ……..51

Figure S2.2. *Hoxa11eGFP*-expressing cells from tibia bone marrow and from periosteum are identified as mesenchymal stem/stromal cells……52

Figure S2.3. FACS analysis controls for *Hoxa11eGFP* expression……..53

Figure S2.4. *Hoxa11eGFP*-expressing cells throughout fracture healing maintain the FACS profile from uninjured bone……54

Figure S2.5. *Hoxa11eGFP*-expressing cells in *Hox11* compound mutant animals are non-hematopoietic and non-endothelial……55

Figure S2.6. *Hoxa11eGFP* expression maintains regional specificity in response to repair ……...56

Figure 3.1. *Hoxa11eGFP* is expressed throughout fracture injury repair of the limb zeugopod ……...73

Figure 3.2. Loss of Hox11 function results in defects following fracture injury……..75

Figure 3.3. *Hox11* compound mutant fractures display altered callus composition..78

Figure 3.4. Chondrocyte differentiation and endochondral ossification is disrupted in the compound mutant callus ……80

Figure 3.5. Osteoclasts are present and express markers of resorption in the compound mutant callus……83

Figure 3.6. Bone matrix organization is disrupted due to the loss of Hox11 Function ……..…84

Figure S3.1. *Hoxa11eGFP* is expressed in the ulna fracture model of repair…….....88

Figure S3.2. Sox5 expression is not affected by the loss of Hox11 function……89

Figure 4.1. *Hoxa11eGFP* is expressed in adult skeletal muscle and expands during regeneration following injury……103

ABSTRACT

The mammalian skeleton boasts a remarkable capacity to completely restore the original structure and function of a bone following injury. Interestingly, the biological processes of fracture repair recapitulate many of the mechanisms of embryonic skeletal development. The *Hox* genes are critical regulators of skeletal development, yet the function of these genes during adult fracture repair is largely unknown. Ongoing research in the Wellik lab is focused on understanding the role(s) of these genes in this context.

The *Hox* genes encode evolutionarily conserved transcription factors that are imperative for patterning of the axial and limb skeleton in the developing embryo. Specifically, *Hox11* genes function to instruct growth and morphology of the lumbar elements of the axial skeleton and the zeugopod elements (radius/ulna and tibia/fibula) of the limbs. Previous work using a *Hoxa11eGFP* allele showed that *Hox11* is expressed through the latest stages of embryonic development. We have now discovered that *Hox11* genes continue to be expressed in the adult skeleton and are largely restricted to the previously characterized PDGFRα^+/CD51$^+$/Leptin Receptor(LepR)$^+$ mesenchymal stem/stromal cell (MSC) population in bone marrow. These *Hox11*-expressing MSCs expand in response to fracture injury and are maintained throughout repair. Loss of *Hox11* function results in a significantly reduced ability to generate cartilage early in repair, and at late stages, the hard callus persists

and is incompletely remodeled. Together, our data suggests that *Hox11* functions in MSCs at multiple stages of repair, first, for endochondral ossification and later for bone remodeling. In addition, we show more generally that the *Hox* expression pattern established during embryonic development is maintained in the adult skeleton. Overall, this research provides novel evidence that *Hox* genes have critical roles beyond embryonic patterning and that these genes are expressed and function in adult MSCs.

CHAPTER 1

INTRODUCTION

Hox Genes

The *Hox* genes are a group of homeodomain-containing transcription factors that are essential for patterning the anterior to posterior axis of the developing embryo. First described in *Drosophila,* mutations in *Hox* genes drive unique homeotic (segment identity transformation) phenotypes. This was first described by William Bateson and Calvin Bridges in the late 19th and early 20th centuries through observations of spontaneous mutations in *Drosophila Melanogaster*, and later by Edward B. Lewis in seminal work on the Bithorax complex (Bateson, 1909; Lewis, 1978; Maeda and Karch, 2009). Interested in understanding basic gene evolution, Lewis studied the *Bithorax* complex of *Hox* genes in *Drosophila* to understand "pseudoallelic genes": genes that are similar to and likely evolve from one another with mutations that equate to new evolutionary functions (Lewis, 1951, 1978). Through a series of studies, Lewis discovered that the *Bithorax* complex is a cluster of genes that each maintain a specific function in patterning adjacent, yet phenotypically different, body segments of the posterior embryo (Figure 1.1A) (Lewis, 1978). Loss-of-function mutations result in anterior homeotic transformations in which entire body segments acquire the identity of the segment that is next most anterior to it (Figure 1.1B) (Lewis, 1978). It was later discovered that gain-of-function mutations in segments more anterior to normal

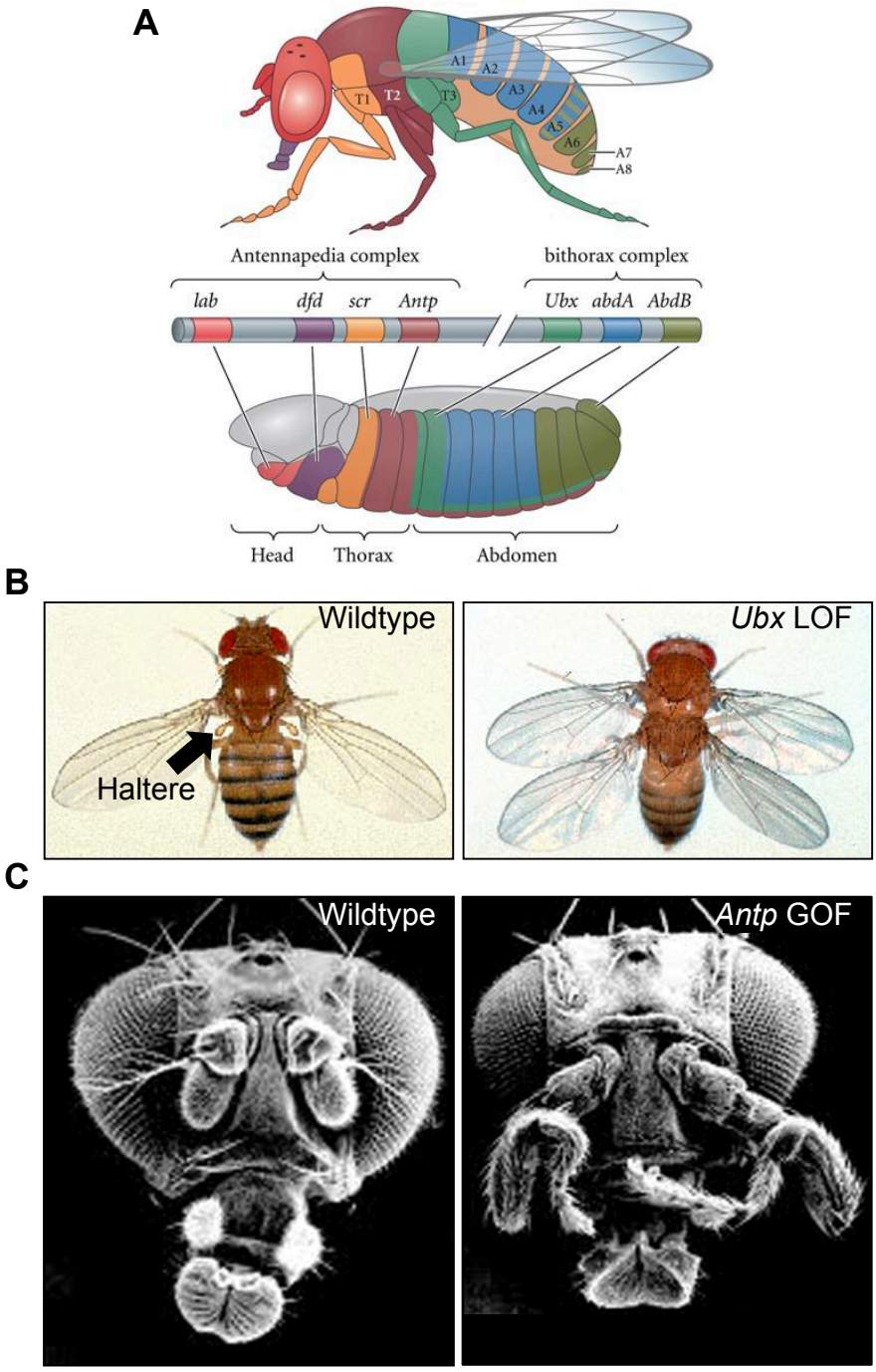

Figure 1.1. *Hox* mutations in *Drosophila Melanogaster* result in homeotic transformations.
(A) Schematic of the *Drosophila Melanogaster Hox* complex of 8 genes (B) Loss of function (LOF) mutations of the *ultrabithorax* (*ubx*) *Hox* gene results in duplication of the closest anterior body segment. (C) Gain of function (GOF) insertion of the *antennapedia* (*antp*) *Hox* gene in a more anterior anatomical location results in the patterning of legs in place of antennae. (Figure adapted from (Lewis, 1978; Schneuwly et al., 1987)).

expression and function, result in homeotic transformations that resemble the posterior segment (Figure 1.1C) (Kaufman et al., 1990; Schneuwly et al., 1987). Taken together, these findings demonstrate that *Hox* genes are, by themselves, capable of driving the pattern of specific body segments in the embryo.

The *Hox* genes are deeply evolutionarily conserved and common to all bilaterian animals (Garcia-Fernandez, 2005). In *Drosophila,* a single eight-gene *Hox* complex is responsible for embryonic patterning. During vertebrate evolution, *cis* and *trans* amplifications and duplications gave rise to the 39-gene, 4-cluster complex found in all mammals (Figure 1.2A) (Garcia-Fernandez, 2005; Krumlauf, 1994; Scott, 1992). The cluster is further subdivided into 13 paralogous groups based on sequence similarity and position within the cluster. A conserved characteristic of the *Hox* genes through evolution is the spatio-temporal genetic organization of the genes, referred to as collinearity. The organization of the genes on each of the four chromosomes (1 cluster per chromosome) from 3' to 5' mirrors their expression patterns and functions in the embryo. In general, 3' genes are expressed earlier in development in the most anterior regions of the embryo while 5' genes are expressed later and in more posterior regions. As the embryo develops, each of the 13 paralogous groups of mammalian genes establishes an anterior limit of expression that will later define positional identity of segments (Dressler and Gruss, 1989; Duboule and Dolle, 1989; Gaunt, 1991; Gaunt and Strachan, 1996; Graham et al., 1989; Izpisua-Belmonte et al., 1991). For example, the anterior limit of expression for *Hox11* genes are the sacral elements of the axial skeleton. *Hox11* expression is restricted to these posterior axial segments and overlaps with the more anterior expression of *Hox9* and *Hox10*, but does not extend beyond the

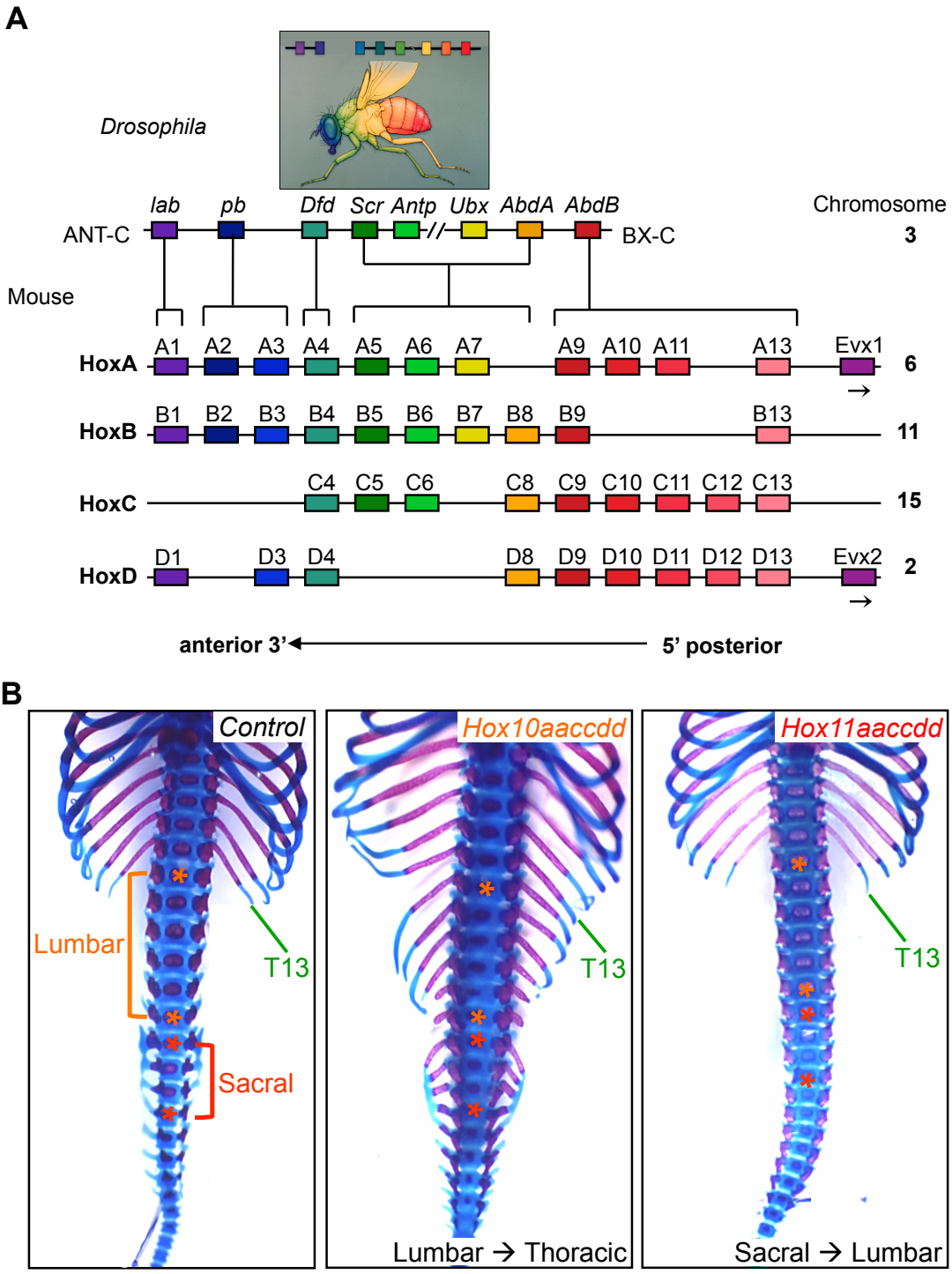

Figure 1.2. The mammalian *Hox* complex and axial skeleton transformations. (A) Schematic of the evolutionary expansion of the *Hox* complex from 1 cluster in *Drosophila* to 4 clusters in mammals. Color-coding signifies the different paralogous groups and their function in anterior to posterior patterning. (B) Loss of function of entire paralogous groups in mammals results in anterior homeotic transformations similar to *Drosophila* (Figure adapted from (Wellik and Capecchi, 2003)).

limit of what will become the sacral elements. This nested and sequential expression is critical for proper patterning of the axial skeleton and also contributes to the overall timing of embryonic development (Duboule, 1994; Iimura and Pourquie, 2006; Payumo et al., 2016; Zakany et al., 1997).

Each of the 13 paralogous groups of mammalian *Hox* genes corresponds to region-specific expression patterns and functions in the embryo. Members of each group are display a high degree of functional redundancy with one another. While minor defects are sometimes observed in single mutants, the most dramatic phenotypes are only observed with loss of an entire paralogous group of genes. Similar to what is observed in *Drosophila*, genetic mutations in mouse models also show anterior homeotic transformations of the axial skeleton (Condie and Capecchi, 1994; Fromental-Ramain et al., 1996a; Horan et al., 1995; Kostic and Capecchi, 1994; Mallo et al., 2010; McIntyre et al., 2007; van den Akker et al., 2001; Wellik, 2009; Wellik and Capecchi, 2003). For example, loss of function of all three of the *Hox10* paralogous genes results in a transformation of the lumbar region to the posterior thoracic region (Wellik and Capecchi, 2003). The result is an animal with a dramatic extension of floating ribs through the sacral elements. Similarly, loss of *Hox11* group function results in transformation of the sacral region to the lumbar region (Figure 1.2B) (Wellik and Capecchi, 2003). These studies, among others, have shown that *Hox* genes in mammals maintain similar genetic functions as in *Drosophila.*

Hox genes and limb development

During embryonic development, the limb buds emerge from the lateral plate mesoderm at around E9.0 (the hindlimbs develop slightly later than the forelimbs). At the earliest stages, mesenchymal cells proliferate rapidly away from the body wall and, in a coordinated effort, the apical ectodermal ridge (AER) and the zone of polarizing activity (ZPA) are established. The AER comprises of a layer of ectoderm that surrounds the distal end of the developing limb bud and is a signaling center for FGF family members (mainly FGF4 and FGF8) (Boulet et al., 2004; Lewandoski et al., 2000; Sun et al., 2002). The ZPA consists of a specific region of mesenchymal cells in the posterior region of the distal limb bud that highly expresses sonic hedgehog (*Shh*) and is critical in establishing the anterior to posterior limb axis (Niswander et al., 1994; Riddle et al., 1993). As the limb bud continues to develop, the proliferating mesenchymal cells condense and differentiate to form the cartilage anlagen that will later become the skeletal elements of the limbs in a process known as endochondral ossification (Reviewed extensively in (Karsenty and Wagner, 2002; Kronenberg, 2003). In brief, for each skeletal element, chondrocytes proliferate rapidly to extend the ends of the cartilage anlagen and progressively differentiate before they exit from the cell cycle and undergo hypertrophy at the center. Overall, this forms a distinct structure called the growth plate, defined by zones of cartilage differentiation that are tightly controlled by a feedback loop of *PTHrP* (parathyroid hormone-related protein, from the ends) and *Ihh* (indian hedgehog, from the pre-hypertrophic zone). Surrounding each skeletal element is a mesenchymal layer of cells called the perichondrium that is the continuous progenitor source for chondrocytes (cartilage) and osteoblasts (bone). At around E14.5,

vascularization from the perichondrium and into the center of the growth plate is induced by VEGF secretion from hypertrophic chondrocytes. Consequently, hematopoietic cells develop at the site that will become the bone marrow cavity. It has also been shown that this vascularization is critical for establishment of mesenchymal cells in the nascent bone marrow cavity to generate trabecular bone and to establish bone marrow mesenchymal stem/stromal cells (MSCs, discussed later) (Maes et al., 2010). Through the latest stages of embryonic development and into postnatal development, the long bones of the limb continue to elongate by chondrocyte proliferation in the growth plate and by rapid bone deposition by osteoblasts along the shaft.

In addition to their roles in axial skeleton patterning, the posterior *Hox* genes (*Hox9* to *Hox13*) were co-opted during vertebrate evolution to pattern the limbs from proximal to distal. Emulating their roles in the axial skeleton, the expression and function of individual paralogous groups is restricted to a specific segment of the limb as it continues to develop. The limb is subdivided into three elements patterned in a one-two-many pattern from proximal to distal: the stylopod (humerus and femur), the zeugopod (radius/ulna and tibia/fibula), and the autopod (the many digits of the forelimb and the hindlimb) (Figure 1.3A). Similar to the axial skeleton, dramatic phenotypes are observed with loss-of-function mutations of entire paralogous groups. However, instead of anterior homeotic transformations, severe, region-specific malformations result from the loss of paralogous group function in the limb. Loss of *Hox9* and *Hox10* function results in severe malformation of the stylopod region, *Hox11* of the zeugopod region

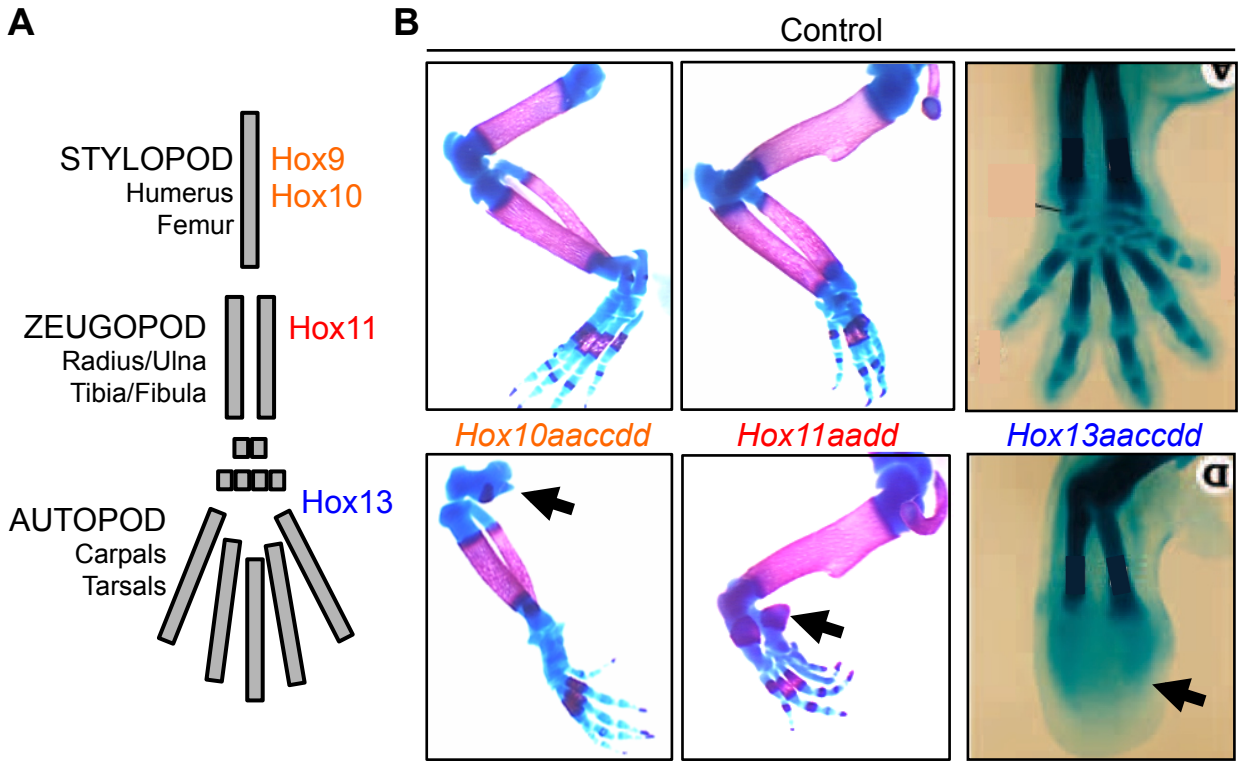

Figure 1.3. Loss of Hox function results in region-specific limb malformations. (A) Schematic representation of the limb and the *Hox* paralogous group of genes that function in patterning each segment. (B) Limb malformation phenotypes of paralogous group loss of function mutations. (Figure adapted from (Fromental-Ramain et al., 1996b; Wellik and Capecchi, 2003))

and *Hox13* of the autopod region (Figure 1.3B) (Boulet and Capecchi, 2004; Davis et al., 1995; Fromental-Ramain et al., 1996b; Wellik and Capecchi, 2003).

Loss of *Hox* gene function has also been implicated in early limb bud formation for establishment of both the AER and the ZPA. Mutations in more anterior paralogous groups (*Hox1* to *Hox9*) demonstrate an additional requirement for these groups in proper anterior to posterior patterning of the limb. Loss of all members in the *Hox9* paralogous group results in loss of *Shh* expression in the ZPA and disrupted patterning of the limb (Xu and Wellik, 2011). Similarly, loss of *Hox5* results in anteriorized *Shh* expression and anterior limb patterning defects (Xu et al., 2013).

Large *Hox* cluster deletions highlight the earliest requirement for *Hox* genes in limb formation. Loss of the entire *HoxA* and *HoxD* posterior clusters (*Hox10* to *Hox13*) results in loss of posterior *Shh* expression in the limb bud and a severe truncation of the skeletal elements of the limb(Kmita et al., 2005). Loss of anterior *HoxD* cluster genes (*Hoxd1* to *Hoxd10)* in the absence of Gli3, displays the most severe limb truncation defect (Zakany et al., 2007). In the presence of Gli3, these animals do not display an overt limb defect likely due to the resultant ectopic expression of the more posterior *Hox* genes, *Hoxd11, Hoxd12* and *Hoxd13* (Zakany et al., 2004). Taken together, results from genetic studies in early limb bud development highlight not only a critical function for *Hox*, but also that *Shh* signaling mediates these functions.

Critical to understanding the function of *Hox,* is in defining which cell type(s) *Hox* is expressed. *Hox* expression analyses have largely been limited to *in situ* experiments, which have been informative for understanding broad expression domains, but are difficult to use for identifying a specific cell type. In order to study *Hox* expression more

rigorously during embryonic limb development a *Hoxa11eGFP* knock-in allele was generated conferring live reporter expression of *eGFP* in cells that express *Hoxa11* (Nelson et al., 2008). Importantly, the region-specific expression pattern that this reporter displays is consistent with previous results from *in situ* hybridization studies (Figure 1.4A) (Haack and Gruss, 1993; Hsieh-Li et al., 1995; Peichel et al., 1997; Small and Potter, 1993). Further, the expression pattern of *Hoxd11* is similar to that of *Hoxa11* and the *Hoxa11eGFP* reporter, suggesting that the paralogs are expressed in the same cells (Pineault et al., 2015).

During mammalian limb development, *Hoxa11eGFP* is dynamically expressed throughout limb development. It is first expressed broadly throughout the limb bud mesenchyme and quickly becomes restricted to the zeugopod region by E12.5 (Figure 1.4B-C). *Hoxa11eGFP* is maintained in the zeugopod through late stages of embryonic development (Figure 1.4D-E). This reporter also shows that *Hox11* is not expressed in the skeletal elements (chondrocytes), but is instead expressed in the surrounding perichondrium (Figure 1.4F-I). Specifically, it is expressed in the outer perichondrium above the layer of osteoblasts that actively lay down bone matrix (Swinehart et al., 2013). This is consistent with a single report of *Hox11* and *Hox13* expression in the developing elements of the chick wing bud, suggesting that this is a generalized expression pattern for *Hox* in the limb (Suzuki and Kuroiwa, 2002).

Hoxa11eGFP is also expressed in the muscle connective tissue fibroblasts and has an additional role in muscle and tendon patterning in the limb. It is well established that musculoskeletal patterning must be a highly integrated process, but little is known about the factors controlling this integration. In a cleverly designed experiment, *Hox11*

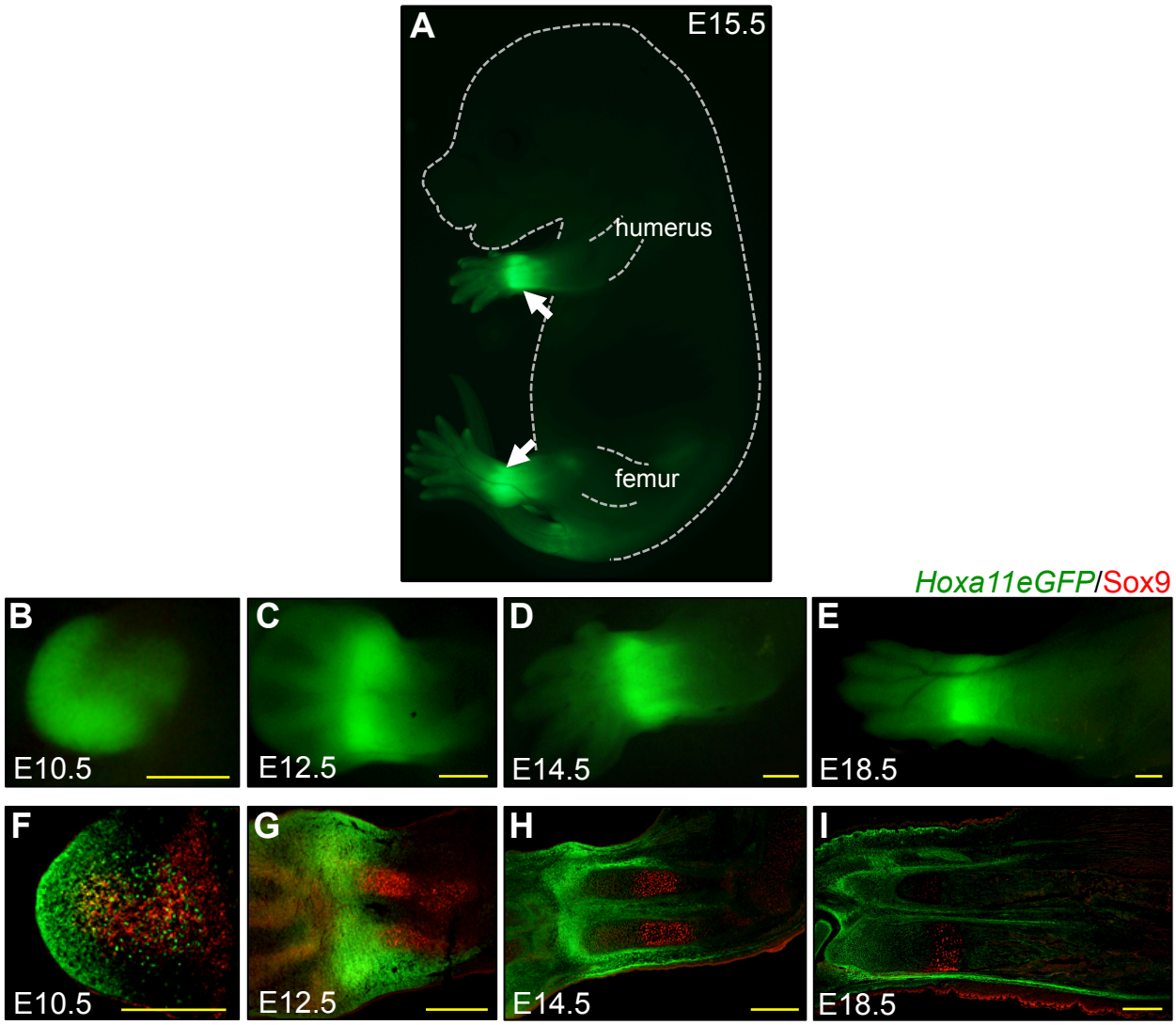

Figure 1.4. Expression of *Hoxa11eGFP* through embryonic limb development. (A) *Hoxa11eGFP* is restricted to specific regions in which it functions during embryonic development. (B-E) Wholemount expression of *Hoxa11eGFP* through forelimb development. (F-I) Section immunofluourescence co-stained with Sox9 to visualize the developing skeletal elements of the forelimb. (Figure adapted from (Swinehart et al., 2013))

compound mutants (maintaining one wildtype *Hox11* allele) were analyzed for muscle and tendon patterning defects because they do not have a skeletal phenotype. In these animals, tendon and muscle patterning is disrupted, providing strong evidence that muscle and tendon defects in *Hox11* mutants are distinct functions for Hox11 and do not occur because of their skeletal perturbations (Pineault et al., 2015; Swinehart et al., 2013).

Significant to the work presented in this thesis, the most surprising finding using this *Hoxa11eGFP* mouse model is that *Hox11* remains expressed into late stages of embryonic development (Swinehart et al., 2013). Previous work had concluded that the *Hox* transcription factors were likely to serve as initial patterning factors. The results reviewed here suggest that the function of *Hox* genes is likely much broader than initial patterning and, possibly, continue into postnatal stages. This observation directly influenced the investigative efforts described in this thesis.

***Hox* genes beyond embryonic patterning: dissecting current literature**

Hox expression in adults is a topic of great interest, and has been suggested by several independent studies. Whole transcriptomic expression analyses of cultured fibroblasts dissected from various human anatomic locations have shown broad and differential *Hox* gene expression patterns. Unbiased approaches such as these have suggested that profiles of *Hox* gene expression may predict the anatomical location origin from which adult skin fibroblasts are dissected and cultured (Chang et al., 2002; Rinn et al., 2006; Rinn et al., 2008). A similar study of fibroblasts from adult human organs also shows differential *Hox* expression profiles suggesting that regional *Hox*

expression patterns are maintained broadly in adult tissues and organs (Takahashi et al., 2004). In a study where bone marrow cells were dissected and plated at low density, colonies of fibroblasts that formed from single cells (CFU-Fs), a defining *in vitro* feature of a mesenchymal stem/stroma cell (MSC), were subjected to unbiased expression analysis. These CFU-Fs from different anatomical locations also displayed differential *Hox* expression profiles (Ackema and Charite, 2008). Related to this, cord blood MSCs and bone marrow MSCs, populations that are used widely for tissue engineering and regenerative medicine, show different *Hox* gene signatures (Liedtke et al., 2010). These data suggest that cells defined as MSCs *in vitro* maintain a differential *Hox* expression profile based on anatomical location. It is important to note, however, that recent work has redefined use of the term MSC to include *in vivo* functions; these latter findings need to be assessed further taking this into consideration (discussed at length in the next section).

The expression of *Hox* genes during skeletal regeneration has also been explored. The first of these studies shows that at least some homeodomain-containing genes (*Msx-1*, *Msx-2*, *rHox*, *Hoxa2* and *Hoxd9*) are reactivated during repair of the femur by *in situ* hybridization and by qPCR (Gersch et al., 2005). In a similar study, calluses from femur fractures were subjected to microarray analysis at several stages following injury. Results show expression of nearly all of the 39 mammalian *Hox* genes throughout the repair process and suggest differential input from different *Hox* genes depending on the stage of the healing process (Bais et al., 2009). Finally, in a transplant study where tibial and mandibular periosteal cells were switched during a fracture healing study, a function for Hox in the repair process was suggested. Results

of the study show formation of cartilage in the mandibular injury when tibial cells were transplanted there. The authors owe this observation to differential Hox function in tibial cells compared to mandibular cells and that mismatching caused the cartilage "scar" formation (Leucht et al., 2008). These data all suggest exciting new roles for *Hox* genes in adult fracture repair, however, taken together, the results of these studies are contradictory with respect to region specificity and do not outline a specific function for *Hox* in the repair process.

It is of intriguing that *Hox* genes apparently maintain a regional "fingerprint" that correlates to the anatomical location from which the cells were collected, however, the aformentioned studies are hard to interpret in the context of embryonic functions for *Hox* genes. The embryonic expression and function of *Hox* genes that is collinear with their chromosomal arrangement is a defining feature of Hox function in the embryo. Moreover, this is a conserved feature through evolution of the cluster, underscoring its potential importance in the broader context of Hox function. However, the embryonic region-specificity of *Hox* paralogous groups is largely ignored in these currently described adult studies. Indeed, in many cases several paralogous groups exhibit expression in any given context suggesting that either specific regional restriction from embryonic development is lost or that these studies are not of high enough rigor to demonstrate region specificity. Using previously generated genetic models that have informed embryonic expression and function, the objective of this thesis work was to characterize expression and function in the adult in a scientifically satisfying manner. As a direct result of this work, two topics are discussed: adult mesenchymal stem/stromal cells and adult fracture healing.

Adult Mesenchymal Stem/Stromal Cells (MSCs)

Adult bone marrow mesenchymal stem cells (BM-MSCs) are widely used as a source of progenitors for *in vitro* experimental studies as well as for use in regenerative medicine. Alongside the discovery of bone marrow resident hematopoietic stem cells in the 1960s (Becker et al., 1963; McCulloch and Till, 1960; Till and Mc, 1961), a population of fibroblastic cells in the bone marrow of rodents was also described. Initial functional characterization of these fibroblastic cells, pioneered by the work of Friedenstein and colleagues in the early 1970s, showed that these cells are non-hematopoietic, that they form fibroblastoid colonies *in vitro,* and that they are progenitors for bone formation (Friedenstein et al., 1970; Friedenstein et al., 1987; Friedenstein et al., 1974; Friedenstein et al., 1976; Friedenstein et al., 1982). In addition, whole bone marrow transplantation studies under the rodent renal capsule showed that bone marrow fibroblast cells are also capable of supporting reconstitution of a hematopoietic environment *in vivo* (Friedenstein et al., 1974; Friedenstein et al., 1968). Multi-lineage potential *in vitro* (to osteoblasts, adipocytes, chondrocytes and myoblasts) of bone marrow fibroblast cells from rodents and from humans was described over the next two decades (Beresford et al., 1992; Friedenstein et al., 1987; Howlett et al., 1986; Mardon et al., 1987; Owen and Friedenstein, 1988; Pittenger et al., 1999; Wakitani et al., 1995). The term “mesenchymal stem cell” (MSC) was coined in 1991 by Arnold Caplan and was thereby adopted broadly to describe these cells (Caplan, 1991). *In vivo* clonal transplantation and reconstitution of the bone marrow microenvironment from human cells was demonstrated in 1997, showing that bone marrow mesenchymal stem cells from humans are equally capable of the functions

described in animal studies (Kuznetsov et al., 1997). Together, these early studies demonstrated that bone marrow stromal cells of both human and animal origin were capable of three basic functions: self-renewal, multi-lineage differentiation *in vitro*, and reconstitution of the hematopoietic microenvironment *in vivo.*

While initial studies were informative, it became clear that the definition of a mesenchymal stem cell needed improvement. The defining features of a bone marrow mesenchymal stem cell were based almost entirely on *in vitro* assays and there existed little data to provide information on how these cells behaved *in vivo.* Moreover, cells with properties similar to those isolated from bone marrow were identified in a variety of other tissues (da Silva Meirelles et al., 2006), highlighting a need for further characterization of MSCs that might be tissue-specific. In an effort to standardize the definition, the International Society for Cellular Therapy (ISCT) recommended use of the term Multipotent Mesenchymal Stromal Cells (MSCs), and a set of properties to define a prospective cell type (cell-surface markers and *in vitro* assays) (Dominici et al., 2006). However, a major gap remained: these standards still only reflected cell-surface markers and functional assays *in vitro*. Given their prospective use in regenerative medicine (stem cell therapies and tissue engineering) it was important to also understand the *in vivo* function(s) of MSCs. The *in vivo* characterization of MSCs has been the dominant focus of several groups in the most recent decade of research.

In the re-evaluation of surface markers used to enrich for MSCs *in vitro,* several changes to the definition of an MSC were made. Instead of culturing cells and then using cell-surface markers to identify cells that function like MSCs, a large of amount of work was done to characterize cells from fresh bone marrow. Through these

experiments, the cell-surface marker CD44, which was often used in culture, failed to identify freshly isolated MSCs and therefore is no longer used to identify MSCs (Qian et al., 2012). In addition, other cell surface markers were identified that enrich for cells that display MSC characteristics: CD105, PDGFRα, Sca1 and CD51 to name a few (Chan et al., 2009; Chan et al., 2013; Morikawa et al., 2009). In comparison to other populations, non-hematopoietic cells that express these markers enrich for CFU-F formation and trilineage *in vitro* and have held up to mark cells that also carry out *in vivo* functions of MSCs.

Genetic mouse models have also proven very useful in the context of understanding *in vivo* functions of MSCs. *In vivo* characterization of MSCs using live reporters and lineage trace models has drastically expanded knowledge regarding the developmental origin and behavior of these cells. The first rigorously characterized mouse model was the *Nestin-GFP* transgenic mouse in which *GFP* is under the control of the *Nestin* promoter and 1.8Kb of the second intron enhancer (Mignone et al., 2004). In a series of studies from Paul Frenette's group, *Nestin-GFP* was defined as marking a subset of perivascular bone marrow multipotent stromal cells. *In vitro,* these cells are capable of multi-lineage differentiation and mesenphere formation, a three-dimensional self-renewal assay in which a single cell is capable of forming a colony of cells in suspension (Mendez-Ferrer et al., 2010). Serial transplantations *in vivo* provided convincing evidence that the cells marked by this transgene were indeed a progenitor cell population capable of self-renewal (Mendez-Ferrer et al., 2010). In a follow-up study, they reported that cell surface markers CD51 (IntegrinαV) and PDGFRα enriched for this GFP+ population and could also enrich for human fetal bone marrow

mesenchymal stromal cells (Pinho et al., 2013). In addition, this group demonstrated that the Nestin-GFP+ cells could be sub-fractionated into Nestin-GFP^{HI} and NestinGFP^{LO} populations: the 'hi' population representing a rare cell type associated with bone marrow arterioles (also marked by the pericyte marker, NG2), and the 'lo' population representing a more abundant population associated with bone marrow sinusoids (also marked by Leptin Receptor, LepR) (Kunisaki et al., 2013). The cell surface markers identified in these studies, including CD105 and Sca1, have since been used to continue to enrich for bone marrow mesenchymal stem/stromal cells *in vivo.* These studies also provided strong evidence that MSCs play important roles in the bone marrow hematopoietic stem cell niche (Kunisaki et al., 2013; Mendez-Ferrer et al., 2010), expanding on previous suggestions of this by others (Adams et al., 2007; Calvi et al., 2003; Zhang et al., 2003).

Leptin Receptor (LepR), and the *Leptin Receptor-Cre* mouse model, is considered to be the marker that most highly enriches for progenitor activity. In a comprehensive study from Sean Morrison's group, LepR+ cells were reported to enrich higher than most other makers for CFU-F potential and were capable of tri-lineage differentiation *in vitro.* Importantly, the CFU-F capacity of LepR+ cells is similar to that of PDGFRα+/Sca1+ and Nestin-GFP^{LO} cells consistent with a previous report that LepR also defines these cells (Kunisaki et al., 2013). PDGFRα+/CD51+ co-staining (Pinho et al., 2013) also overlaps with the LepR+ population. *In vivo,* LepR+ cells can be lineage-traced to differentiated cells following fracture injury, another critical function for MSCs. Upon fracture injury, LepR-lineage cells expand at the site of injury and contribute substantially to cartilage and bone in the fracture callus. Interestingly, despite the fact

that *LepR-Cre* is a constitutive reporter, these cells do not lineage-trace to bone cells (osteoblasts and osteocytes) in an uninjured setting until very late stages of life. Taken together, these data support that LepR+ cells are largely quiescent MSCs until they are required to respond in an injury setting (Zhou et al., 2014), all consistent with properties displayed by stem cells

LepR+ cells also display essential *in vivo* functions in the bone marrow stem cell niche and contribute to bone maintenance and repair. These cells highly express CXCL12 (chemokine (C-X-C motif) ligand 12 CXCL12) and SCF (stem cells factor), important factors in the stem cell niche (Ding and Morrison, 2013; Ding et al., 2012). Conditional deletion of CXCL12 or SCF specifically in LepR+ cells using *LepR-Cre* (DeFalco et al., 2001) reveals important functions for these two factors in LepR+ cells. Deletion of SCF results in increased cycling of HSCs and their subsequent depletion from bone marrow. Deletion of CXCL12 does not deplete bone marrow HSCs but promotes their mobilization into the blood stream and spleen, suggesting that CXCL12 from these cells is required for HSC homing to the bone marrow niche. In addition, secretion of angiopoietin-1 (*Angpt1*) from LepR+ cells (and from HSCs) is required for niche regeneration following irradiation. Together, these data show that LepR+ cells have vital functions in maintaining the bone marrow stem cell niche (and HSCs) at steady state and in recovering the niche following irradiation (Ding and Morrison, 2013; Ding et al., 2012; Oguro et al., 2013; Zhou et al., 2015). Overall, this mouse model is an extremely useful tool for marking mouse bone marrow MSCs as it fulfills most of the requirements necessary to be identified as a stem cell compared to other currently defined populations. Finally, Leptin Receptor is also expressed on human bone marrow

mesenchymal stem/stromal cells (Hess et al., 2005) suggesting that functions defined in animal models may directly translate to humans.

A series of live reporter and lineage tracing studies using genes that are important for embryonic skeletal development also make it possible to understand the origin of adult MSCs, either in the embryo or during postnatal development. In a study aimed at identifying the origin of bone-forming cells during limb formation, perichondrial Osterix(Osx)+ pre-osteoblasts were shown to migrate into the bone marrow with vasculature during endochondral bone formation (Maes et al., 2010). Using *Osx-Cre*, it was later shown that this population of cells is capable of *in vitro* multi-lineage differentiation, gives rise to the majority of osteoblasts and osteocytes during postnatal development, and is maintained in MSCs in the adult (Mizoguchi et al., 2014). Given that osterix is a transcription factor required at the earliest stages of osteoblast differentiation, it is unclear, whether *Osx-Cre* is marking a progenitor cell or early, incompletely committed osteoblast lineage cells. It is likely that this genetic model labels mostly progenitors to osteoblasts, but also comes on in cells that remain progenitors as well. In another study, Henry Kronenberg's group provided evidence that *Collagen2-Cre* (driven by the Collagen 2 promoter/enhancer) marks cells of the perichondrium and of the periosteum at early postnatal stages and lineage labels to MSCs in adult bone marrow (Ono et al., 2014). In the same study, lineage tracing of *Sox9-CreER* and *Aggrecan-CreER*, additional models that show expression in the periosteum when induced at postnatal stages, also gave rise to adult bone marrow mesenchymal cells (Ono et al., 2014). Collectively, these data suggest that adult MSCs

arise from embryonic and early postnatal perichondrial and periosteal cells that migrate to the bone marrow with vasculature (likely as a pericyte).

The genetic tools described have been invaluable in providing information with regard to *in vivo* MSC functions, however it is important to note that the genes associated with these mouse models may not be specific to functions for MSCs. They are often classically known for their roles either in a differentiation pathway or in a completely different population of cells. To highlight this, osterix (*Osterix-Cre*) and lepr (*LepR-Cre*) are typically known for their roles in osteoblast and adipocyte differentiation, respectively. Similarly, sox9 (*Sox9-CreER*), collagen 2 (*Col2-CreER*) and aggrecan (*Acan-CreER*) are essential for chondrocyte differentiation. *Nestin-GFP* is a transgene that was originally generated to study neuronal differentiation (Mignone et al., 2004). Gremlin1, an antagonist of bone morphogenetic proteins (BMP) that has a defined role in development of the skeleton (Canalis et al., 2012) has also recently been shown to lineage trace to adult MSCs that contribute to fracture repair and display self-renewal by serial transplantation (Worthley et al., 2015). Gremlin1 functions in bone formation, yet the genetic tool lineage traces to these mesenchymal stem/stromal cells. Genetic tools that reflect specific functions in progenitor cells may provide more specificity in marking adult MSCs. To this point, CXCL12, described above, drives an important function in HSC niche maintenance and the *cxcl12-GFP (*or *cxcl12-dsred*) genetic mouse model also faithfully marks many of the lineage-trace models for MSCs already described here (Omatsu et al., 2010; Sugiyama et al., 2006). This mouse model, among others not yet discovered, may be important in future studies to continue to compare and contrast currently defined mouse models and markers.

Despite all of the efforts to understand MSCs, their origins and their functions, it still remains indefinable that a ”true” mesenchymal stem cells exists. One of the defining features of a stem cell is self-renewal. Such a quality has been shown for hematopoietic stem cells (HSCs) (Osawa et al., 1996), embryonic stem (ESCs) cells (Evans and Kaufman, 1981; Martin, 1981) and induced pluripotent stem cells (iPSCs) (Takahashi and Yamanaka, 2006). Though this demonstration has been attempted for MSCs, bona fide evidence has not been displayed. It has been suggested that the survival and expansion of MSCs *in vivo* require transplantation of many cells either from a single clone of in co-transplantation with other fibroblastic cells, all of which require *in vitro* expansion (Chan et al., 2015). Serial transplantations (an experiment done to provide evidence of self-renewal) of MSCs do show continued expansion and incorporation in subsequent transplants, however it remains unclear specifically which cells are incorporating. This is in contrast to the single-cell transplants demonstrated for HSCs, ESCs and iPCSs. This limitation begs the question of if a “true” mesenchymal stem cell actually exists. It is possible that all of these genetic tools are marking a similar, smaller population of “true” mesenchymal stem cells but the potential overlap in all of the described lineage-trace models has yet to be resolved. An alternative to the “true stem cell” theory is that among all of the MSC populations that have been described to reside in bone marrow, there are subsets of stem-like cells that are predetermined to differentiate to a specific cell type. It may be that all of the currently defined MSCs are capable of differentiation of multiple lineages when forced, but that this is not the case during normal maintenance. To this point, it will be important to clearly define the differences and similarities of all of the mouse models directly. This

understanding will be critical in determining how these cells may be used for regenerative medicine purposes.

Adult fracture repair

Fracture injury repair is one of the few truly regenerative processes in adults. The result of a properly healed fracture injury is unscarred bone that has restored the original structure and function. The reasons for this are two-fold: 1) two stem cell populations reside in the bone marrow space (HSCs and MSCs) and, 2) mechanisms of fracture healing recapitulate those used in embryonic development. Still, there are many cases in which malunion or non-union fractures occur. Most commonly, this is seen in elderly patients and in patients that have a pre-existing disease. Understanding the mechanisms that govern fracture healing can provide useful information to treat and/or cure these fractures.

The repair of bone following fracture injury can be defined by four overlapping stages: inflammation, soft callus, hard callus and remodeling (Figure 1.5) (Schindeler et al., 2008). Immediately following injury, an inflammatory response is initiated and hematopoietic cells, especially macrophages, expand at the site to clear debris and work to prevent infection. Following this, MSCs migrate to and proliferate at the center of the injury before differentiating to chondrocytes that form the soft cartilage callus. The soft callus acts to stabilize the injury site while it is being replaced by a hard, bony callus. Ossification during healing occurs via two distinct mechanisms. Endochondral ossification takes place at the center of the callus. In this process, cartilage is ossified and is eventually replaced by bone. Simultaneously, intramembranous ossification,

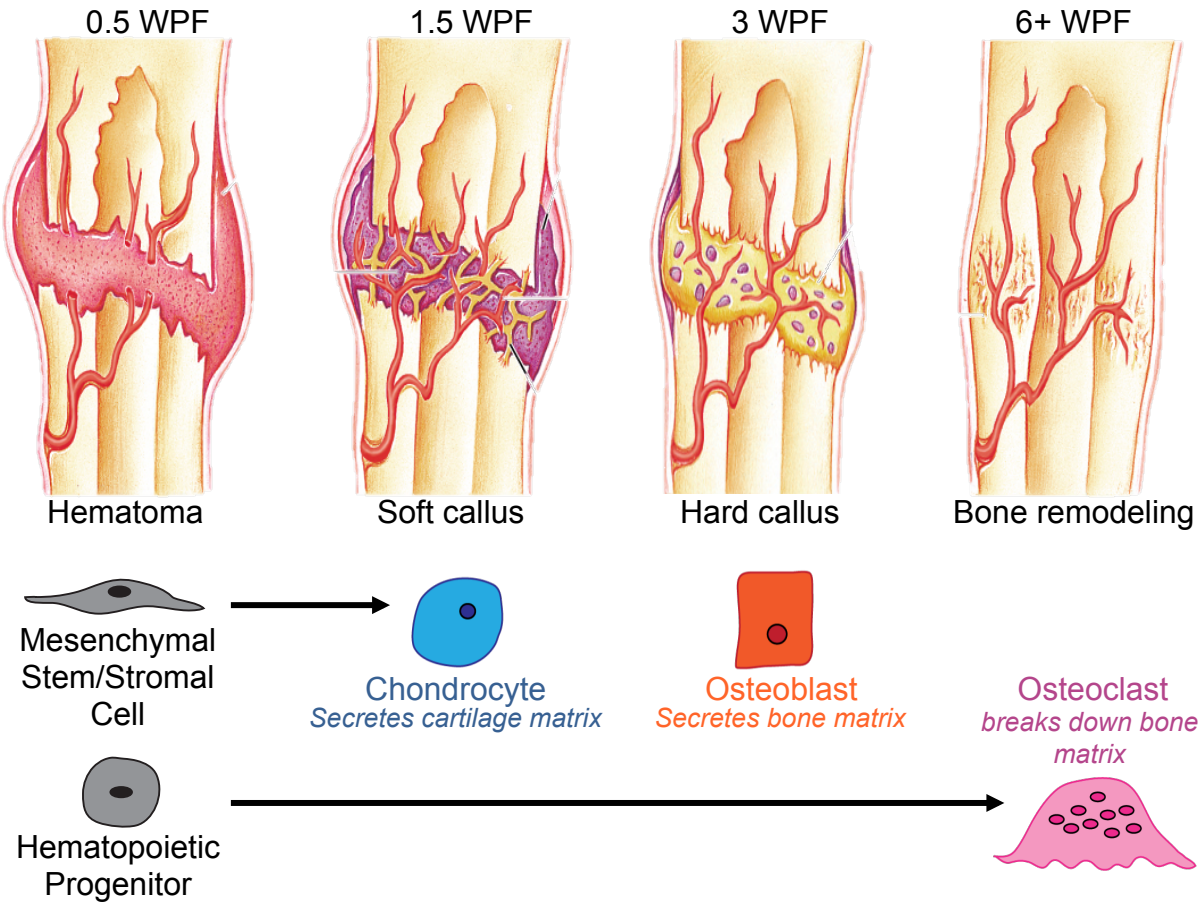

Figure 1.5. The stages of fracture healing.
The process of fracture healing is defined by four consecutive and overlapping stages. Cell types involved include mesenchymal stem/stromal cells that differentiate to chondrocytes and osteoblasts, and hematopoietic progenitors that differentiate to osteoclasts. Time points reflect typical semi-stabilized long bone fractures. (Figure modified from Human Anatomy and Physiology, Copyright © 2001 Benjamin Cummings, an imprint of Addison Wesley Longman, Inc.)

wherein mesenchymal cells differentiate directly to osteoblasts occurs adjacent to the existing cortical bone. Combined, these processes function to efficiently generate new bone that stabilizes the injury. In the final and longest stage of fracture healing, the new bone is remodeled to regenerate its original structure. This function is largely carried out by large, multinucleate, phagocytic cells called osteoclasts whose specific function is to degrade bone matrix and allow osteoblasts space to lay down proper cortical bone matrix (Shapiro, 2008). The fracture healing process results in a scarless, intact skeleton that is capable of the same functions that it performed prior to injury.

Mesenchymal stem/stromal cells are critical for fracture healing and several sources have been shown to contribute to mesenchymal cells of the callus. The periosteum has been implicated as the primary source of progenitor cells as it contains both mesenchymal cells and osteoblasts that can contribute to both methods of endochondral and intramembranous ossification (Nakahara et al., 1990). Bone marrow stem/stromal cells also contribute largely to the fracture callus as discussed in the preceding section (Colnot et al., 2006; Mizoguchi et al., 2014; Park et al., 2012; Worthley et al., 2015; Zhou et al., 2014). The relative contribution of bone marrow and periosteum to fracture healing is contradictory. Using lineage tracing combined with a grafting study of fracture injuries, Celine Colnot's group found that the periosteum gave rise to osteoblasts, osteocytes and chondrocytes, while the endosteum and bone marrow gave rise to osteoblasts and osteocytes and only to a few chondrocytes (Colnot, 2009). This study, while not definitive, is the most direct evidence that the periosteum contributes substantially to the fracture callus.

Fracture repair, with the exception of the inflammatory phase, has been described as a recapitulation of developmental processes. Many of the developmental pathways that are critical for proper long bone development are recapitulated during fracture repair (Ferguson et al., 1999; Vortkamp et al., 1998). Specifically, transcription factors, growth factors and matrix proteins involved in endochondral ossification are highly expressed from the earliest stages of facture repair (Ferguson et al., 1999; Vortkamp et al., 1998). This is consistent with the observation that the overall morphology of the fracture callus mirrors the embryonic growth plate during development (Gerstenfeld et al., 2003). As described already in this thesis, the *Hox* genes have critical functions in skeletal patterning during embryonic development skeletal patterning. Studies have reported that *Hox* genes are re-expressed during repair (Bais et al., 2009; Gersch et al., 2005; Leucht et al., 2008), however there exists very little knowledge to substantiate this claim and it has not been explored functionally. Defining functions for *Hox* genes during adult fracture repair was a major aim of this thesis work.

CHAPTER 2

Regionally Restricted Hox11 Function in Adult Bone Marrow-Multi-potent Mesenchymal Stem/Stromal Cells

Summary

Posterior *Hox* genes (*Hox9-13)* are critical for patterning the limb skeleton along the proximodistal axis during embryonic development. Here we show that *Hox11* paralogous genes, which developmentally pattern the zeugopod (radius/ulna and tibia/fibula), remain expressed regionally in the adult skeleton. Using *Hoxa11eGFP* reporter mice, we demonstrate expression exclusively in multipotent mesenchymal stem/progenitor cells (MSCs) in the bone marrow of the adult zeugopod. These Hox+ cells express PDGFRα and CD51, are marked by *LepRCre*, exhibit CFU-F activity and can tri-lineage differentiate, demonstrating MSC activity. Loss of Hox11 function leads to defects in fracture repair, including reduced cartilage formation and delayed ossification. In tri-lineage differentiation experiments, *Hox* mutant cells are defective in osteoblastic and chondrogenic differentiation. These defects are zeugopod-specific. In the stylopod (humerus and femur), progenitors express other *Hox* genes and femur fractures heal normally in *Hox11* mutants. Together, our data supports regional *Hox* expression and function in skeletal MSCs.

Introduction

Hox genes are responsible for critical patterning events along regionally restricted, overlapping domains of the anteroposterior axis of the axial skeleton (Mallo et al., 2010; McIntyre et al., 2007; Wellik, 2009; Wellik and Capecchi, 2003; Zakany and Duboule, 2007). In addition to this highly conserved role, the posterior *Hox* group genes 9 through 13 play critical roles in the development of the proximodistal skeleton of the limbs (Boulet and Capecchi, 2004; Davis et al., 1995; Fromental-Ramain et al., 1996a; Fromental-Ramain et al., 1996b; Wellik and Capecchi, 2003; Xu and Wellik, 2011). *Hox9* and *Hox10* function is required for patterning of the most proximal element of the limb, the stylopod (femur and humerus) (Fromental-Ramain et al., 1996a; Wellik and Capecchi, 2003; Xu and Wellik, 2011). *Hox11* genes are required for the middle limb elements or zeugopod (radius and ulna; tibia and fibula) (Boulet and Capecchi, 2004; Davis et al., 1995; Wellik and Capecchi, 2003), and the *Hox13* group genes are critical for establishment of the autopod skeleton (carpals and metacarpals; tarsals and metatarsals) (Fromental-Ramain et al., 1996b).

The establishment of the spatial restriction of *Hox* expression has been investigated in detail (Lonfat and Duboule, 2015; Montavon and Duboule, 2013), but much less is understood regarding how *Hox* genes function in establishing skeletal morphologies and pattern that are unique to each region of the vertebrate skeleton. In an attempt to gain insight into this question, we previously generated and examined a GFP insertion allele in one of the *Hox11* paralogs, *Hoxa11*, and closely followed its expression from its initiation in the limb bud mesenchyme (Nelson et al., 2008). As *Sox9*-expressing cells condense to form the two zeugopod anlage (radius/ulna or tibia/fibula), *Hoxa11eGFP*

expression is excluded from these cells. Instead, it can be visualized in the outer perichondrium surrounding these elements as they condense and grow (Nelson et al., 2008; Swinehart et al., 2013). *Hoxd11* is expressed with a similar pattern in the embryo, suggesting that the paralogs are expressed in the same cells (Pineault et al., 2015). As the cartilage matures and bone formation initiates, *Hox* expression remains excluded from differentiated cell types. *Hoxa11eGFP* is not expressed in differentiating cartilage, in osteoblasts, or in endothelial cells in the limb. During developmental stages, *Hoxa11eGFP* is only expressed in the outer perichondrial stromal cells just outside the osteoblast layer surrounding both zeugopod elements, and it persists through newborn stages (Nelson et al., 2008; Swinehart et al., 2013).

In this study, we pursue analyses of these *Hoxa11eGFP*+ cells into postnatal and adult stages. We find that the pattern of *Hox11* expression established during development is maintained through postnatal and adult stages in the periosteum of the adult animal. Intriguingly, we find that *Hoxa11eGFP* becomes additionally visualized in the bone marrow. We identify these adult *Hoxa11eGFP*+ cells as a population of bone marrow mesenchymal stem/stromal cells (BM-MSCs) (Kfoury and Scadden, 2015). *In vivo*, *Hoxa11eGFP*-expressing cells are identified by PDGFRα, CD51 and Leptin Receptor, and they expand at the site of injury following fracture. *In vitro, Hox11*-expressing cells are capable of tri-lineage differentiation (to osteoblasts, chondrocytes and adipocytes) and they exhibit greater self-renewal potential (colony forming unit-fibroblast, CFU-F) than previously described MSC populations (PDGFRα+/CD51+). In addition, we find that Hox11 functions in these cells *in vitro* for proper differentiation to the mesenchymal osteogenic and chondrogenic lineages. Importantly, we show that

Hox genes maintain regional specificity upon fracture injury and that this regional *Hox+* population is functionally important in fracture repair. *Hox11* mutant animals have significant defects in repair of the zeugopod, with decreased cartilage formation and delayed osteogenesis *in vivo.* Taken together, our data shows that *Hox* genes are exclusively expressed in region-specific adult BM-MSCs and that Hox function is critical for regional osteochondral progenitor activity of MSCs *in vitro* and *in vivo.*

Results

***Hox11* expression is maintained in undifferentiated stromal cells through postnatal and adult stages.**

We have previously shown that, during embryonic stages, *Hoxa11eGFP* becomes localized to the zeugopod (radius/ulna or tibia/fibula) region, it is found in the perichondrium surrounding the skeletal elements where it persists through newborn stages (Figure 2.1) (Nelson et al., 2008; Swinehart et al., 2013). Maintenance of this expression during development prompted us to examine expression at post-natal and adult stages using this knock-in reporter. At all time points, we find that *Hoxa11eGFP* remains restricted to the zeugopod region of both forelimbs and hindlimbs, consistent with the regional expression observed during development (Figure 2.1A, 2.2A and S2.1A). Further, we find that the perichondrial expression established in the embryo is preserved in the periosteal region through adult stages (Figure 2.1B, 2.2B, and S2.1B-C). Additionally, during postnatal growth and development, *Hoxa11eGFP* expression becomes visualized at the endosteal surface of the zeugopod bone and throughout the bone marrow (Figure 2.2B and S2.1B-C). qRT-PCR analysis of the skeleton at

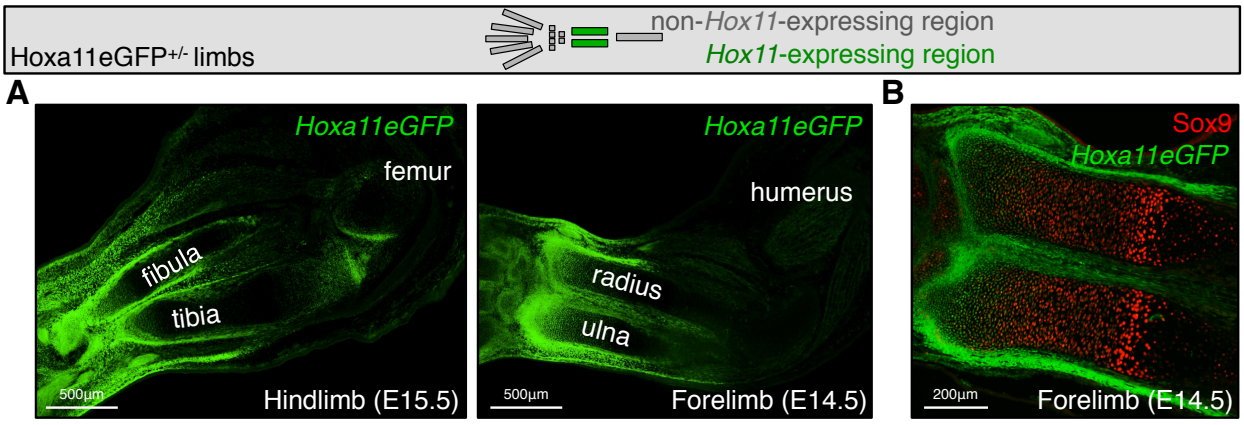

Figure 2.1. *Hoxa11eGFP* surrounds the zeugopod skeletal elements of the developing limbs.
Limb schematic depicts *Hoxa11eGFP* regional expression (green). (A) *Hoxa11eGFP* expression is shown in embryonic hindlimbs (tibia/fibula) and forelimbs (radius/ulna). (B) Sox9 expression depicts the developing cartilage skeletal elements of the forelimb. *Hoxa11eGFP* surrounds the skeletal elements, largely excluded from the differentiating cartilage anlage.

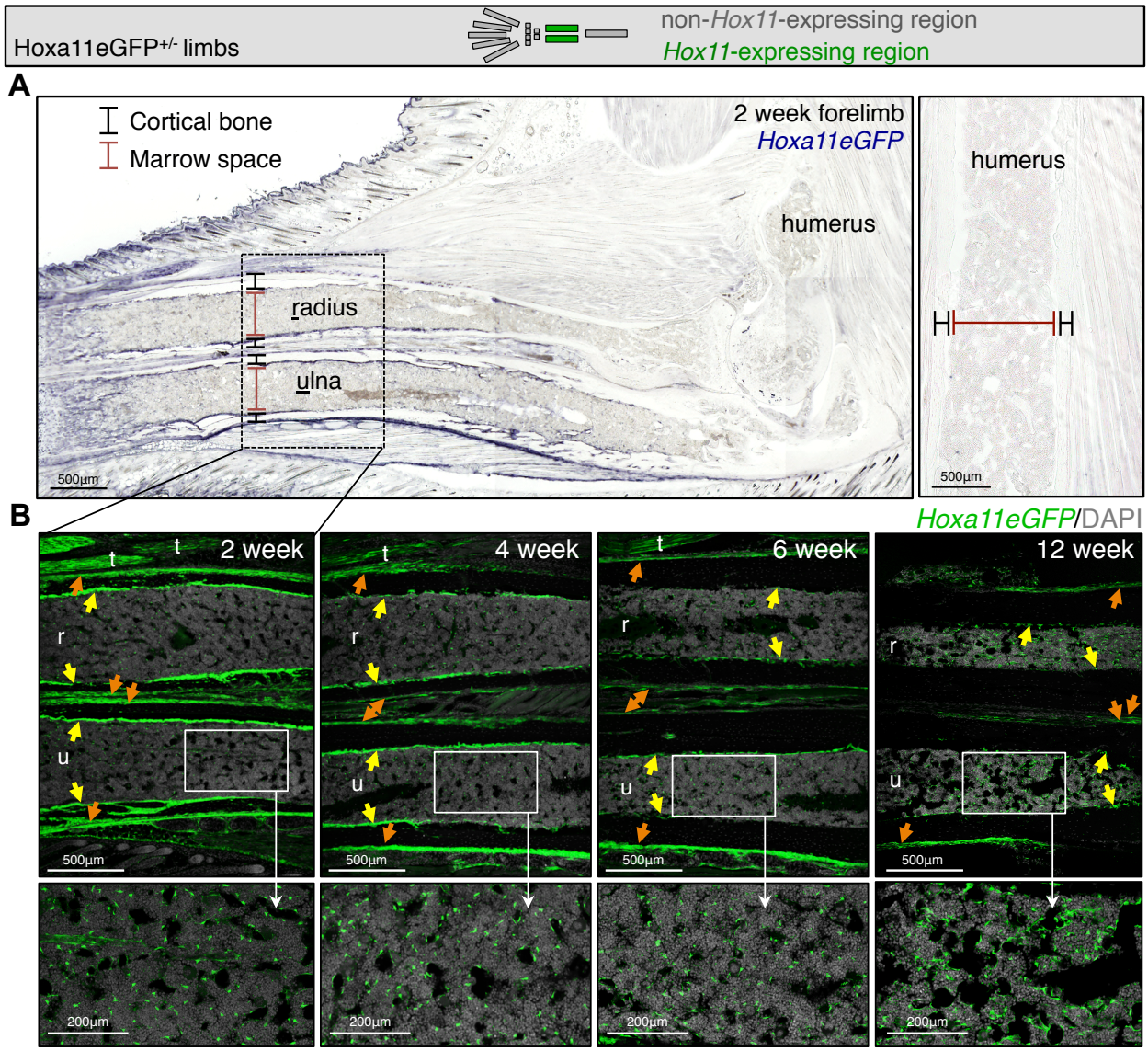

Figure 2.2. *Hoxa11eGFP* is maintained regionally through postnatal and adult stages.
Limb schematic depicts *Hoxa11eGFP* regional expression (green). (A) Low magnification images of the forelimb at 2 weeks show that *Hoxa11eGFP* expression is restricted to the zeugopod and absent from the stylopod. (B) High magnification images show strong periosteal expression (orange arrows) through postnatal stages and into adulthood. *Hoxa11eGFP* expression is additionally observed in endosteal regions (yellow arrows) and in the bone marrow (higher magnification insets). (r) radius; (u) ulna; (t) tendon. See also Figure S2.1.

postnatal stages also shows expression of *Hoxd11,* suggesting that both *Hox11* paralogs function in the postnatal skeleton (Pineault et al., 2015). Consistent with what we have previously shown at embryonic stages, *Hoxa11eGFP* expression does not overlap with any differentiated cell types (Swinehart et al., 2013). *Hox11* expression is excluded from macrophages, endothelial cells, adipocytes, neurons, osteoblasts and osteoclasts (Figure 2.3). Of note, high magnification visualization of *Hoxa11eGFP* reveals a distinct stromal appearance, and many GFP+ cells are observed in close association with bone marrow vasculature (Figure 2.3B). Taken together, these observations led us to explore whether *Hox11*-expressing cells are a mesenchymal progenitor population.

Adult *Hox11*-expressing cells are MSCs.

Bone marrow is comprised largely of hematopoietic cells (~98-99%), while the remaining 1-2% of cells are bone marrow stromal cells. Among stromal cells, approximately 15% are endothelial cells with the remaining 85% being non-endothelial stroma. Bone marrow multipotent mesenchymal stem/stromal cells (BM-MSCs) are contained within the non-endothelial stromal population, but comprise only a small subset of these cells (Kfoury and Scadden, 2015). In recent years, a number of methods have been described that enrich for BM-MSCs. Co-labeling with cell surface markers PDGFRα and CD51, and genetic lineage labeling using Leptin Receptor Cre (LepRCre) are two methods that have been reported to most highly enrich for mesenchymal progenitor cell activity (Kunisaki et al., 2013; Pinho et al., 2013; Zhou et al., 2014).

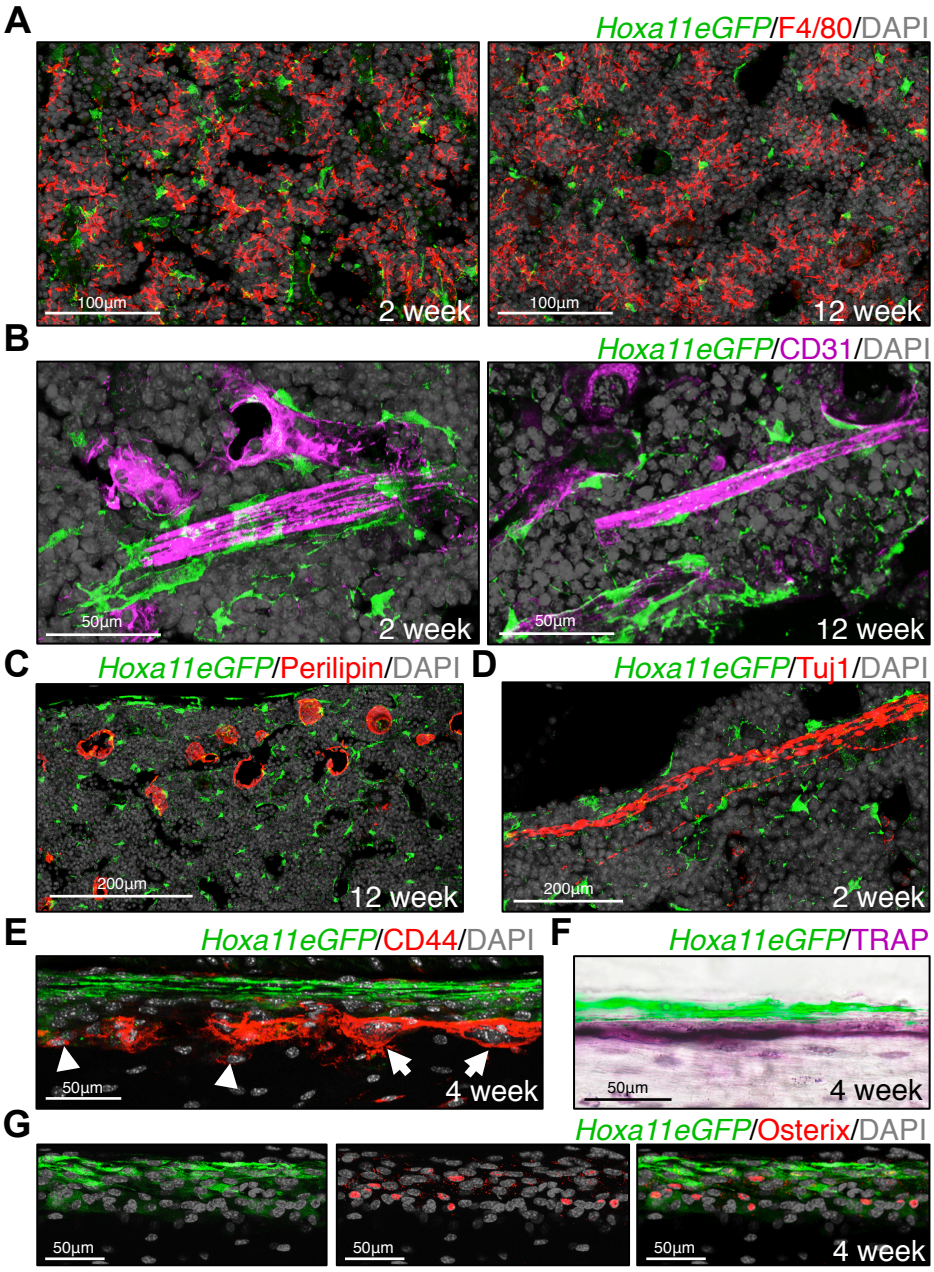

Figure 2.3. *Hoxa11eGFP* is not expressed in differentiated cell types. Co-expression analyses using known markers for differentiated cell types and *Hoxa11eGFP*. (A) *Hoxa11eGFP* is excluded from F4/80+ macrophages in bone marrow. (B) *Hoxa11eGFP* is excluded from CD31+ endothelial cells, but GFP+ cells closely associate with bone marrow vasculature. (C) *Hoxa11eGFP* is excluded from Perillipin+ adipocytes in bone marrow. (D) *Hoxa11eGFP* is excluded from Tuj1+ neurons in the bone marrow. (E) *Hoxa11eGFP* is excluded from CD44+ small, mononucleate osteoblasts (arrow heads) and from CD44+ large, multinucleate osteoclasts (arrows) on the bone surface. (F-G) Co-expression analysis for specific markers of osteoclasts and osteoblasts, TRAP (F) and osterix (G), are consistent with CD44 staining.

Using FACS analyses, we examined the bone marrow from zeugopods of *Hoxa11eGFP* heterozygous mice, and we find that GFP+ cells are not observed in the hematopoietic compartment (CD45+Ter119+) and do not sort with the endothelial stroma (CD31+, Figure 2.4A and S2.2A). *Hoxa11eGFP* sorts entirely within the non-endothelial stromal compartment, and the majority of GFP+ cells are additionally positive for both PDGFRα and for CD51 (Figure 2.4B, and S2.2A-B). We additionally find that *Hox11*-expressing cells are Leptin Receptor (LepR)+ using an antibody to LepR for FACS analyses (Figure 2.4C and S2.2A). To examine this further, we generated mice carrying single alleles of each *Hoxa11eGFP*, LepRCre, and ROSA-LSL-tdTomato (DeFalco et al., 2001; Madisen et al., 2010; Nelson et al., 2008). Bone marrow was examined at adult stages, and virtually all *Hoxa11eGFP*-expressing cells in these populations were co-labeled with ROSA-Tomato (Figure 2.4D and S2.3A). These data suggest that *Hoxa11eGFP*+ cells represent a subset of BM-MSCs within this previously defined population. Interestingly, we also find that *Hoxa11eGFP*+ periosteal cells lining the surface of the zeugopod skeletal elements demonstrate high co-expression with PDGFRα/CD51 and, to a lesser extent, LepR (Figure 2.4E-F and S2.2C). Of note, GFP+ cells were not detected in any populations of non-GFP animals or in the stylopod (humerus) of *Hoxa11eGFP* heterozygous (*Hoxa11eGFP*$^{+/-}$) animals, consistent with maintainence of the regionally restricted *Hox* expression pattern that is established during limb development (Figure S2.3B).

Hallmark functions of BM-MSCs are self-renewal and differentiation into mesenchymal lineages. If *Hox11*-expressing cells are mesenchymal progenitor cells, sorted *Hoxa11eGFP*+ cells should be capable of tri-lineage differentiation into three

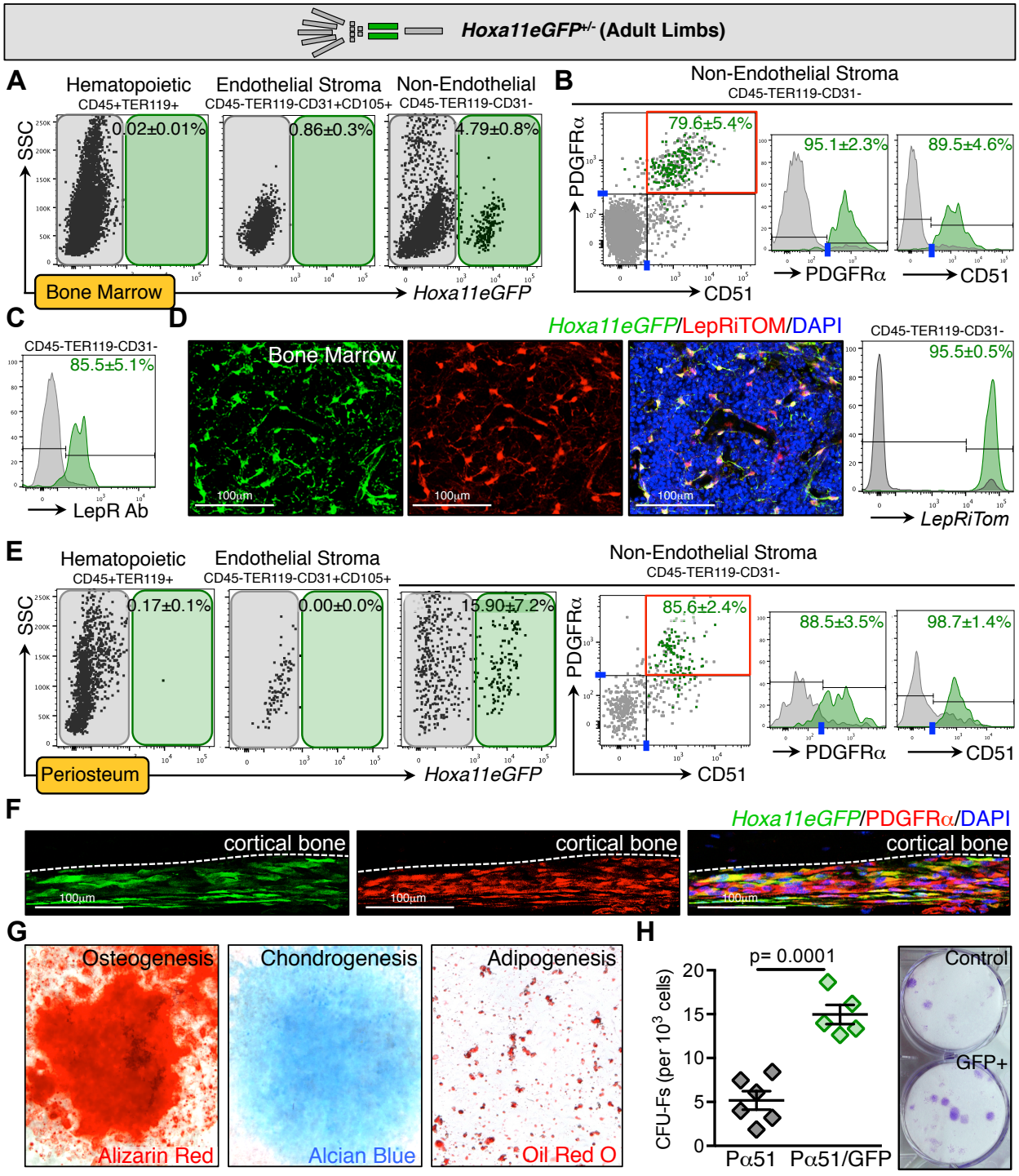

Figure 2.4. *Hoxa11eGFP*-expressing cells are a subset of bone marrow mesenchymal stem/stromal cells (BM-MSCs).
Limb schematic depicts *Hoxa11eGFP* regional expression (green).
(A-B) FACS analysis of live bone marrow cells from the unfractured zeugopod skeleton reveals *Hoxa11eGFP* is not expressed in CD45+/TER119+ hematopoietic cells or in CD105+/CD31+ endothelial cells. *Hoxa11eGFP* is expressed in CD45-/TER119-/CD31-

non-endothelial stromal cells. Overlaid FACS plots or histograms display GFP+ (green) and GFP- (gray) cells from non-endothelial stromal compartment. *Hoxa11eGFP*+ cells predominantly sort with the PDGFRα+/CD51+ cells. Data are represented as mean ± SEM. See also Figure S2.2A-B. (C) Using an antibody against Leptin Recteptor (LepR), FACS analysis shows that *Hoxa11eGFP*+ cells are also marked by LepR. Data are represented as mean ± SEM. See also Figure S2.2A (D) Mice carrying alleles for *Hoxa11eGFP*, LepRCre, and ROSA-tdTomato show high overlap of *Hoxa11eGFP*+ and LepRiTom+ cells in immunofluorescent sections. Analogous FACS analysis shows that 95.5±0.5% of all GFP+ cells are also LepRiTom+. Data are represented as mean ± SEM. See also Figure S2.3A. (E) FACS analysis of live periosteal cells shows that *Hoxa11eGFP*+ cells are also non-hematopoietic, non-endothelial cells that co-express PDGFRα and CD51. See also Figure S2.2C. (F) Immunofluoresence for PDGFRα shows co-expression of *Hoxa11eGFP*+ cells and PDGFRα in the periosteum. (G) *In vitro* analyses reveal that sorted *Hoxa11eGFP*+ bone marrow cells are capable of trilineage differentiation. (H) Sorted *Hoxa11eGFP*+/PDGFRα+/CD51+ cells exhibit increased CFU-F formation compared to cells sorted only as PDGFRα+/CD51+. Data are represented as mean ± SEM.

mesenchymal lineages: chondrocytes, osteoblasts and adipocytes; and should be able produce self-renewing fibroblast colony-forming units (CFU-Fs) *in vitro*. These standard assays were performed and we find that *Hoxa11eGFP*+ cells are able to differentiate into all three lineages (Figure 2.4G). Interestingly, examination of CFU-F formation reveals very high progenitor activity in the *Hox*+ BM-MSCs. Figure 2.4H shows that PDGFRα+/CD51+ cells show significant CFU-F potential, as previously published (Pinho et al., 2013). When zeugopod bone marrow cells are additionally sorted for *Hoxa11eGFP* (PDGFRα+/CD51+/*Hoxa11eGFP*+), these cells demonstrate approximately three-fold higher colony forming activity than cells sorted only for PDGFRα and CD51 (Figure 2.4H). Combined, these data strongly support that *Hoxa11eGFP*+ bone marrow stromal cells represent a mesenchymal stem/progenitor population.

Hox11 functions during fracture repair and maintains regional specificity.

It has been previously demonstrated that MSCs expand in response to fracture injury and are required for repair (Gerstenfeld et al., 2003; Mizoguchi et al., 2014; Park et al., 2012; Schindeler et al., 2008; Shapiro, 2008; Worthley et al., 2015; Zhou et al., 2014). To examine whether Hox+ cells display this response, we fractured the zeugopod of *Hoxa11eGFP* heterozygous animals (forelimb ulna or hindlimb tibia, in separate analyses) and show that *Hoxa11eGFP*+ cells expand at the site following injury (Figure 2.5A). *Hox11*-expressing cells do not overlap with differentiated cell types, including macrophages, endothelium, osteoblasts or osteoclasts (Figure 2.5B-D). We find that *Hox11*-expressing cells are highly associated with the

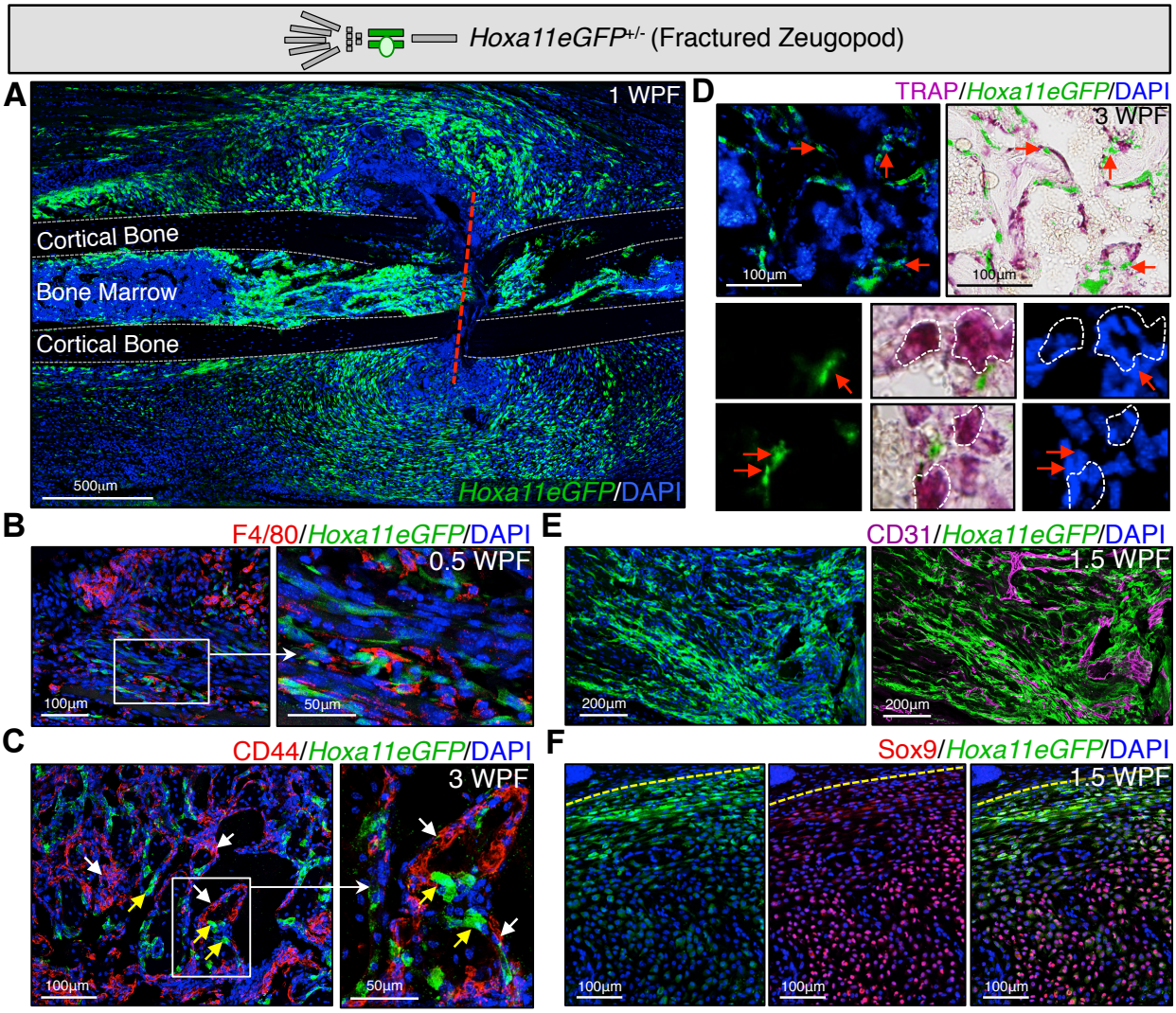

Figure 2.5. *Hoxa11eGFP*-expressing cells expand following injury and do not overlap with differentiated cell types.
Limb schematic depicts *Hoxa11eGFP* regional expression (green) and the fracture callus in the zeugopod region (ulna or tibia) in Hoxa11eGFP$^{+/-}$ mice. (A) At 1 week post-fracture (WPF), *Hoxa11eGFP*+ cells are visualized at the site of fracture (red dashed line) expanded in the forming callus. (dashed grey line) outline of cortical bone. (B) At 0.5WPF, *Hoxa11eGFP* does not overlap with F4/80+ macrophages. (C) At 3WPF, *Hoxa11eGFP*-expressing cells are near bone surfaces and excluded from CD44+ osteoblasts and osteoclasts. (D) At 3WPF, *Hoxa11eGFP*-expressing cells are distinct from TRAP+ osteoclasts, but are closely associated with them near the bone surface. (E) At 1.5WPF, *Hoxa11eGFP* is excluded from CD31+ endothelial cells, but are closely associated with new vasculature in the callus. (F) At 1.5WPF, *Hoxa11eGFP* is highly expressed in the expanded periosteum (yellow dashed line) surrounding the callus and dramatically decreases as sox9 expression increases in differentiating chondrocytes closer to the center of the callus.

vasculature in the fracture callus and that, during soft callus formation, the highest expression of *Hoxa11eGFP* is in cells surrounding the callus, largely excluded from the *sox9*-expressing differentiating chondrocytes closer to the center of the callus (Figure 2.5E-F).

We find that the expanded GFP+ population sorts with the same FACS profile observed prior to fracture – non-hematopoietic, non-endothelial stroma, and double-positive for both PDGFRα and CD51 (Figure 2.6A), as well as co-labeled *in vivo* using LepRCre (Figure 2B). Interestingly, we find that this PDGFRα+/CD51+ profile is maintained throughout the fracture repair process (Figure 2.6C and S2.4A-B). Together, these observations are consistent with cellular activity expected for MSCs following fracture injury.

To further test the potential of these cells in fracture repair, LepRCre/tdTomato/ *Hoxa11eGFP*$^{+/-}$ from adult bone marrow was transplanted into the four-day old fracture callus of wild-type animals. After six days (10 days post-fracture), the callus was assessed for tdTomato-lineage traced cells and we find that the transplanted cells are capable of differentiating to sox9+ chondrocytes and osterix+ osteoblasts (Figure 2.6D). These results show that cells that are *Hoxa11eGFP*+ at the time of transplant are capable of differentiating to skeletal lineages critical for fracture repair *in vivo.*

Data presented herein strongly supports the assertion that *Hoxa11eGFP* marks an MSC population. Further, MSCs are the only cell population in which Hoxa11eGFP cells can be identified; *Hoxa11eGFP* does not co-express with any differentiated cell types. To provide evidence regarding whether *Hox* genes function in the context of the adult skeleton *in vivo*, we performed fracture analyses on *Hox11* compound mutants

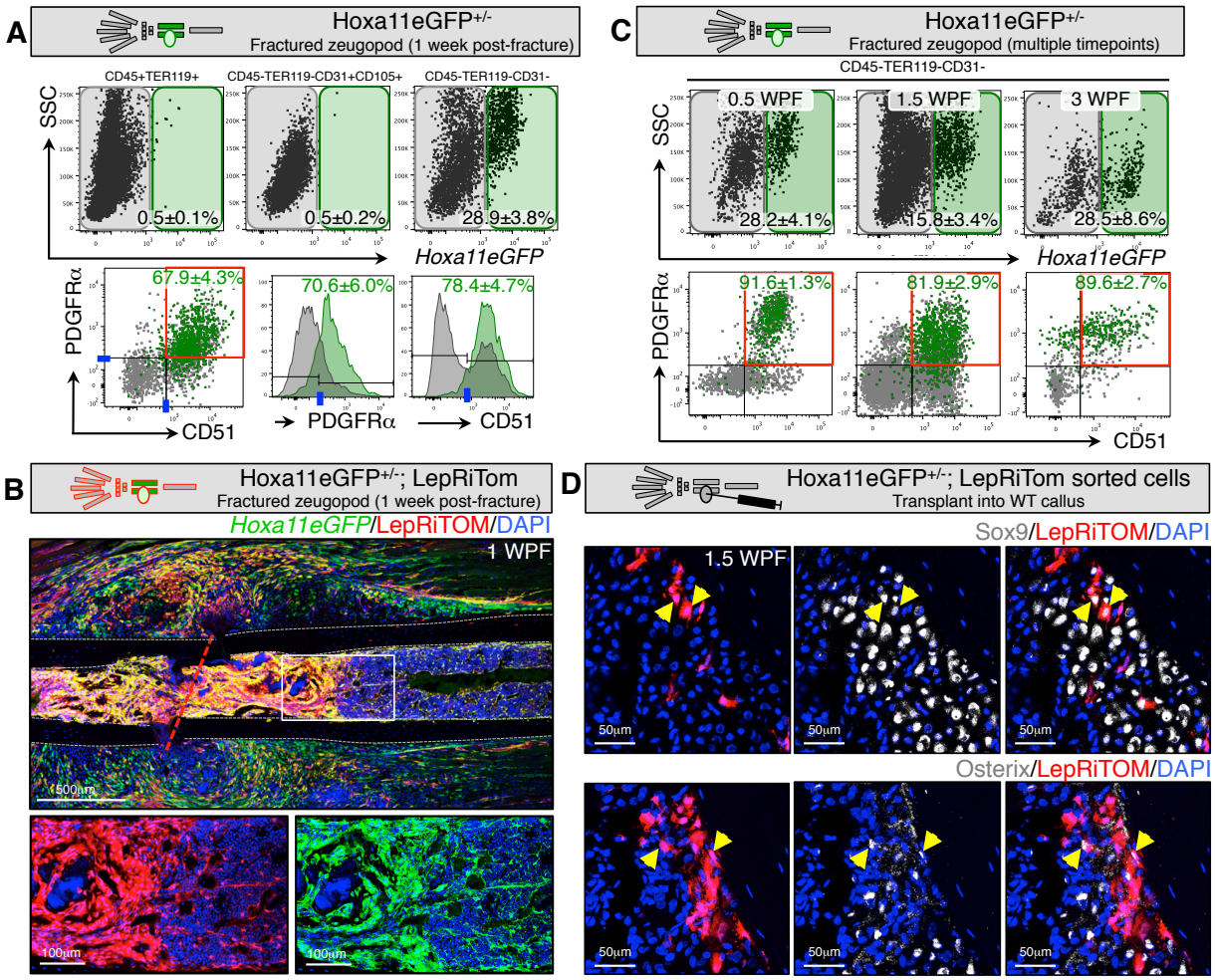

Figure 2.6. *Hoxa11eGFP*-expressing cells in the fracture callus are progenitors that give rise to differentiated cell types.
Limb schematic depicts *Hoxa11eGFP* regional expression (green) and the fracture callus in the zeugopod region (tibia or ulna). (A) Live-cell FACS analysis of the callus at 1WPF, reveals that *Hoxa11eGFP* is only expressed in CD45-/TER119-/CD31- non-endothelial stromal cells. Overlaid GFP+ (green) and GFP- (grey) FACS plots and histograms display GFP+ (green) and GFP- (gray) non-endothelial stroma show *Hoxa11eGFP* in the PDGFRα+/CD51+ progenitor population. Data are represented as mean ± SEM. (B) Immunofluorescent sections of fractured mice carrying alleles for *Hoxa11eGFP*, LepRCre, and ROSA-tdTomato show overlap of *Hoxa11eGFP*+ and LepRiTom+ cells, especially in the expanded bone marrow population closest to the fracture site (higher magnification images). (dashed grey line) outline of cortical bone, (red dashed line) fracture line. (C) Live-cell FACS analysis at 0.5WPF, 1.5WPF, and at 3WPF reveals that *Hoxa11eGFP* is expressed in PDGFRα+/CD51+ cells at all stages of repair. Data are represented as mean ± SEM. See also Figure S2.4. (D) Sorted and transplanted, LepRiTom+(LepRCre lineage trace)/*Hoxa11eGFP*+ cells transplanted into a wild-type, 4-day old tibia fracture callus differentiate to Sox9+ chondrocytes (upper panel, yellow arrowheads) and Osterix+ osteoblasts (lower panel, yellow arrowheads) at 10 days post-fracture (6 days post-injection).

(animals in which three of the four functioning *Hox11* alleles are mutated, *11Aadd*) and littermate controls (*Hoxa11eGFP* heterozygous, *11Aa*^{G}, mice and wild-type, *11AADD*, mice, which were indistinguishable in these experiments). Control mice heal normally, ossifying across the fracture gap by 3 weeks post-fracture (WPF) and remodeling almost completely by 12 weeks after fracture (Figure 2.7A). In fractures of *Hox11* compound mutant mice, ossification across the fracture gap is delayed, although most show a completely ossified callus by 6 WPF. Even by 12 WPF, *Hox11* compound mutants do not approach the level of repair observed in controls (Figure 2.7A). These observations were quantified using a rated scale and blind scoring of microCT images in two orthogonal visual planes (Figure 2.7B).

Unstabilized fractures, like the ulnar fractures described here, typically heal through endochondral ossification whereby new bone is formed from a cartilage anlagen (Gerstenfeld et al., 2003; Schindeler et al., 2008). We find that cartilage formation is reduced in the compound mutants and the amount of cartilage produced never reaches the levels observed in controls (Figure 2.7C). Importantly, *Hoxa11eGFP*+ cells in compound mutant animals display the same FACS profile observed in control animals and the proportion of *Hoxa11eGFP*+ cells in the bone marrow of controls and compound mutants is also unchanged (Figure 2.7D-E and S2.5A-B). Additionally, the CFU-F capacity of *Hoxa11eGFP*+ cells from compound mutant cells is not diminished compared to controls (Figure 2.7F). Together, these results suggest that the defects in skeletal healing are not due to a diminished number of MSCs, but that the *Hox11* mutant MSCs are not producing cell types required for efficient repair.

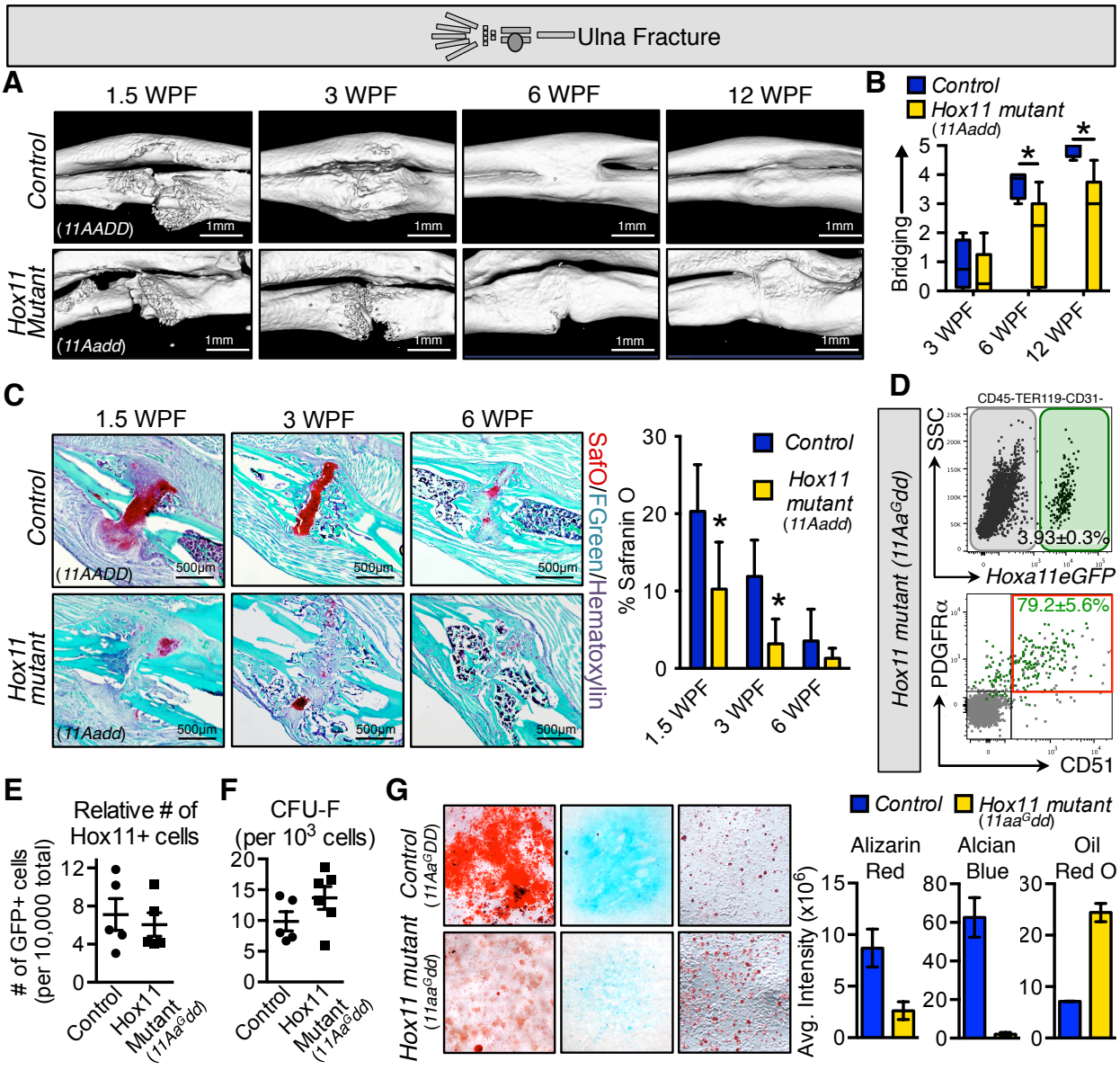

Figure 2.7. Loss of Hox11 function impairs fracture healing *in vivo* and results in *in vitro* differentiation defects.

Limb schematic depicts ulna fracture in control and *Hox11* compound mutant (*11Aadd*) animals. (A) MicroCT isosurfaces show defects in repair of *Hox11* mutants (*11Aadd*, lower panels) compared to controls (*11AADD*, upper panels). (B) Blinded scoring of microCT saggital and coronal images highlight the defects in bridging of the fracture gap in mutants (*11Aadd*, yellow) compared to controls (*11AADD*, blue). (C) Safranin O-stained callus sections and histomorphometric quantification at 3 timepoints post-fracture show a significant decrease in the amount of cartilage formed in the *Hox11* mutant (*11Aadd*) callus. (D) *Hoxa11eGFP*+ cells from the bone marrow of adult *Hox11* compound mutant (*11Aa^{G}dd*) animals are PDGFRα+/CD51+ non-endothelial stromal cells. See also Figure S2.5. (E) The relative number of *Hoxa11eGFP*+ cells from the bone marrow of control (*11Aa^{G}DD*) or *Hox11* compound mutant (*11Aa^{G}dd*) animals is

unchanged. Data is represented as number of GFP+ cells per 10,000 live cells. (F) The CFU-F capacity of *Hoxa11eGFP*+ cells from the bone marrow of control (*11Aa^{G}DD*) and *Hox11* compound mutant (*11Aa^{G}dd*) animals is unchanged. Data is represented as number of colonies per 1,000 GFP+ sorted cells. (G) *In vitro* trilineage differentiation analysis was performed on sorted *Hoxa11eGFP*+ cells from E18.5 control (*Hox11Aa^{G}DD*) and *Hox11* mutant (*Hox11aa^{G}dd*) animals. *Hoxa11eGFP*+ cells from *Hox11* mutant animals (yellow) have decreased capacity for osteogenic and chondrogenic differentiation in micromass and increased capacity for adipogenic differentiation compared to controls (blue). Data represented as average staining intensity quantified using ImageJ software. All statistics represented with a student T-test; * $p<0.05$.

If the defects in skeletal healing result from loss of Hox11 function in the MSC population, *Hox11* mutant MSCs should show similar defects during *in vitro* differentiation assays. To assess this, we performed tri-lineage differentiation on *Hoxa11eGFP*+ cells from control and *Hox11* mutant animals. In these assays, isolated mutant *Hoxa11eGFP*+ cells are defective in osteoblast formation and in chondrogenic ability *in vitro*, analogous to what is observed *in vivo*. Intriguingly, *Hox11* mutant cells showed an increased propensity to differentiate to adipose cells compared to controls (Figure 2.7G). Combined with *in vivo* fracture data, these analyses strongly support that *Hox11* genes function in adult mesenchymal stem/stromal cells to regulate differentiation to skeletal lineages.

An important characteristic of *Hox* expression, developmentally, is the restriction of Hox paralogs along the anteroposterior axis of the axial skeleton and the proximodistal axis of the limbs. Here, we demonstrate that adult limbs maintain the same zeugopod-specific expression of *Hoxa11eGFP* that is observed developmentally. If *Hox*-expressing MSCs serve as a regionally restricted mesenchymal progenitor population, we should not observe expression of *Hox11* in other skeletal areas and there should be no defects in fracture repair in *Hox11* compound mutants in other regions of the skeleton where they are not normally expressed. This is supported by experiments in which the stylopod (femur) of *Hox11* compound mutants and controls were fractured and followed after injury to assess healing. Figure 2.8A (and Figure S2.6B) shows that *Hox11* expression is not initiated ectopically upon injury in this region (Figure 2.8A and S2.6A-B). Further, there are no differences between controls and

Hox11 compound mutant animals in repair of the femur in response to fracture injury (Figure 2.8B). Thus, Hox11 functions in a regionally restricted manner in this process.

Further support for regional *Hox* expression and function is supported by qRT-PCR analyses of bone marrow stromal cells from other regions of the skeleton. In these experiments, stromal cells from the stylopod and zeugopod were isolated and expanded separately *in vitro*. Stylopod stromal cells exhibit preferential expression of *Hox9* and *Hox10* genes, with low *Hox11* gene expression. In zeugopod stromal cells, *Hox11* genes are preferentially expressed over the adjacent *Hox* genes (Figure 2.8C), mirroring the *Hox* expression profile observed *in vivo*. We additionally sorted and performed qRT-PCR on LepRiTom+ and LepRiTom- non-endothelial stromal cells (CD45-TER119-CD31-) from fresh bone marrow from the stylopod, zeugopod, and sternum. Due to limited cell number, we analyzed only a limited set of *Hox* genes, but we find that these cells also display a *Hox* expression profile that is consistent with regionalized embryonic expression patterns. *Hoxa9* and *Hoxa10* are expressed in the stylodpod, but not the zeugopod. *Hoxa11* is expressed in the zeugopod, but not the stylopod or the sternum, and *Hoxa5*, *Hoxb6*, and *Hoxc6* is expressed in the sternum (Figure 2.8D). This analysis further showed *Hox* expression is observed only in the Leptin Receptor lineage-labeled cells. *Hox* expression is not detected in any Leptin Receptor-negative, non-endothelial stromal cells from any region examined, further supporting a role for *Hox* genes in progenitor-enriched (functional) MSCs.

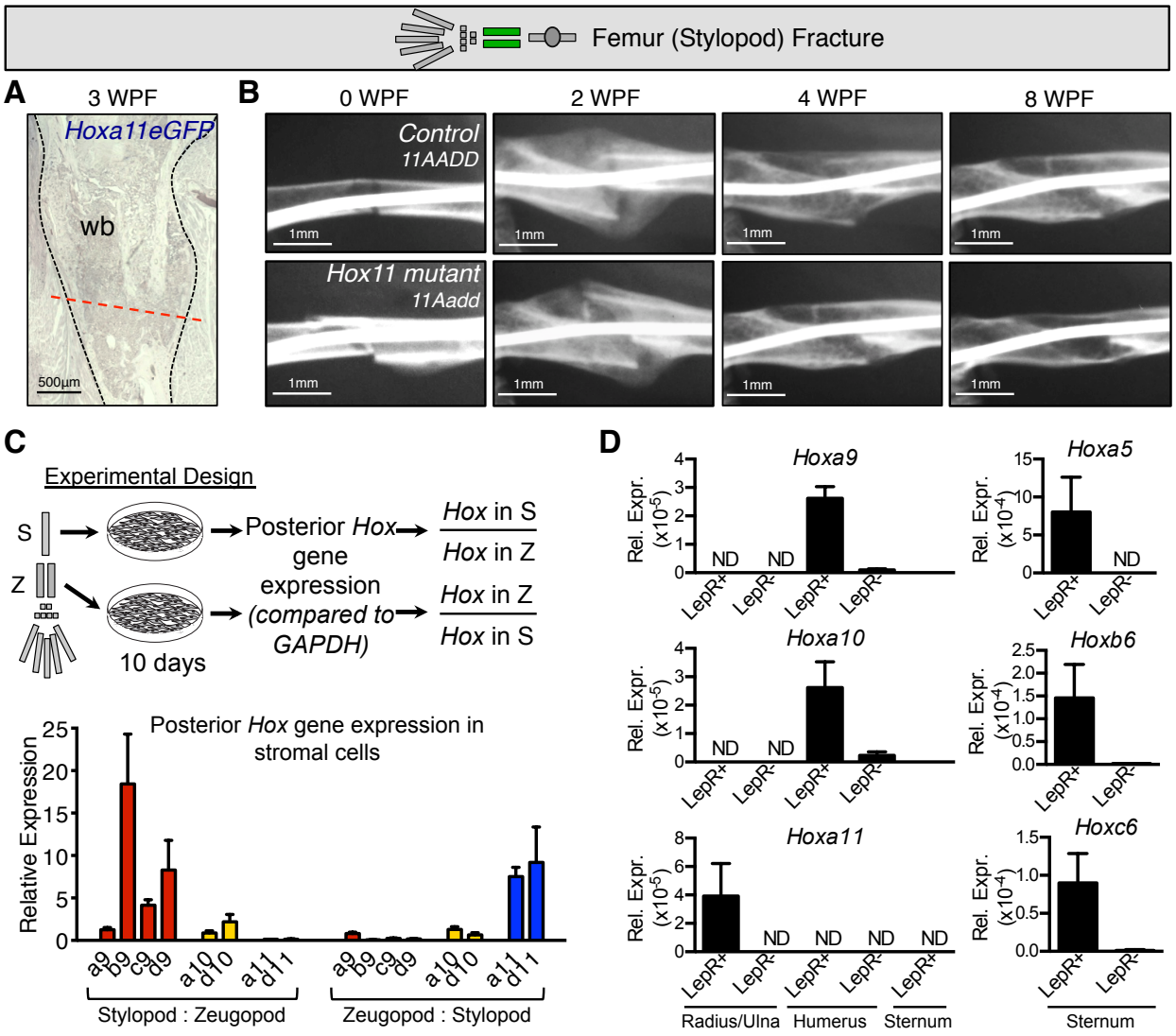

Figure 2.8. *Hox* expression and function is regionally restricted.
(A-B) Limb schematic depicts *Hoxa11eGFP* regional expression (green) and fracture callus in the femur. (A) Femur fractures in *Hoxa11eGFP*$^{+/-}$ animals show no ectopic expression of *Hox11*. (wb) woven bone; (dashed black line) outline of fracture. See also Figure S2.6B. (B) X-ray time-course analyses show that loss of Hox11 function (*11Aadd*, bottom) does not affect the rate of repair of a femur fracture compared to controls (*11AADD*, top). (C) The posterior *Hox* expression profile (*Hox9-11*) was assessed in cultured bone marrow stromal cells. A schematic of the experiment is shown: the fold change (relative to GADPH) for each *Hox* gene in each limb segement (stylopod ad zeugopod) was calculated for each animal. Results show expression profiles of the posterior *Hox* genes compliment the expression patterns established during development. (D) Differential *Hox* gene expression is displayed in freshly-sorted CD45-TER119-CD31-LepRiTom+ and LepRiTom- cells from the bone marrow of various skeletal elements were analyzed by qPCR for *Hox* expression. In all analyses, *Hox* expression is only detected in LepR+ cells. Data is represented relative to housekeeping gene, Rn18s, using the delta delta cT method.

Discussion

Taken together, numerous lines of evidence support *Hoxa11eGFP*+ zeugopod cells as a regional, functionally relevant BM-MSC population in adult animals. This builds on work reported by others that have previously shown that regionally-restricted *Hox* expression persists in adult fibroblast populations (Ackema and Charite, 2008; Chang et al., 2002; Leucht et al., 2008; Rinn et al., 2006; Rinn et al., 2008), but it represents the first demonstration that *Hox*+ cells can be identified and function as BM-MSCs and that these genes function in this population of cells to directly provide skeletal lineages *in vivo*. It remains to be determined whether other *Hox* paralogous groups function as MSCs in other skeletal regions, however the retention of regionally restricted *Hox* expression in the stylopod and sternum, in addition to the zeugopod, only in LepR+ MSC populations and not in the remainder of the bone marrow stromal population, supports this possibility.

The data reported herein demonstrates continuous *Hoxa11eGFP* expression through postnatal and adult stages in the periosteum of the zeugopod skeleton, with increased and persistent expression in bone marrow stroma. Our previously published work examining expression through embryonic stages showed that expression is rapidly restricted to the zeugopod perichondrium during early stages of limb development and that this perichondrial/periosteal expression is maintained through newborn stages (Nelson et al., 2008; Swinehart et al., 2013). It is interesting to correlate real-time *Hoxa11eGFP* reporter expression with results from a recent study that closely examined the lineage-tracing profile of a conditional *Osterix-Cre (Osx-Cre).* When Osx-Cre is initiated at perinatal stages, a subset of lineage-traced cells, which are initially found

perichondrially/periosteally, become long-lived BM-MSCs that can be observed in the adult bone marrow (Mizoguchi et al., 2014). This profile is similar to the live *Hoxa11eGFP* reporter. It will be interesting to further compare the populations marked by this, and other Cre lines, with *Hoxa11eGFP*. Our results are consistent with the possibility that *Hox*-expressing mesenchymal cells represent an initial mesodermal stem/progenitor cell population that is maintained throughout the life of the animal, but this possibility will require further testing in future experiments.

In this study, we highlight significant new evidence that *Hox11* genes function regionally in adult BM-MSCs. *Hox11* mutants are unable to repair properly in response to zeugopod injury, exhibiting delayed osteogenic bridging and reduced cartilage formation but show no defects in repair of the stylopod. *In vitro*, *Hox11* mutant MSCs are unable to differentiate into skeletal lineages. The collective phenotypes through development, postnatal growth and adult stages are consistent with a model whereby *Hox* genes regulate the proper differentiation to mesenchymal skeletal lineages throughout the life of the animal.

Regionalized expression of *Hox* genes in MSC populations adds a new level of complexity to the increasingly broad roles that skeleton-associated MSCs play in the adult animal. Whether distinct *Hox* paralogs impart differential functional information within this population that informs patterning, repair, and morphology of specific regions of the skeleton is perhaps the most intriguing new question raised by this work. Our data indicate that mesenchymal stem/stromal cells have regional signatures of *Hox* gene expression that are functionally relevant. If every BM-MSC population retains unique functional characteristics imparted by differential *Hox* expression, there are

critical implications for use of mesenchymal progenitor cells obtained from bone marrow in regenerative therapies (Bianco et al., 2013; Frenette et al., 2013). It is possible that the location from which MSCs are isolated have important influences on how they behave *in vivo, in vitro,* and in transplantation for regenerative purposes. This should be further explored and considered in therapeutic approaches using MSCs.

Supplemental Figures

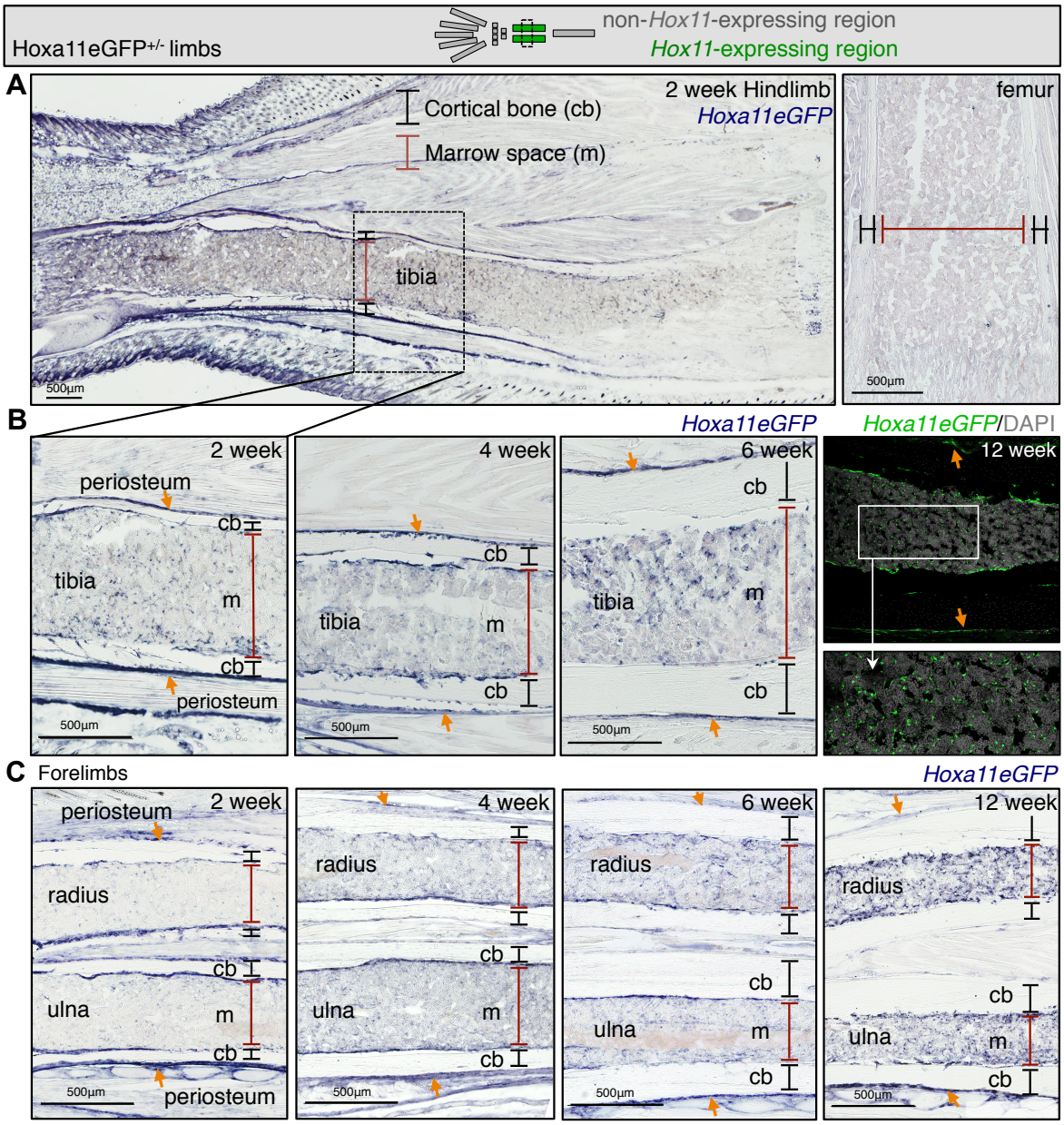

Figure S2.1. *Hoxa11eGFP* is regionally expressed through postnatal and adult stages in hindlimbs and forelimbs.
Limb schematic depicts *Hoxa11eGFP* regional expression (green). (A) *Hoxa11eGFP* is expressed in the hindlimb zeugopod (tibia/fibula). Low magnification images at 2 weeks show *Hoxa11eGFP* restricted to the zeugopod and absent from the stylopod (femur). (B) High magnification images through 12 weeks show expression in the periosteum (orange arrows) and increasing in the bone marrow. (C) High magnification forelimb images analogous to Figure 2.2 are shown developed with alkaline phosphatase. (m and red bar) marrow; (cb and black bar) cortical bone. See also Figure 2.2.

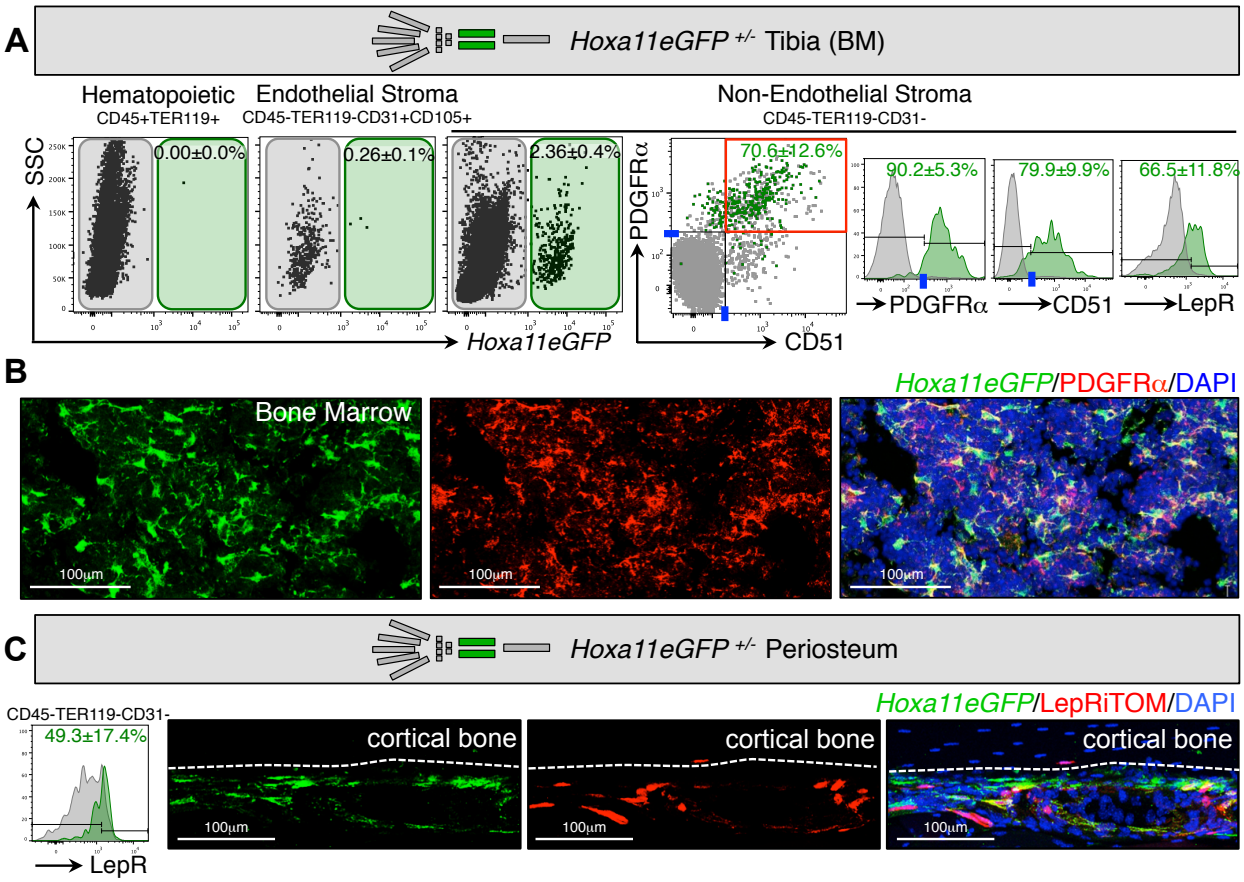

Figure S2.2. *Hoxa11eGFP*-expressing cells from tibia bone marrow and from periosteum are identified as mesenchymal stem/stromal cells.
(A) Limb schematic depicts *Hoxa11eGFP* regional expression (green). Live-cell FACS analysis of unfractured zeuogpod limbs from tibia bone marrow. *Hoxa11eGFP* is not expressed in CD45+/TER119+ hematopoietic cells or in CD105+/CD31+ endothelial cells. *Hoxa11eGFP* is expressed in CD45-/TER119-/CD31- non-endothelial stromal cells. Overlaid FACS plots or histograms display GFP+ (green) and GFP- (gray) cells from non-endothelial stroma. *Hoxa11eGFP*+ cells are predominantly PDGFRα+, CD51+, LepR+ cells. See also Figure 2.4A-B. Data are represented as mean ± SEM. (B) Immunohistochemsitry shows co-expression of *Hoxa11eGFP*+ cells and PDGFRα staining in the bone marrow. (C) In the periosteum, fewer *Hoxa11eGFP*+ cells, compared to bone marrow, are positive for LepR shown by FACS antibody and by mice carrying alleles for *Hoxa11eGFP*, LepRCre, and ROSA-tdTomato. Data are represented as mean ± SEM.

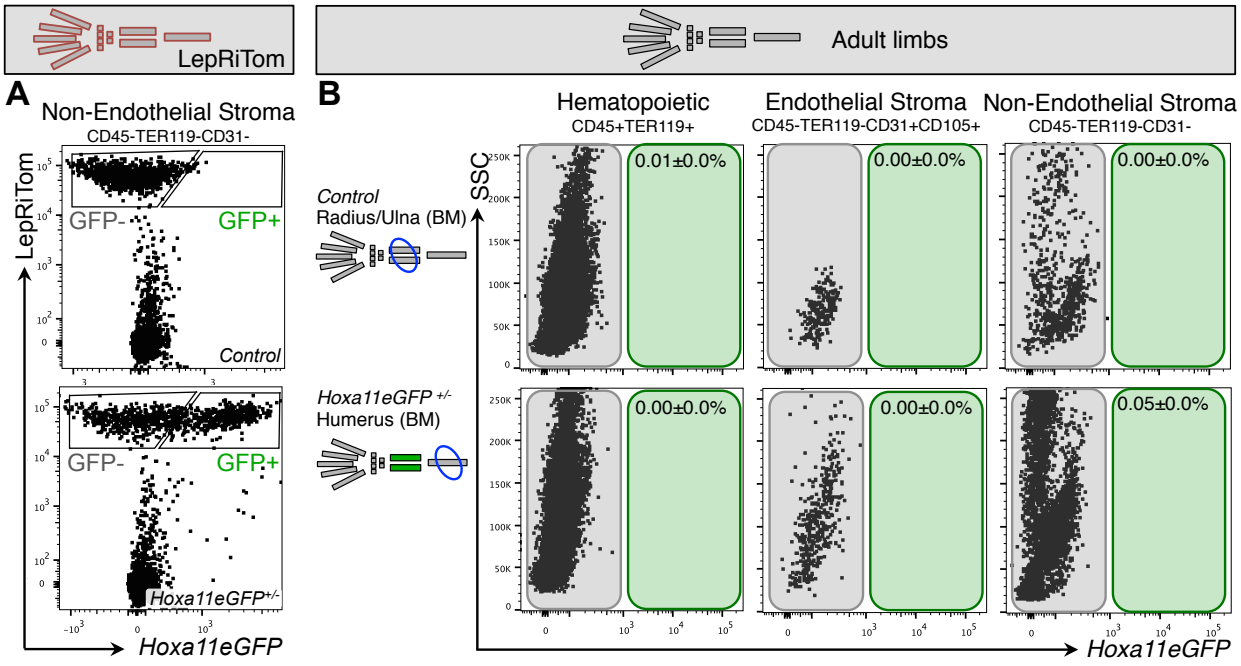

Figure S2.3. FACS analysis controls for *Hoxa11eGFP* expression.
(A) Limb schematic depicts tdTomato+ cells in the limb of LepRCre/tdTomato mice. Live-cell FACS analysis of bone marrow from control (LepRCre/tdTomato) and from LepRCre/tdTomato/Hoxa11eGFP mice confirms there are no GFP+ cells found in control LepR/tdTomato mice. GFP+ cells are only found in mice carrying the *Hoxa11eGFP* knock-in allele. (B) Live-cell FACS analysis of bone marrow from unfractured zeugopod control (non-GFP) limbs and the stylopod region of *Hoxa11eGFP*$^{+/-}$ animals shows no GFP+ cells. Data are represented as mean ± SEM.

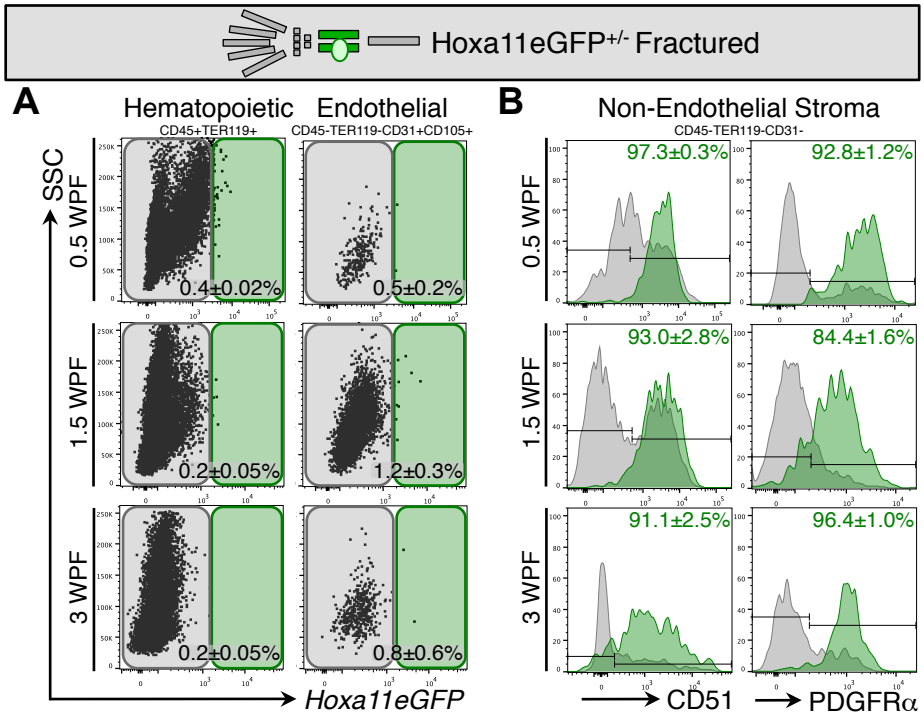

Figure S2.4. *Hoxa11eGFP*-expressing cells throughout fracture healing maintain the FACS profile from uninjured bone.
Limb schematic depicts *Hoxa11eGFP* regional expression (green) and the fracture callus in the zeugopod region (tibia or ulna). (A and B) Live cell FACS analysis of the fracture callus from Hoxa11eGFP+/- animals shows GFP+ cells excluded from CD45-TER119- (hematopoietic) cells and from CD105+CD13+ (endothelial) cells at 0.5WPF, 1.5WPF and 3WPF. GFP+ cells are largely CD45-TER119-CD31-PDGFRα+CD51+ cells. Data are represented as mean ± SEM. See also Figure 2.6.

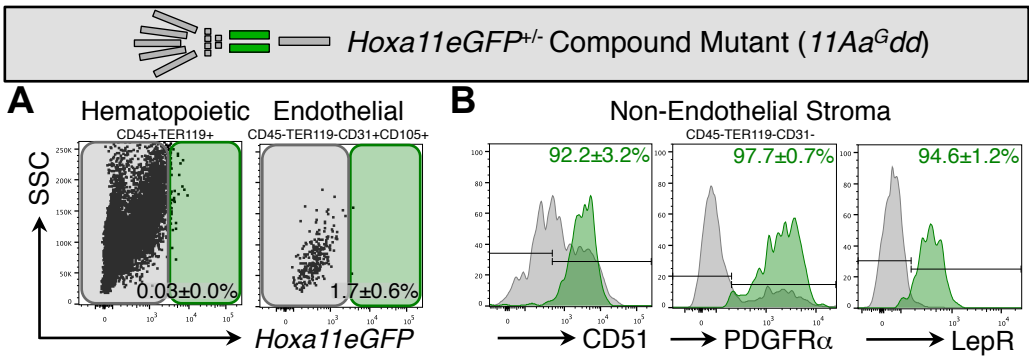

Figure S2.5. *Hoxa11eGFP*-expressing cells in *Hox11* compound mutant animals are non-hematopoietic and non-endothelial.
Limb schematic depicts *Hoxa11eGFP* regional expression (green). (A and B) Live cell FACS analysis of the fracture callus from *Hoxa11eGFP* compound mutant (*Hox11Aa^{G}dd*) animals shows GFP+ cells excluded from CD45-TER119- (hematopoietic) cells and from CD105+CD13+ (endothelial) cells in the bone marrow. GFP+ cells are largely CD45-TER119-CD31-PDGFRα+CD51+LepR+ cells. Data are represented as mean ± SEM. See also Figure 2.7D.

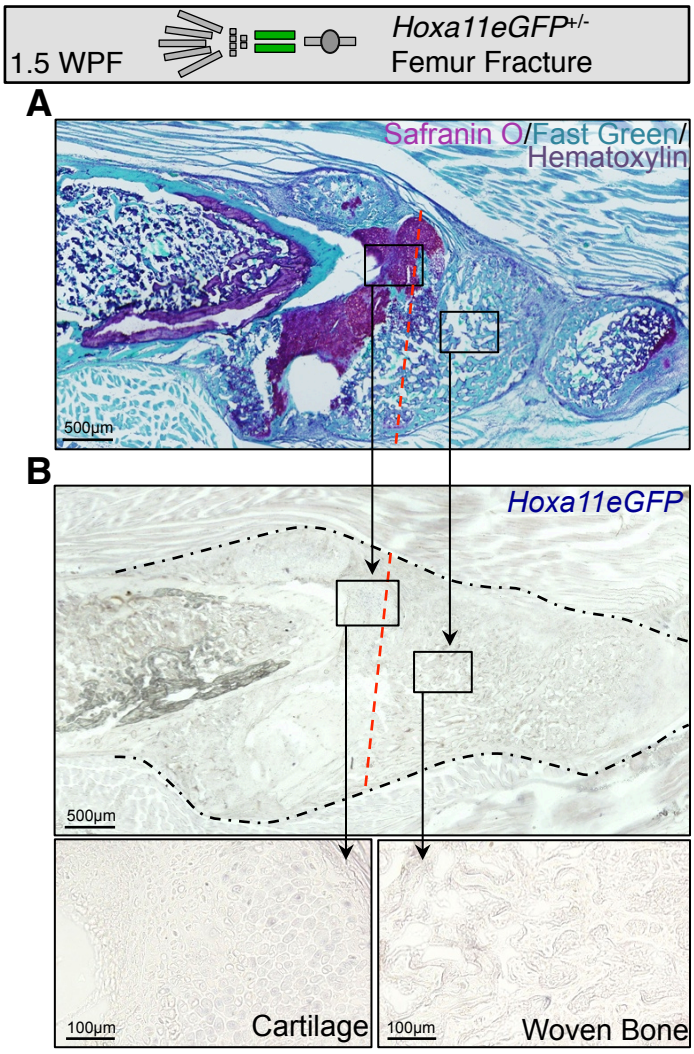

Figure S2.6. *Hoxa11eGFP* expression maintains regional specificity in response to repair.
(A-B) Limb schematic depicts Hoxa11eGFP regional expression (green) and the fracture callus in the stylopod region (Femur) of *Hoxa11eGFP*$^{+/-}$ mice. (A) Fractures collected at 1.5 WPF show endochondral ossification at the site of injury, consistent with tibial and ulnar fracture injuries as show by Safranin O staining. (B) *Hoxa11eGFP* is not expressed in any region of the femur fracture at 1.5 WPF. See also Figure 2.8A.

Materials and Methods

Mice. All mice were maintained in a C57BL/6 background. Male and female mice either double or single heterozygous for the *Hoxa11* and *Hoxd11* null alleles were mated to generate compound mutant animals (Boulet and Capecchi, 2004). Animals heterozygous for the *Hoxa11eGFP* allele were generated by traditional breeding strategies as previously described. LepR-Cre (DeFalco et al., 2001) mice were crossed to the Rosa26-CAG-loxp-stop-loxp-tdTomato (Madisen et al., 2010) line to obtain LepRiTom. To assess spatial variation in bone fracture repair based on local *Hox* expression levels, three distinct fracture-healing models were employed. All animals were anesthetized with isofluorane during each procedure and provided buprenorphine pre- and post-operatively. Carprofen was also given during the recovery period. Post-operative radiographs were taken immediately following fracture (Faxitron X-Ray) to ensure proper fracture location. All animals were fully weight bearing within 1 hour following surgery and were given chow and water ad libitum until the time of death. All animal experiments described in this article were reviewed and approved by the University of Michigan's Committee on Use and Care of Animals, Protocol #08787 (Wellik) and Protocol #09757 (Goldstein).

Fracture Methods. *Tibial fracture:* Following procedures previously described in detail,(Hiltunen et al., 1993; Taylor et al., 2009) mice were anesthetized with Isofluorane gas, and a small incision was made medial to the tibial tuberosity. A 26-gauge needle was used to bore a small hole into the medial-proximal cortex. The needle was withdrawn and replaced with a sterile 0.009 mm diameter stainless steel wire (McMaster-Carr) that was passed through the marrow space and compacted firmly into

the distal tibial bone. The wire was trimmed flush with the cortex, and skin was closed with skin glue. While still anesthetized, mice were placed on a custom guillotine device, with the tibial midshaft placed on top of a two-point support surface. An anvil striker was placed on the anter-medial surface of the tibia at approximately mid-shaft. A weight of ~290 g was dropped from 8 cm to fracture the bone. Tibial "splints" were placed with surgical tape to prevent initial rotational stability to the fracture site over the first 48 hours. *Femoral fracture:* Following procedures similar to the tibial fracture, and outlined in rats by Bonnarens and Einhorn (Bonnarens and Einhorn, 1984), a small lateral parapatellar incision was made and the patella was dislocated medially exposing the distal femoral notch. A 26-gauge needle was used to bore a hole into the distal femoral notch. The needle was replaced with a sterile 0.014mm diameter stainless steel wire (McMaster-Carr), which was passed retrograde up through the femoral diaphysis and compacted firmly into the proximal femoral bone. The wire was trimmed flush with the femoral notch, the patella reduced and a suture was used to close the incision through the capsule followed by skin closure using glue. While still anesthetized, mice were placed on a custom guillotine device, with the femoral midshaft placed on top of a two-point support surface. An anvil striker was placed on the anterior surface of the femur, and a ~290 g weight was dropped from 8 cm to fracture the bone. *Ulnar fracture:* A small incision was made along the posterior surface of the ulna. The mid-ulnar diaphysis was exposed via blunt dissection through the overlying soft tissues and periosteum. Using a fine wire cutter, the ulna was cut at the mid-shaft, taking care not to extend the wire cutters into the radius during the fracture process. Skin was closed with skin glue.

X-ray and microCT. X-ray scans were collected using a benchtop x-ray imager by Faxitron at 3X magnification. For timecourse analyses, animals were anesthetized before x-ray imaging. Samples were scanned using an eXplore Locus SP microCT system (GE Healthcare). All specimens were scanned in water using the following parameters: voltage 80 kVp; current 80 μA; exposure time 1600 ms; voxel size in the reconstructed image 18 μm, isotropic. The data were processed and analyzed using MicroView (v2.1.2 Advanced Bone Application; GE Healthcare Preclinical Imaging).

Rating of callus bridging. MicroCT scans were reoriented for analysis and snapshots of the callus were captured in two planes; a transverse plane to capture the radius and ulna together and an orthogonal plane to capture the callus at a 90 degree angle to the transverse plane. Both images were placed side-by-side and blindly rated based on a scale, from 0 to 5, to assess the progression of fracture gap bridging. The following guidelines were used for each score: 0 = bony callus present, not bridged; 1 = woven bone connected on one side of the callus, no cortical bone bridging; 2 = woven bone connected throughout the callus, no cortical bone bridging; 3 = some cortical bone bridging present, woven bone may still be apparent, non-continuous bone marrow space; 4 = predominantly cortical bone bridging, continuous bone marrow space, noticeable cause still present; 5 = exclusively cortical bone bridging, continuous bone marrow space, little to no callus present. Data is presented as a box-and-whisker plot of time points (3 WPF: control n = 5, Hox11 mutant n = 6; 6 WPF: control n = 4, Hox11

mutant n = 6). Statistical analyses were carried out by an unpaired Student's t-test; * $p<0.05$.

Histology, immunohistochemistry and histomorphometric measurements. Limbs were collected at the indicated ages or time points following fracture surgery. Intramedullary pins were removed if present. All specimens were dissected in PBS on ice and scanned immediately for microCT (if required for fracture analyses). Specimens for frozen sections were fixed for three days in 4% paraformaldehyde in PBS at 4°C, decalcified in 14% EDTA for 7 days and then sunk in 30% Sucrose in PBS overnight prior to embedding into OCT media. Cryosections were collected at 18μm through indicated segments of the limb or through the entire fracture callus. Immunohistochemical staining was performed using standard methods. Sections were blocked with donkey serum and incubated with primary antibodies overnight at 4°C against Sox9 (Millipore, AB5535, 1:500), CD44 (Southern Biotech, 1500-01,1:200), PECAM/CD31 (Developmental Studies Hybridoma Bank, 1:10), Perillipin (Sigma, P1873, 1:100), or βIII-tubulin/Tuj-1 (Santa Cruz, sc-58888, 1:100). F4/80 (Abd Serotec, MCA497RT, 1:100) was incubated for 2 hours at 37°C. Secondary antibodies were incubated at room temperature for 2 hours: donkey anti-goat-alexafluor488, donkey-anti-rabbit-alexafluor555, donkey-anti-Armenian hamster-alexafluor594, and donkey-anti-mouse-alexafluor555. To minimize complications resulting from high auto-fluorescence in adult tissues, we used an antibody against GFP (Invitrogen, A-11122, 1:200) followed with either an alkaline phosphatase conjugated (Jackson ImmunoResearch, 111-055-003, 1:500) or an alexafluor488 conjugated (Invitrogen,

A21206, 1:1000) anti-rabbit secondary antibody for all above analyses of *Hoxa11eGFP* expression. For *Hoxa11eGFP* co-expression analyses that required rabbit antibodies, tissue was fixed overnight in 4% paraformaldehyde and decalcified for 1-2 days in 14% EDTA before cryoembedding. PDGFRα (Cell Signaling, 3174S, 1:10) or Osterix (Abcam, ab22552, 1:300) primary antibodies were incubated overnight at 4°C in combination with chicken-anti-GFP (Abcam, ab13970, 1:1500). Secondary antibodies were incubated at room temperature for 2 hours: donkey-anti-rabbit-Cy3 and donkey-anti-chicken-488. tdTomato was imaged directly without use of an antibody. TRAP staining was performed using a leukocyte acid phosphatase kit (Sigma).

To quantify the amount of cartilage within each callus, every 10th section from cryopreserved tissue was stained with Safranin O/Fast Green/Hematoxylin as previously described (Kahveci et al., 2000; Tran et al., 2000). The callus area and cartilage area on each section was measure manually using ImageJ software. A minimum of three tissue sections per callus was measured and the average was calculated among all animals per time point (1.5 WPF: control n = 8, *Hox11 mutant* n = 11, 3 WPF: control n = 6, *Hox11 mutant* n = 6; 6 WPF: control n = 7; *Hox11 mutant* n = 6).

All brightfield images were captured on an Olympus BX-51 upright light microscope with an Olympus DP70 camera. Fluorescent images were captured on a Leica Upright SP5X Confocal Microscope with 2-Photon. Confocal Z stacks through entire sections were taken at a thickness of 2μm, stacked using ImageJ software, and stitched together using Photoshop software (when required) to obtain high-resolution images of entire limbs and fracture calluses.

Flow Cytometry. Bone marrow cells were harvested by flushing the marrow cavity with digestion buffer (2mg/mL Collagenase IV and 3mg/mL Dispase in 1xPBS) using an appropriate sized needle for each bone. Periosteum was harvested by careful dissection from the tibia after removing muscle tissue and immediately washing in PBS. To obtain cells from the fracture callus, skin and muscle tissue was carefully dissected away from the callus prior to excision with a razor blade (including cortical bone). The callus/cortical bone tissue was then transferred to a dish with 1ml of digestion buffer and cortical bone was dissected away from the callus. For all dissections, three digestion steps were carried out at 37°C with periodic agitation to obtain a single cell suspension. After each period of digestion, cells in suspension were collected into ice-cold staining buffer (1X PBS, 0.5% BSA, 2mM EDTA). Red blood cells were lysed on ice at a final concentration of 0.5X. For staining, cells were resuspended in staining buffer at a concentration of $1x10^6$ cells/30ul in a solution containing the following antibodies: For hematopoietic exclusion; Ter119-AF700 (Biolegend, Clone TER119, 1:100) or TER119-APC (BD, clone TER119, 1:100) and CD45-APCeFluor780 (ebioscience, Clone 30-F11, 1:200) or CD45-APC-Cy7 (BD, clone 30-F11, 1:200). For endothelial cell exclusion: CD31-PerCPCy5.5 (BD, Clone MEC13.3, 1:100) and CD105-PeCy7 (Biolegend, Clone MJ7/18, 1:200). For non-endothelial stroma and MSC exclusion; PDGFRα/CD140a-APC (ebioscience, Clone APA5, 1:100) or PDGFRa/CD140a-PECF594 (BD, clone APA5, 1:100), CD51-PE (ebioscience, Clone RMV-7, 1:100), Biotinylated-goat-anti-Leptin Receptor (R&D, Cat. BAF497, 1:200), and Streptavidin-Qdot565 (Invitrogen, Cat. Q10133MP, 1:500) or BV605 (Biolegend, 405229, 1:500). For LepR-

Cre/tdTomato/*Hoxa11eGFP* samples, cells were collected, digested and stained with CD45-APC-Cy7 and TER119-APC-Cy7 (BD, clone TER119, 1:100) for hematopoietic exclusion. After staining, all samples were washed twice with staining buffer and resuspended in staining buffer with DAPI (1:10,000) for analysis and sorting. Analysis was carried out on an LSRII Fortessa flow cytometer (BD), sorting was performed on a FACSAria II (BD) with 4 lasers (407nm, 488nm, 561nm, 640nm). Results were analyzed with FlowJo (v10.0.7) software.

CFU-F Assays. CFU-F assays were performed either from freshly isolated or from briefly cultured cells. For freshly isolated assays, cells from bone marrow were obtained using a modified version of the above mentioned protocol. Between digestion steps, cells were collected into warm MSC complete media (DMEM with 4.5 g/L D-glucose (Gibco), 1X Glutamax (Gibco), 1mM Sodium Pyruvate, 15% FBS, 100ug/mL streptomycin, 100U/mL Penicillin) supplemented with 2mM EDTA. After all digestions, cells were allowed to rest at 37°C for 10min and cooled on ice before continuing with the above mentioned RBC lysis and staining protocol. $1x10^3$-$3x10^3$ cells were sorted and plated into a single well of a 6-well plate. Cells were maintained at 37°C with 5% CO_2 in a water-jacketed incubator and left untouched for 5 days in phenol red-free a-MEM (Gibco) containing 20% FBS (HyClone), 10% MesenCult stimulatory supplement (STEMCELL Technologies), and 100ug/mL Streptomycin, 100U/mL Penicillin. One-half media was replaced every three days following initial incubation. After 10-14 days, cells were stained with Giemsa and adherent colonies were counted.

For cultured assays, bone marrow from control (*11Aa^{G}DD*) or from Hox11 compound mutant (*11Aa^{G}dd*) animals was flushed and cultured in DMEM (Gibco) containing 1X Glutamax (Gibco), 1mM Sodium Pyruvate (Gibco), 20% FBS (HyClone), 10% Mesencult stimulatory supplement (STEMCELL Technologies), and 100ug/mL Streptomycin, 100U/mL Penicillin for 7 days. $1.5x10^3$ non-hematopoietic *Hoxa11eGFP*+ cells were sorted and plated in a single well of a 6-well plate. One-half media was replaced every three days following initial incubation. After 10-14 days, cells were stained with Giemsa and adherent colonies were counted.

Transplantation Studies. Bone marrow cells from LepRCre/tdTomato/*Hoxa11eGFP* adult animals were expanded in culture with DMEM media containing supplements described above. CD45-/*Hoxa11eGFP*+/tdTomato+ were sorted and recovered in culture for 24 hours prior to transplantation. Tibia fractures were performed on wildtype animals as described above. $3.5x10^5$ GFP+/tdTomato+ cells were injected 4 days post-fracture in 20μl of 1x sterile PBS. Immunofluorescence for Osterix and Sox9 was performed as described above at 10 days post-fracture.

Trilineage differentiation and quantification. To isolate adult *Hoxa11eGFP*+ cells, bone marrow from the radius and ulna of adult mice was flushed and bones were minced. In order to test the function of Hox11 from full mutants, cells from whole bones were isolated from E18.5 control and mutant embryos (control: *Hoxa11eGFP*+/-, Mutant: *11aa^{eGFP}dd*). For both isolations, cells were cultured for 7-10 days before sorting for live CD45- (CD45-APC-Cy7) GFP+ cells to plate for differentiation. For

chondrogenic differentiation, $5x10^4$ cells were plated in micromass, cultured for 21 days (StemPro Chondrogenic differentiation kit) and stained for alcian blue. For osteogenic differentiation,$1x10^4$ cells were plated in micromass, cultured for 12-14 days (StemPro Osteogenic differentiation kit) and stained for alizarin red. For adipogenic differentiation, $3x10^4$ cells/well were plated in monolayer, cultured for 10 days (StemPro Adipogenic differentiation kit) and stained for oil red O. All experiments were carried out with technical replicates (Adult: 4 Hoxa11eGFP+/- animals; E18.5: 1 control and 1 Hox11 mutant animal). For quantification, captured images were converted to binary format in ImageJ software. For alizarin red and alcian blue stains, the mean intensity of the stain was measured by drawing a box surrounding the colored stain. For oil red O staining, the entire image was measured. Measured mean intensities were normalized to background. Background was calculated by taking an average measurement among three different areas within the image (excluding the stain).

qPCR. For analysis of expanded, adherent marrow cells, bone marrow was flushed with needles from the tibia, femur, humerus, and radius/ulna of three wild-type animals and cultured separately in DMEM with 4.5 g/L D-glucose (Gibco), 1X Glutamax (Gibco), 1mM Sodium Pyruvate, 15% FBS, 100ug/mL streptomycin, 100U/mL Penicillin. Cells were passaged once and allowed to grow to confluence before they were collected directly into Trizol. RNA was extracted by phenol choloroform. cDNA synthesis was performed with SuperScript II (Invitrogen). For analysis of freshly isolated LepRCre/tdTomato bone marrow cells, bone marrow was digested as described previously and non-hematopoietic, non-endothelial, LepR lineage-positive or negative

cells were sorted directly into trizol. RNA was extracted with phenol chloroform and RNeasy micro kit (Qiagen). Due to low cell number collection, cDNA synthesis was performed from the entire sample with EcoDry system (Clontech, random hexamers). All qPCR was performed with the following primer sets using Roche FastStart SYBR Green Mastermix:

Hoxa5F – CAGGGTCTGGTAGCGAGTGT, Hoxa5R – CTCAGCCCCAGATCTACCC;

Hoxb6F – GAGACCGAGGAGCAGAAGTG, Hoxb6R – CAGGGTCTGGTAGCGTGTG;

Hoxc6F – CCAGGACCAGAAAGCCAGTA, Hoxc6R – CCTTCTCCAGTTCCAGGGTCT;

Hoxa9R- GTAAGGGCATCGCTTCTTCC, Hoxa9L – ACAATGCCGAGAATGAGAGC,

Hoxb9R – TCCAGCGTCTGGTATTTGGT, Hoxb9L – GAAGCGAGGACAAAGAGAGG,

Hoxc9R – AATCTGTCTCTGTCGGCTCC, Hoxc9L – AGTCTGGGCTCCAAAGTCAC,

Hoxd9R – TTGTTTGGGTCAAGTTGCTG, Hoxd9: - CTCAGCTTGCAGCGATCA,

Hoxa10R – GTGTAAGGGCAGCGTTTCTT,

Hoxa10L – CAGCCCCTTCAGAAAACAGT, Hoxc10R – ACCTCTTCTTCCTTCCGCTC,

Hoxc10L ACTCCAGTCCAGACACCTCG, Hoxd10R – TTTCCTTCTCCTGCACTTCG,

Hoxd10L – GGAGCCCACTAAAGTCTCCC, Hoxa11R – CCTTTTCCAAGTCGCAATGT,

Hoxa11L – AGGCTCCAGCCTACTGGAAT, Hoxc11F – GCGGCCGACGAGCTTAT,

Hoxc11R – TTTTTCATGAGGATCTCAGTGACTGT,

Hoxd11R – AGTGAGGTTGAGCATCCGAG,

Hoxd11L – ACACCAAGTACCAGATCCGC.

Delta Ct values were calculated for each primer set relative to GAPDH or to Rn18s. To analyze each paralogous group (*Hox9*, *Hox10* and *Hox11*) as a whole in cells cultured from stylopod or zeugopod regions, the ratio of stylopod:zeugopod or

zeugopod:stylopod was calculated for each primer set in each animal, separately, before it was averaged and graphed.

CHAPTER 3

Hox11 Genes Are Required For Region-Specific Fracture Repair.

Summary

The processes that govern adult bone fracture repair rely to some degree on recapitulated mechanisms from embryonic skeletal development. The *Hox* genes are transcription factors that are expressed and perform critical patterning functions in regional domains along the axial and limb skeleton during development, however, much less is known about roles for these genes in the adult skeleton. We recently reported that *Hox11* genes remain expressed in the adult skeleton in regionally restricted PDGFRα+/CD51+/LepR+ MSCs. Importantly, we find that this expression is restricted to the region of the limb in which it functions during embryonic development. In this study, we report that the loss of *Hox11* function results in significant defects during the fracture repair process at adult stages. *Hox11* compound mutant animals generate much less cartilage in response to fracture. Later in the repair process, the hard callus persists and is incompletely remodeled in mutant animals. Together, our data suggests that *Hox11* genes function at multiple stages of repair; first, for endochondral ossification and later in bone remodeling.

Introduction

The mammalian skeleton boasts a remarkable capacity to repair following injury. Mechanisms that govern callus formation and remodeling include many events that recapitulate embryonic skeletal development (Bolander, 1992; Einhorn, 1998; Ferguson et al., 1999; Gerstenfeld et al., 2003; Vortkamp et al., 1998). For this reason, it is considered one of few postnatal processes that are truly regenerative, resulting in the reestablishment of the original structure and function of bone without the formation of a scar. The expression of several genes required for embryonic long bone formation (endochondral ossification) are also expressed in the fracture callus, and the patterns of expression and overall histology are similar to those observed in the embryonic growth plate (Ferguson et al., 1999; Gerstenfeld et al., 2003; Vortkamp et al., 1998). *Hox* genes are critical transcription factors required regionally for proper embryonic skeletal development. While several studies have reported *Hox* expression during fracture healing (Bais et al., 2009; Gersch et al., 2005; Leucht et al., 2008), their function in this process has not been directly tested.

Hox genes encode evolutionarily conserved transcription factors that are essential for patterning the axial and limb skeleton during embryonic development. The 39 mammalian *Hox* genes are subdivided into 13 paralogous groups (*Hox1*-*Hox13*) based on sequence similarity and position within the *Hox* cluster. Genetic studies show that members of each paralogous group show remarkable functional redundancy with one another. A defining feature of the *Hox* genes through evolution is the collinear arrangement of the cluster along chromosomes. 3' *Hox* genes (*Hox1*) are expressed earlier in development and in more anterior regions of the skeleton while 5' genes

(*Hox13*) are expressed later and in more posterior regions (Condie and Capecchi, 1994; Fromental-Ramain et al., 1996a; Horan et al., 1995; Kostic and Capecchi, 1994; Mallo et al., 2010; van den Akker et al., 2001; Wellik, 2009; Wellik and Capecchi, 2003). A similar pattern for the posterior *Hox* genes (*Hox9* to *Hox13)* is observed for the proximal to distal patterning of the limbs (Boulet and Capecchi, 2004; Davis et al., 1995; Fromental-Ramain et al., 1996a; Fromental-Ramain et al., 1996b; Izpisua-Belmonte and Duboule, 1992; Mallo et al., 2010; Wellik and Capecchi, 2003; Xu and Wellik, 2011; Zakany and Duboule, 2007). The *Hox11* genes, the focus of this study, instruct proper development of the zeugopod (radius/ulna and tibia/fibula) as well as sacral patterning and morphology in the axial skeleton (Boulet and Capecchi, 2004; Davis et al., 1995; Wellik and Capecchi, 2003). Loss of *Hox11* function results in severe patterning defects of these regions while the remainder of the skeleton develops normally.

Using a *Hoxa11eGFP* knock-in allele, we previously reported that *Hox11* is expressed in the perichondrium/periosteum surrounding the developing skeletal elements into late stages of postnatal development (Swinehart et al., 2013). This result suggests that *Hox* genes may continue to function beyond initial patterning events in the embryo. My work described in the previous chapter additionally shows that *Hox11* genes are expressed in adult mesenchymal stem/stromal cells (MSCs) present in the bone marrow and in the periosteum (Chapter 2). Hox11+ cells are a subset of PDGFRα+/CD51+/Leptin Receptor+ cells that have been previously characterized by other groups to highly enrich for mesenchymal stem/stromal progenitor activity and to contribute to the fracture healing process (Kunisaki et al., 2013; Pinho et al., 2013; Zhou et al., 2014). Importantly, expression and function of Hox11 in these cells is maintained

in the same region it functions in the embryo. Further, the expression of other *Hox* genes are also restricted regionally in LepR+ MSC populations, suggesting this is a general function for *Hox* genes in adult MSCs.

In this study, we explore the cellular defects associated with loss of Hox11 function in fracture repair. At early stages of repair, Hox11 function is critical for chondrocyte differentiation and endochondral ossification. At later stages of repair, hard callus remodeling does not occur properly in *Hox11* mutants. Interestingly, while osteoclasts are present and express cathepsin K in the mutant callus, they fail to attach appropriately to the bony matrix and the bone matrix in mutants is abnormal. Taken together, our work demonstrates continued function for *Hox11* genes at adult stages in the skeleton.

Results

Hox11 is expressed throughout fracture repair.

The fracture healing process can be loosely defined by distinct phases of anabolic and catabolic responses to the injury (Einhorn and Gerstenfeld, 2015; Schindeler et al., 2008). A period of inflammation is the immediate response to fracture injury. Macrophages and other immune cells invade the site to clear debris and results in the formation of a hematoma that expands into the soft tissue areas surrounding the broken bone. Following this, a distinctly anabolic phase of healing occurs; this is defined by mesenchymal stem/stromal cell proliferation and differentiation to form cartilage (chondrocytes) and bone (osteoblasts). A soft callus is formed first, comprised mostly of cartilage, and replaces the hematoma to stabilize the site of injury. As the

cartilage matrix ossifies, it is replaced by new bone matrix laid down by osteoblasts, resulting in the formation of a hard callus. The final phase of healing is defined by a long catabolic process of woven bone matrix breakdown and replacement with lamellar bone that coalesces with the surrounding intact cortical bone. Osteoclasts, phagocytic cells that specifically breakdown bone matrix, are critical in this process.

We have previously shown that *Hoxa11eGFP* is restricted to the zeugopod region of the limb during development (Nelson et al., 2008; Swinehart et al., 2013). It is expressed in the perichondrium/periosteum surrounding the skeletal elements through late embryonic stages of development. We have also reported that expression of *Hoxa11eGFP* persists in the zeugopod through postnatal stages in the skeletal connective tissues: the periosteum, the endosteum and the bone marrow. We identified these *Hox11*-expressing cells as a subset of mesenchymal stem/stromal cells (MSCs) that express PDGFRα, CD51 and Leptin Receptor, defined markers that enrich for adult stem cell properties (Kunisaki et al., 2013; Pinho et al., 2013; Zhou et al., 2014).

One of the functions of MSCs is to provide a progenitor cell pool for repair following fracture injury. We examined the expression of *Hoxa11eGFP* following fracture injury of either the ulna of the tibia (forelimb or hindlimb zeugopod). During hematoma formation, the initial stage of fracture repair, Hoxa11eGFP+ cells begin to expand from the periosteum (Figure 3.1A and S3.1A). During the soft (cartilage) callus and the hard (bony) callus stages, cells expressing *Hoxa11eGFP* expand significantly throughout the site of fracture. *Hoxa11eGFP*-expressing cells are observed in the center of the soft callus in the intramedullary space and in the expanded periosteal stromal layer that surrounds the newly formed fracture callus (Figure 3.1B and S3.1B).

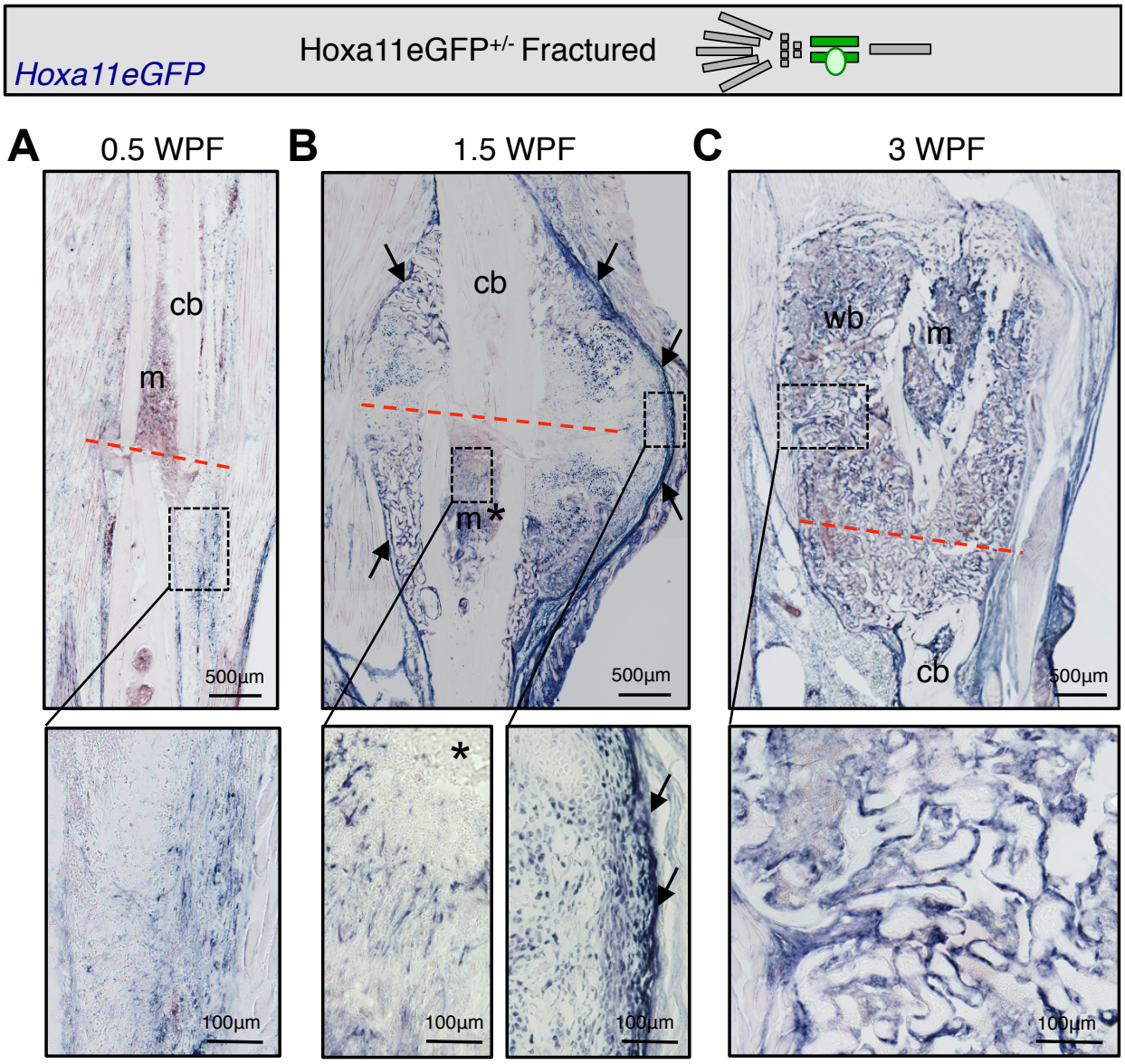

Figure 3.1. *Hoxa11eGFP* is expressed throughout fracture injury of the limb zeugopod.
Limb schematic depicts *Hoxa11eGFP* regional expression (green) and the fracture callus in the zeugopod region (tibia). *Hoxa11eGFP* expression is shown using a GFP antibody and developing with alkaline phosphatase. (A) *Hoxa11eGFP* is expressed at low levels in the hematoma. (B) *Hoxa11eGFP* expression expands in the soft callus including the intramedullary space (*) and the expanded periosteum surround the callus (arrows). (C) *Hoxa11eGFP* is expressed near woven bone surfaces in the hard callus.

In the hard callus, *Hoxa11eGFP*-expressing cells are observed throughout, lining the woven bone surfaces (Figure 3.1C). Critically, our previous work shows that *Hox11*-expressing cells do not overlap with any markers of differentiated cells throughout the fracture healing process (Chapter 2). FACS analysis at all stages following injury demonstrates that the *Hox11*-expressing cells maintain an MSC marker profile consistent with *Hoxa11eGFP* only being expressed in progenitor cells throughout the repair process (Chapter 2).

Loss of Hox11 function results in defects following fracture injury.

To assess a role for *Hox11* in the fracture repair response, we employed an ulnar fracture model in *Hox11* compound mutants. Three *Hox11* alleles are mutated in compound mutant animals and retention of one wild-type allele is sufficient to prevent the developmental skeletal defects observed in the four-allele mutant animal (Davis et al., 1995; Swinehart et al., 2013). X-rays and microCT scans performed at several time points following fracture injury reveal defects in the healing response in compound mutants compared to controls. At 1.5 weeks post-fracture (WPF), during soft callus formation, there are no apparent differences in ossification between mutants and controls (Figure 3.2A). However, by 3 WPF, controls develop hard, bony calluses, while *Hox11* mutants have not fully bridged the fracture gap (Figure 3.2B). At 6 WPF, most compound mutant animals have completed bridging the fracture gap (though 27% result in non-union fractures). At this stage, the remodeling process lags significantly behind that of control animals (Figure 3.2C and F). By 12 WPF, control animals display near completely remodeled bony surfaces. Conversely, *Hox11* mutants that have bridged

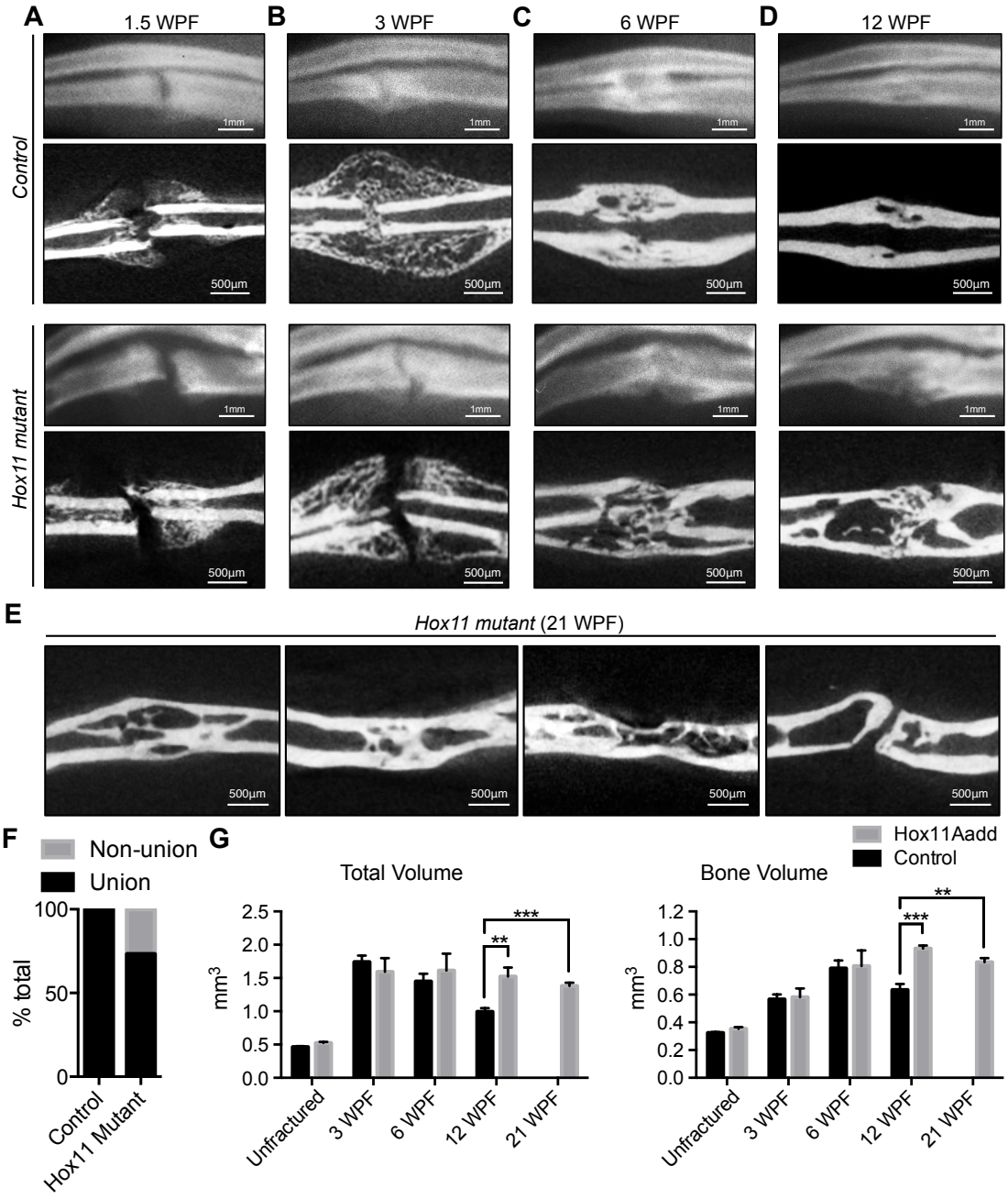

Figure 3.2. Loss of Hox11 function results in defects following fracture injury. (A-D) Xrays (top panels) and cross-sectional views of microCT (lower panels) in control and in *Hox11* compound mutant animals. (A) At 1.5WPF, x-ray and microCT analysis are comparable. (B) At 3WPF, controls are bridged and mutants are not. (C-D) At 6WPF and 12WPF, mutants are bridged, but are delayed in remodeling compared to controls. (E) Cross-sectional views of microCT at 21WPF show incomplete bone remodeling in compound mutant animals. (F) Quantification of non-unions in control and Hox11 compound mutant animals shows an increase in mutants (G) MicroCT analysis shows increased total and bone volume at late stages of fracture repair in compound mutant animals.

Measured Parameter	*Unfractured*		*1.5 weeks post fracture*		*3 weeks post fracture*	
	Control (n=6)	*Hox11 mutant (n=8)*	*Control (n=5)*	*Hox11 mutant (n=7)*	*Control (n=5)*	*Hox11 mutant (n=6)*
Total Volume (mm^3)	0.45 (0.03)	0.52 (0.04)*	1.81 (0.45)	2.75 (0.72)*	1.74 (0.22)	1.59 (0.50)
Bone Volume (mm^3)	0.32 (0.01)	0.35 (0.03)*	0.52 (0.13)	0.78 (0.22)*	0.57 (0.08)	0.57 (0.21)
Bone Volume Fraction	.71 (0.02)	0.67 (0.02)*	.32 (0.18)	0.28 (0.03)	0.33 (0.05)	0.35 (0.05)
Bone Mineral Density (mg/cc)	839.6 (40.7)	740.2 (61.8)	486.0 (173.2)	424.1 (101.1)	511.3 (30.4)	480.2 (77.5)
Bone Mineral Content (mg)	.36 (0.01)	0.39 (0.05)	0.82 (0.15)	1.07 (0.31)	0.89 (0.08)	0.78 (0.32)
Tissue Mineral Density (mg/cc)	977.0 (32.0)	905.6 (85.4)	935.3 (101.8)	860.7 (101.4)	838.0 (31.3)	792.5 (74.3)

Measured Parameter	*6 weeks post fracture*		*12 weeks post fracture*		*21 weeks post fracture*	
	Control (n=5)	*Hox11 mutant (n=6)*	*Control (n=5)*	*Hox11 mutant (n=4)*	*Control*	*Hox11 mutant (n=5)*
Total Volume (mm^3)	1.45 (0.25)	1.61 (0.62)	0.99 (0.12)	1.52 (0.27)*	ND	1.49 (0.16)*
Bone Volume (mm^3)	0.79 (0.13)	0.81 (0.28)	0.63 (0.10)	0.93 (0.04)*	ND	0.86 (0.06)*
Bone Volume Fraction	0.55 (0.07)	0.51 (0.05)	0.64 (0.04)	0.63 (0.09)	ND	0.58 (0.04)
Bone Mineral Density (mg/cc)	664.3 (83.7)	606.4 (60.2)	796.2 (49.3)	817.7 (104.3)	ND	751.2 (24.3)
Bone Mineral Content (mg)	0.96 (0.17)	0.97 (0.34)	0.79 (0.13)	1.22 (0.07)*	ND	1.09 (0.12)*
Tissue Mineral Density (mg/cc)	896.8 (48.6)	866.9 (37.1)	1036.2 (26.4)	1054.0 (72.6)	ND	983.3 (57.1)

Table 3.1. MicroCT parameters measured during fracture injury.

have not undergone significant remodeling (Figure 3.2D). Even as late as 21 WPF, compound mutants are unable to remodel and repair the fracture, remaining similar to what is observed at 12 WPF (Figure 3.2E). MicroCT analyses of animals that successfully bridged the fracture gap show no significant difference in bone quality parameters throughout the repair process. Bone mineral density (BMD), bone volume fraction (BVF), bone mineral content (BMC) and tissue mineral density (TMD) are not significantly different in the callus of control and mutants until the latest stages of repair (Table 3.1). At 12 WPF, the bone volume of the callus is significantly increased in mutants compared to controls. This increase in volume is maintained through 21 WPF in mutants (Figure 3.2G). Bone mineral content is also increased in mutants at this stage due to the increase in bone volume (Table 3.1).

Hox11 functions for endochondral ossification during skeletal regeneration.

To understand the cellular defects during repair, we assessed for differences in early callus composition using safranin O and fast green staining. At three time points post-fracture (1.5WPF, 3WPF, and 6WPF), we measured the percentage of the callus that was comprised of mesenchyme, cartilage or new bone in *Hox11* compound mutants compared to controls (Figure 3.3A-B). We find that cartilage formation (safranin O) is significantly reduced in the *Hox11* mutant callus compared to controls. Conversely, the percentage of the *Hox11* compound mutant callus that is made up of undifferentiated mesenchyme is significantly increased at the earliest stages. This increase in undifferentiated mesenchyme may lead to fibrous non-unions we observed

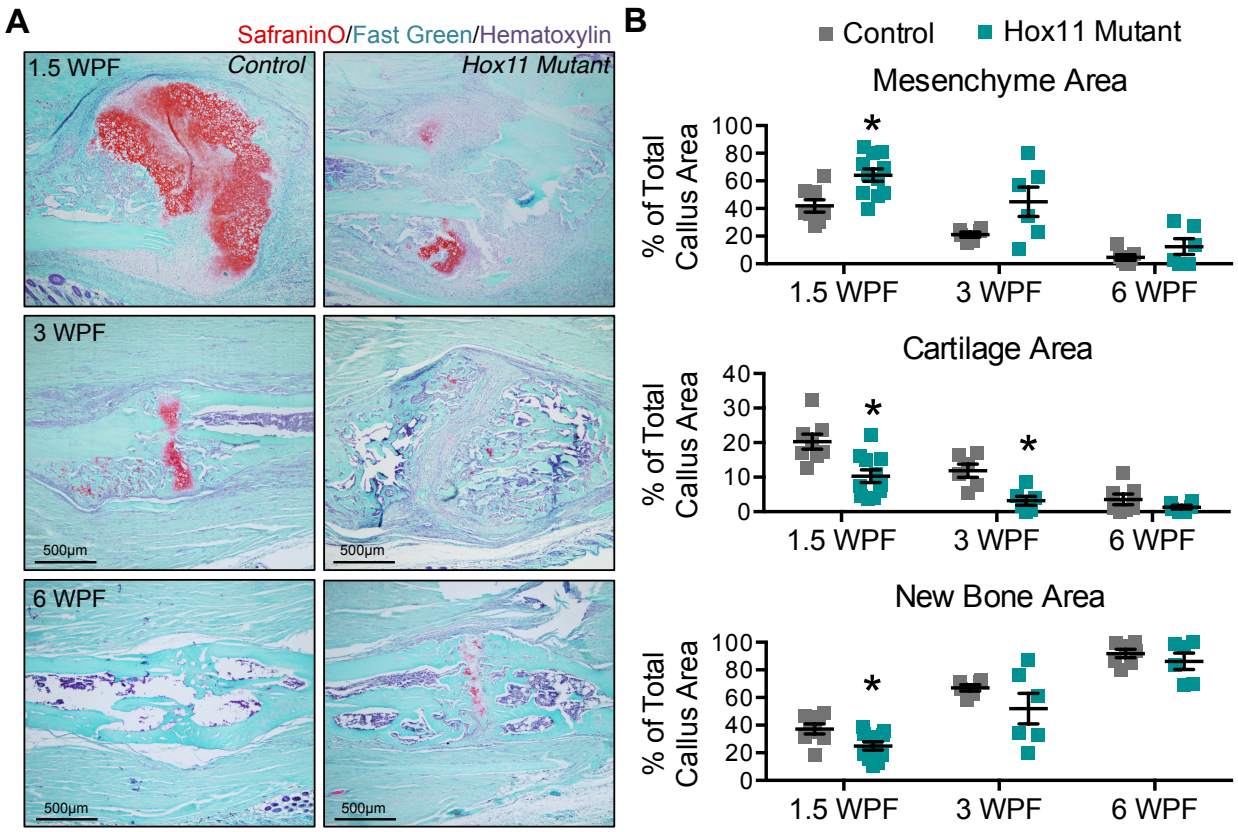

Figure 3.3. *Hox11* compound mutant fractures display altered callus composition
(A) Safranin O/Fast Green-stained callus sections from control and *Hox11* compound mutants at 1.5, 3, and 6 WPF show abundant cartilage formation in center regions of the control calluses. Similar regions of compound mutant calluses are filled with undifferentiated mesenchyme. (B) Histomorphometric quantifications of the cartilage, bone and mesenchymal areas from Safranin O/Fast Green-stained sections.

in some animals. Together these data show an overall altered composition of the callus through the early stages of repair in *Hox11* compound mutant animals.

The process of new bone formation in the callus is completed by two distinct ossification processes: intramembranous and endochondral ossification (Bolander, 1992; Schindeler et al., 2008). In brief, endochondral ossification is bone formation via a cartilage intermediate. In this process, mesenchymal cells differentiate to cartilage and this cartilage template is ossified as osteoblasts replace the matrix with new bone. Intramembranous ossification is characterized by the direct condensation of osteoblasts that secrete bony matrix without prior cartilage matrix formation; this process is the exclusive means of ossification of most of the craniofacial skeleton. Following fracture of long bones, both processes are thought to act simultaneously to heal the site of injury. Typically, intramembranous ossification occurs at the outer regions of the callus, extending from the existing cortical bone area and growing inwards towards the fracture gap, while endochondral ossification occurs at the center.

We find that new bone formation inwards from the cortical bone, characteristic of intramembranous ossification, occurs normally in *Hox11* compound mutants (Figure 3.4A). In both controls and mutants, these regions show high levels of osterix (osteoblasts) expression, are highly vascularized (PECAM) and the general progression of bone formation over time is toward the center of the fracture gap (Figure 3.4B). In addition, we observe no defects in the overall vascularization of the *Hox11* compound mutant callus compared to controls (Figure 3.4C). Taken together, these data support an absence of apparent defects in intramembranous ossification or in callus vascularization.

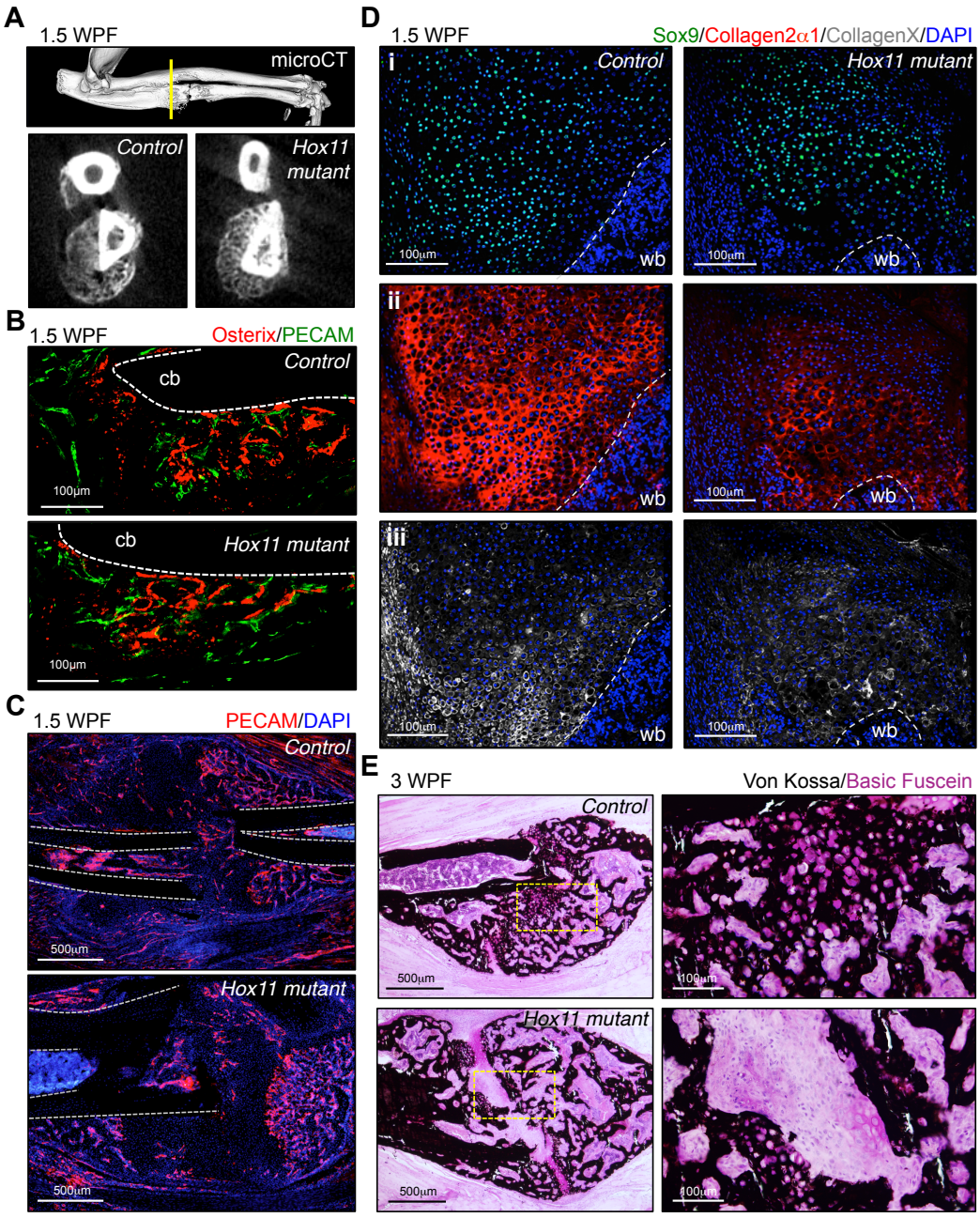

Figure 3.4. Chondroctye differentiation and endochondral ossification is disrupted in the compound mutant callus.
(A) MicroCT analysis of outer regions of callus show comparable bone formation in regions of intramembranous ossification. (B) Osterix and PECAM-stained sections show bone formation and vascularization in regions of intramembranous ossification. (C) PECAM-staining in controls and compound mutants shows comparable vascularization in the early callus (1.5WPF). (D) Sox9, Collagen2 and Collagen 10-stained sections at 1.5WPF show chondrocyte differentiation in control and mutant calluses. (E) Von Kossa-stained sections show unbridged callus at 3WPF in mutant fractures.

Decreased safranin O staining in the *Hox11* mutant callus provides strong evidence that endochondral ossification is disrupted (Figure 3.3A-B). Interestingly, we find that sox9, the earliest marker for chondrocyte differentiation is expressed broadly and at equivalent levels in *Hox11* compound mutant and control calluses (Figure 3.4Di). Sox5, another transcription factor critical for the early differentiation of chondrocytes is also similarly expressed in controls and mutants (Figure S3.2). However, consistent with diminished mature cartilage as evidenced by decreased safranin O staining in mutants, collagen 2 (resting, proliferating and prehypertophic chondrocytes) and collagen 10 (hypertrophic chondorcytes) expression is significantly deceased in mutant calluses compared to similar regions in controls (Figure 3.4Dii-iii). These results are consistent with a defect in the differentiation and/or maturation of chondrocytes with loss of Hox11 function.

To examine ossification directly, we used Von Kossa staining. In control fracture calluses, the ossification of cartilage can be clearly visualized. In the *Hox11* compound mutant callus, ossification is significantly reduced and ossification does not bridge the fracture gap at 3 weeks post-fracture, consistent with x-ray and microCT analysis described previously (Figure 3.4E and Figure 3.2B). Collectively, these results demonstrate disrupted endochondral ossification of the *Hox11* compound mutant fracture callus. This leads to a reduced ability to bridge the fracture gap normally and is likely the cause for the increase in fracture non-unions observed in *Hox11* compound mutant animals.

Loss of Hox11 function results in bone remodeling defects.

By late stages of repair, we find that the majority of *Hox11* compound mutant animals do bridge the fracture gap (Figure 3.2C). Presumably by increased intramembranous ossification, most compound mutant fractures are able to overcome the defects in endochondral ossification to create a bony callus. However, as shown in Figure 3.2, x-ray and microCT analyses reveal a disruption of bone remodeling in these animals at late stages of repair. We used Tartrate Resistant Acid Phosphatase (TRAP) staining, to visualize osteoclasts in the nascent calluses at these stages and find that osteoclasts are present on new woven bone surfaces in mutants and at approximately equal numbers in mutants compared to controls (Figure 3.5A-B). Additionally, cathepsin K, an enzyme that distinguishes a fully differentiated osteoclast that is capable of resorption, is expressed in the osteoclasts that line the woven bone surface (Figure 3.5C). Attachment to bone surfaces is essential for osteoclasts to enact efficient bone resorption. Upon close examination, we find that many osteoclasts in the mutant calluses are detached from the bone surface. These detached osteoclasts are also larger than osteoclasts seen in control calluses (Figure 3.5D), consistent with defects in osteoclast resorption during the remodeling phase of bone healing.

We performed Raman Spectroscopy on new bone within the fracture callus and cortical bone outside of the fracture callus to further investigate matrix abnormalities. This analysis shows no differences in mineral crystallinity in mutants compared to controls however; the mineral to matrix (Proline + Hydroxyproline) ratio is significantly increased in mutants compared to controls both prior to fracture as well as in the woven bone of the fracture callus (Figure 3.6A-B). These data are consistent with a defect in

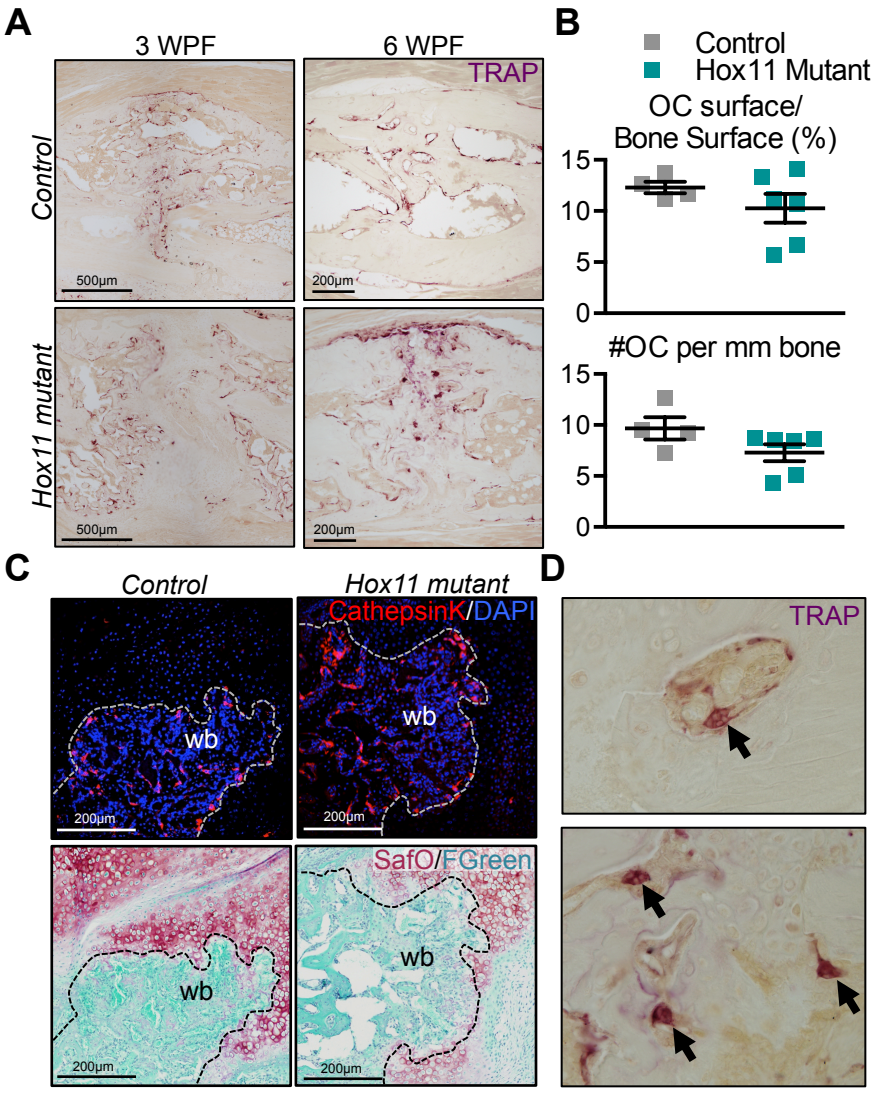

Figure 3.5. Osteoclasts are present and express markers of resorption in the compound mutant callus

(A) TRAP-stained callus sections from control and compound mutant animals at 3 and 6 WPF show TRAP+ osteoclasts in calluses. (B) Histomorphometric quantification of osteoclasts per bone surface (%) and number of osteoclasts per 1mm of bone surface is comparable in controls and mutants. (C) CathepsinK-stained callus sections from control and compound mutant animals show positive staining in controls and mutants. Safranin O/Fast Green staining on the same sections shows the overlap of cathepsinK with woven bone areas. (D) High magnification images of large, detached osteoclasts in the *Hox11* compound mutant callus.

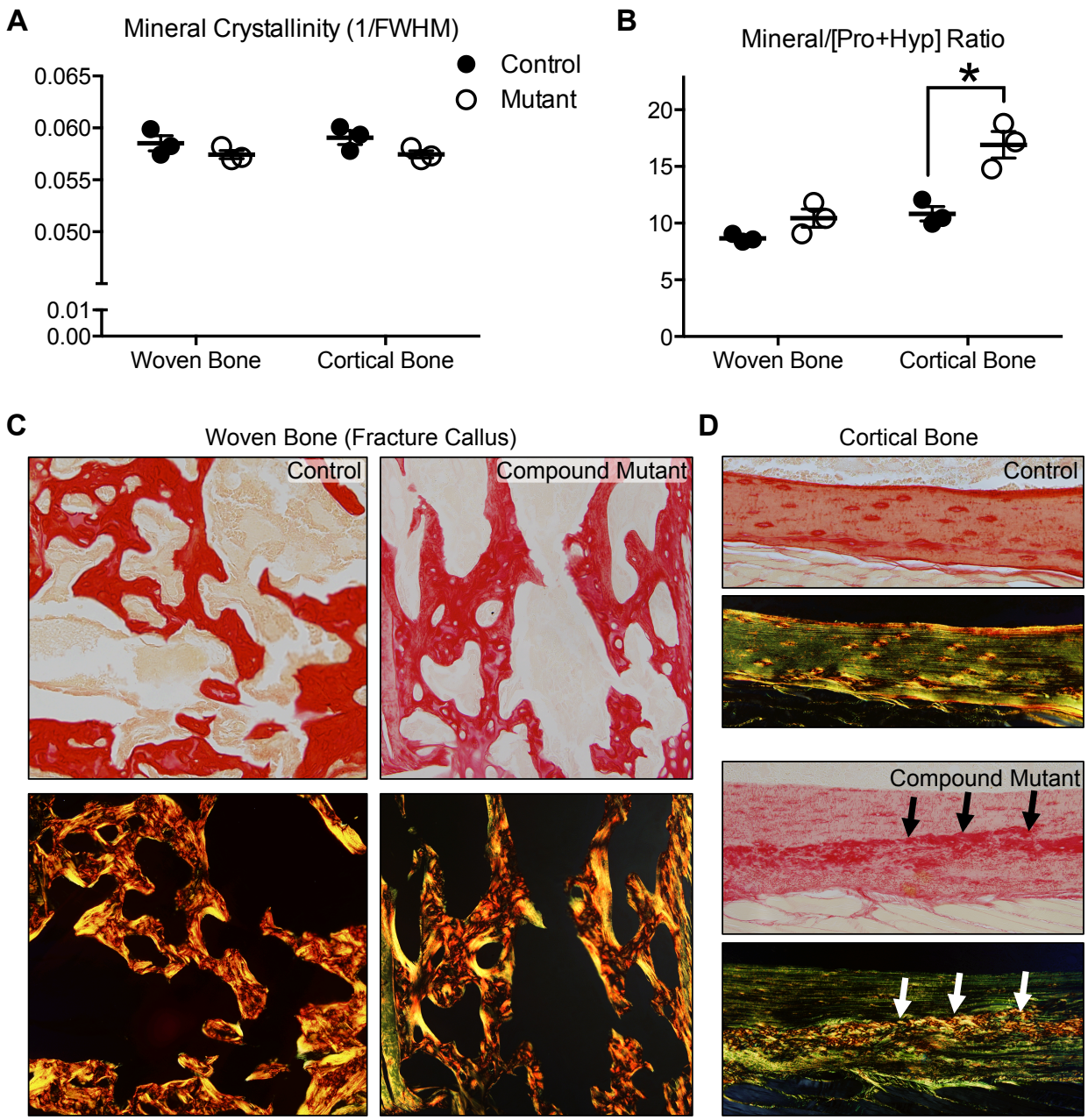

Figure 3.6. Bone matrix organization is disrupted due to the loss of Hox11 function.

(A-B) Raman spectroscopy of woven bone callus and cortical bone outside the callus from controls and *Hox11* compound mutants at 3 WPF. (A) Mineral crystallinity is comparable. (B) Mineral to matrix (proline+hydroxyproline) ratio is increased significantly in mutant cortical bone compared to control. Mutant callus bone is increased, not significantly. (C-D) Picrosirius red-stained sections with brightfield (top panels) or polarize light microscopy (bottom panels).

the bone matrix in *Hox11* compound mutant animals. As further support for defects in matrix organization, picrosirius red staining reveals a highly disorganized matrix in *Hox11* mutants using polarized light microscopy. Using this technique, disorganized matrix appears red/orange and multi-directional yielding a basket weave appearance. An organized matrix is green and linear. New woven bone generated in the fracture callus is highly disorganized in both control and mutant calluses (Figure 3.6C). However, we also observe disorganization in the matrix of cortical bone in compound mutant animals (Figure 3.6D).

Discussion

Our understanding of *Hox* transcription factors in the skeleton is largely limited to embryonic development. Previous studies have shown that *Hox* genes are expressed during repair and suggested that they may be important for efficient regeneration (Bais et al., 2009; Gersch et al., 2005; Leucht et al., 2008; Wang et al., 2009). Transcriptome analyses have shown a broad increase in the expression of various *Hox* genes throughout repair processes (Bais et al., 2009; Gersch et al., 2005). Additionally, differential expression of *Hox* genes was hypothesized to be the cause for scar formation in a transplant study where periosteal progenitor cells from different anatomical locations were swapped in fracture injuries (Leucht et al., 2008). Here, we present several novel findings in the first rigorous, genetic study of Hox function during the fracture repair process. Using our *Hoxa11eGFP* insertion allele, we show clear expansion of *Hox11* expression in response to fracture injury. Complete loss of Hox11 paralogous group function results in severe malformations during embryonic

development and neonatal lethality that preclude adult studies. Using a sensitized background of compound *Hox11* mutants, we show that loss of Hox11 function results in severe repair defects in endochondral ossification and bone remodeling in response to fracture injury.

In this study, we provide evidence that *Hox11* functions for the transition from progenitor cell to mature matrix-producing cells during fracture injury. Our previous work showed that *Hox11*-expressing adult mesenchymal stem/stromal cells of the skeleton expand upon fracture injury. Our data here shows that differentiation to chondrocytes during soft callus formation is disrupted after specification to the chondrocyte lineage. Sox9 and sox5 (expressed in progenitors) turn on normally in the *Hox11* compound mutant callus, however downstream collagen 2, collagen 10, and safranin O are markedly reduced. These results are consistent with previous work in the embryo showing that defects associated with loss of Hox11 function during embryonic limb development are due to defects in chondrogenic differentiation at the earliest stages of maturation (Gross et al., 2012). In addition, these results are consistent with our previous work that demonstrates loss of chondrogenic differentiation *in vitro* from MSCs that carry mutations in all four *Hox11* alleles that function in the forelimb (Chapter 2). It will be interesting in future studies to investigate complete loss of Hox11 function using conditional alleles.

A significant characteristic of the *Hox* gene complex is the restriction of paralogous group expression and function to specific anatomical locations during embryonic development where they elicit essential functions in proper skeletal patterning. The work described here, and in our previous study (Chapter 2), suggests

that these genes may provide a similar function during adult fracture repair. My previous worked showed that *Hox11* expression is regionally restricted throughout postnatal growth and in expansion following fracture injury (Chapter 2). Consistent with this, the function of *Hox11* remains restricted to zeugopod fracture injuries (Chapter 2). Here, we describe clear roles for *Hox11* in response to fracture injury repair. Understanding the function of *Hox* genes in other skeletal locations is of great interest for future study. It remains unclear whether all *Hox* groups provide similar functions at each anatomic location or whether they have unique functions. For example, the *Hox9* and *Hox10* paralogous groups are required for patterning of the humerus and the femur (stylopod limb) during embryonic development. Do these genes function similar to *Hox11* genes during the fracture healing process in these regions? Are there any differences in their respective contribution to this process? This will be an important area of future study. Overall, our results suggest that regionally specific Hox function is an important, and previously unappreciated, mechanism of the fracture healing process.

Supplementary Figures

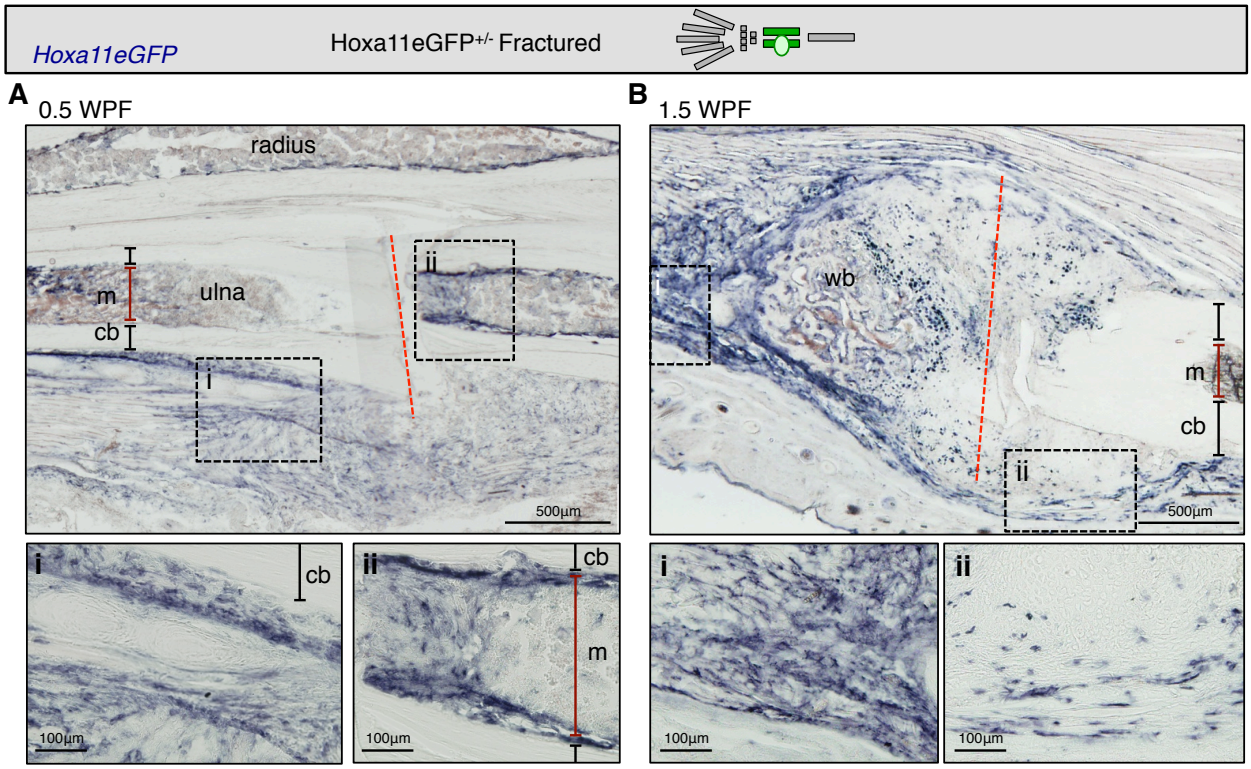

Figure S3.1. *Hoxa11eGFP* is expressed in the ulna fracture model of repair. Limb schematic depicts *Hoxa11eGFP* regional expression (green) and the fracture callus in the zeugopod region (ulna). *Hoxa11eGFP* expression is shown using a GFP primary antibody and developing with alkaline phosphatase. (A) *Hoxa11eGFP* is expressed at low levels in the hematoma near the periosteum and also in the intramedullary space. (B) *Hoxa11eGFP* expression expands significantly at 1.5WPF.

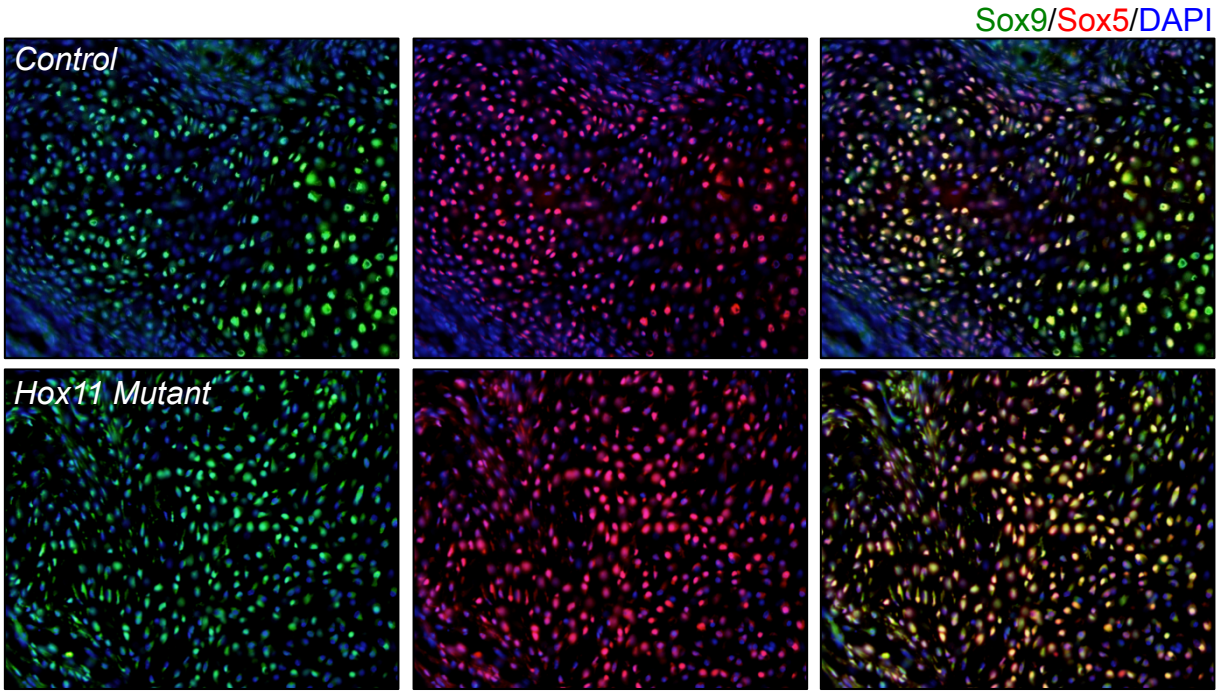

Figure S3.2. Sox5 expression is not affected by the loss of Hox11 function. Sox5/sox9-stainined callus sections at 1.5WPF in controls and *Hox11* compound mutant animals show comparable staining.

Material and Methods

Mice, fracture methods, and X-ray and microCT. *See materials and methods in chapter 2.*

Histology, immunohistochemistry and histomorphometric measurements. Limbs were collected at the indicated ages or time points following fracture surgery. Intramedullary pins were removed if present. All specimens were dissected in PBS on ice and scanned immediately for microCT (if required for fracture analyses). Specimens for frozen sections were fixed for three days in 4% paraformaldehyde in PBS at 4°C, decalcified in 14% EDTA for 7 days and then sunk in 30% Sucrose in PBS overnight prior to embedding into OCT media. Cryosections were collected at 18μm through indicated segments of the limb or through the entire fracture callus. Specimens for paraffin sections were fixed for two days in 10% formalin at 4C, decalcified in 14% EDTA for 7 days and then put into 70% ethanol until paraffin processing overnight. Paraffin sections were collected at 7um thickness.

Immunohistochemical staining was performed using standard methods. Antigen retrieval for paraffin sections was performed by proteinase K (Collagen 2 and Collagen 10) or by a heated citrate buffer (CathepsinK). Sections were blocked with donkey serum and incubated with primary antibodies overnight at 4°C against Sox9 (Millipore, AB5535, 1:500), PECAM/CD31 (Developmental Studies Hybridoma Bank, 1:10), Collagen 2 (Millipore, MAB8887, 1:50), Collagen 10 (Millipore, 234196, 1:50), Osterix (Abcam, ab22552, 1:300) or Cathepsin K (Abcam, ab19027, 1:50). Secondary antibodies were incubated at room temperature for 2 hours. Staining for Sox5 required amplification using a tryamide Cy3 kit from Perkin Elmer. . To minimize complications

resulting from high auto-fluorescence in adult tissues, we used an antibody against GFP (Invitrogen, A-11122, 1:200) followed with an alkaline phosphatase conjugated (Jackson ImmunoResearch, 111-055-003, 1:500). TRAP staining was performed using a leukocyte acid phosphatase kit (Sigma). Picrosirius red staining was performed on paraffin sections using a protocol generously provided by Yugi Mishina at the University of Michigan.

To quantify the amount of cartilage within each callus, every 10th section from cryopreserved tissue was stained with Safranin O/Fast Green/Hematoxylin as previously described (Kahveci et al., 2000; Tran et al., 2000). The callus area and cartilage area on each section was measure manually using ImageJ software. A minimum of three tissue sections per callus was measured and the average was calculated among all animals per time point (1.5 WPF: control n = 8, *Hox11 mutant* n = 11, 3 WPF: control n = 6, *Hox11 mutant* n = 6; 6 WPF: control n = 7; *Hox11 mutant* n = 6).

To perform Von Kossa staining, specimens were collected three weeks after fracture injury, dissected, fixed in 10% neutral buffered formalin for two days, and transferred to 70% EtOH before processing as previously described (Smith et al., 2013). Plastic sections were collected at 11um on a Polycut E (Reichert-Jung) and dried overnight under compression at 45C. Staining was performed slightly modified from a previously described method (Danscher, 1983).

All brightfield images and polarized light microscopy was captured on an Olympus BX-51 upright light microscope with an Olympus DP70 camera. Fluorescent images were captured on a Leica Upright SP5X Confocal Microscope with 2-Photon.

Confocal Z stacks through entire sections were taken at a thickness of 2μm, stacked using ImageJ software, and stitched together using Photoshop software (when required) to obtain high-resolution images of entire limbs and fracture calluses.

Raman Spectroscopy. The Raman microscope was constructed locally as described previously (Sinder et al., 2016) but was fitted with a 785 nm diode laser (Innovative Photonics Solutions, Monmouth Junction, NJ), 25-μm slit, and a 10x/0.50 NA objective (S Fluor, Nikon Instruments, Inc., Melville, NY). The excitation laser was spot-focused to give ~30 mW of laser powder at the specimen. For each *Hoxa11* compound mutant (n = 3) and WT control (n = 3) animal, 6 cortical and 6 woven bone spectra were acquired. Woven bone was taken from the fracture site and cortical bone near to, but outside of the fracture region. Prior to data collection, the site was pre-scanned using a short acquisition time of 20 seconds to check for low background tissue fluorescence and low PMMA contributions. Selected sites were then photobleached for 10-15 minutes prior to collecting a Raman spectrum using an accumulation cycle time of 6 minutes (2X3-minute cycles).

All Raman spectroscopic data were calibrated and processed in MATLAB® software using locally written scripts described elsewhere (Sinder et al., 2016). The script included an automated ‘derivative minimization’ procedure to remove spectral interference from PMMA (Banerjee and Li, 1991), while an ‘adaptive min-max’ polynomial fitting procedure (3rd order, constrained) was used to correct for background tissue fluorescence (Cao et al., 2007). All spectra were imported into GRAMS/AI® software for baseline correction and normalization against the bone mineral phosphate

v1PO4 band at ~959 cm-1. For optimal curve-fitting, second derivative, and constrained mixed Gaussian-Lozentzian deconvolution functions were applied to the following spectral regions: 829-900 cm-1 (833, 853, 872, 891 cm-1) and 901-990 cm-1 (920, 933, 943, 959 cm-1). The following Raman bands pertinent to bone were identified: proline, hydroxyproline, and phosphate bands at 853 cm-1, 872 cm-1, and 959 cm-1, respectively. Mineral-to-matrix ratios were calculated from the intensity ratio of the mineral v1PO4 band to the combined intensity of the proline and hydroxyproline bands (959 cm-1/(853+872) cm-1) (Mandair and Morris, 2015). Mineral crystallinity was calculated as the inverse of the full-width at half maximum (1/FWHM) of the Gaussian-fitted v1PO4 band at 959 cm-1. Mean cortical and woven measurements obtained for each specimen (6 per bone type as described above) were pooled by group to provide a representative mean value.

CHAPTER 4

CONCLUSION

Summary of findings

Knowledge on the function of the *Hox* genes in the mammalian skeleton has been largely limited to the patterning information they provide during embryonic development. Results from this thesis work uncover two major findings that expand knowledge about *Hox* expression and function beyond embryonic development. First, my work demonstrates that *Hox* genes are expressed exclusively in adult LepR+ MSCs and maintain regional restriction established during development. Second, region specific *Hox* function is critical for the differentiation of mesenchymal-lineage cells that are required for adult fracture repair of the skeleton.

Hoxa11eGFP+ cells continue to be expressed through postnatal development of the skeleton and into adulthood. These cells are observed at the outer periosteal surface of the zeugopod long bones, in the endosteal lining the inner bone surface and as a small population within the bone marrow. Extensive molecular analyses show that *Hoxa11eGFP*+ cells do not overlap with any differentiated cell type, but that they overlap exclusively with a recently defined MSC population that expresses PDGFRα, CD51 and Leptin Receptor, three cell-surface markers that label progenitor-enriched MSCs within the bone marrow stroma (Kunisaki et al., 2013; Pinho et al., 2013; Zhou et al., 2014). *In vitro, Hoxa11eGFP*+ cells are capable of multi-lineage differentiation, and

interestingly, sorting additionally on GFP demonstrates enhanced CFU-F capacity compared to the total PDGFRα+/CD51+ population. *In vivo, Hoxa11eGFP*+ cells expand following fracture injury and are capable of differentiating to osteoblasts and to chondroctyes that contribute to callus formation. Finally, and specific to a characteristic of *Hox* genes, LepR+ bone marrow MSCs from different bones display a differential *Hox* expression pattern that matches the expression pattern established during embryonic development. *Hox* gene expression is not detected in LepR- stromal cells. Together, these results support that *Hox11*-expressing cells are a subset of regionally restricted LepR+ MSCs that reside in the adult skeleton.

Given the critical role for *Hox* genes in skeletal development, we also explored whether *Hox11* genes function in the skeleton at adult stages. Using *Hox11* compound mutants (which maintain only one wild-type *Hox11* allele that circumvents developmental defects of the full mutant), we employed an ulnar fracture model. Adult *Hox11* compound mutant animals show perturbations in fracture repair with delayed bridging of bone across the fracture gap and incomplete remodeling. At the earliest stages, chondrocyte differentiation and the subsequent generation of cartilage is severely impaired by the loss of Hox11 function. Mesenchymal cells in the callus initiate expression of early transcription factors required for cartilage differentiation (sox9 and sox5), but are not able to differentiate to cells that generate normal major matrix components including proteoglycans (safranin O), collagen 2 and collagen 10. The result is undifferentiated mesenchyme in the fracture callus, reduced endochondral ossification and delayed bridging of the fracture gap. Consistent with this, differentiation defects using full *Hox11* mutant cells are also seen *in vitro.* At later stages of repair,

most *Hox11* compound mutant animals bridge the fracture gap, but fail to remodel the hard callus generated. Raman spectroscopy and histologic assessments point to a possible bone matrix defect in these animals that contributes to the lack of bone remodeling following injury. Consistent with the regional restriction described for MSCs based on *Hox* expression, *Hox11* expression and function is also restricted during fracture repair. *Hoxa11eGFP* is not ectopically expressed in a femur fracture model and employing this model in *Hox11* compound mutants shows no perturbations in healing compared to control animals. Taken together, our results support a model in which adult expression and function of *Hox* genes maintains the regionally restricted expression and function that is established during embryonic development.

Contributions to the field

The regional restriction of *Hox* gene expression and function during adult fracture repair is a novel finding with important implications for adult skeletal biology. First, this finding reveals that the transcription factors that govern initial skeletal patterning in the embryo also function in regeneration of the adult skeleton. We report here that Hox11 functions for MSC differentiation to skeletal lineages in the fracture callus. This leads to several new considerations in the study of fracture healing. First, it further demonstrates that the healing process of all fractures is not inherently equal. It is well known that fractures in different anatomical locations require various degrees of medical intervention due, in large part, to differing requirements in stabilizing the injury. However, taking our results into consideration, it is also possible that differential Hox function might account for some of the differences. Related to this, it remains unclear

whether each *Hox* paralogous group regulates function in MSCs in a differential manner. Hox function, in general, has not been placed into a specific pathway during embryonic development. A possible explanation for this is that *Hox* genes impart different functions dependent on anatomical location. Despite extensive research since the 1980s, this remains unclear. Elucidating these potential differences, and ones in adut fracture healing, will continue to be the focus of future studies.

Regional specificity in the context of how MSCs function *in vivo* is an interesting new layer of complexity for MSC biology. That *Hox* gene expression is only present in *LepR*-expressing bone marrow MSCs from different anatomical locations is an exciting finding. It supports the idea that the functions defined here for *Hox11* may also be true of paralogous groups in other skeletal locations, though this will need to be formally tested. It also leads to questions about the function of *Hox* genes in contexts that are not specific to skeletal regeneration and that have been implicated as functions for adult MSCs. For example, *leptin receptor*-expressing cells play critical roles in the bone marrow hematopoietic stem cell niche via CXCL12, SCF and ANGPT1 (Ding and Morrison, 2013; Ding et al., 2012; Oguro et al., 2013; Zhou et al., 2015). How or even if *Hox* genes function in this context remains to be seen, but it is an attractive idea that *Hox* genes function for region-specificity in the bone marrow stem cell niche.

Despite the growing body of research regarding *in vivo* functions for adult MSCs, the major interest in these cells remains in regenerative medicine/tissue engineering applications. That MSCs are capable of differentiating into bone and cartilage *in vitro* has been a major influence on tissue engineering strategies and *in vivo* transplantation methods for decades. Stem cells and tissue replacement therapies involving the use of

MSCs are continuously investigated. We, and others, describe that cells dissected from different anatomical locations have differential *Hox* gene expression patterns (Ackema and Charite, 2008; Liedtke et al., 2010; Rinn et al., 2006; Rinn et al., 2008). Understanding the importance of maintaining unique *Hox* genes and what function this serves will be critical in future studies involving MSCs for regenerative medicine. For example, it may be important to derive MSCs from regions that are appropriate for intended use in these applications. "Matching" Hox function *in vitro* to the intended tissue *in vivo,* may prove useful in the viability of transplants as has been suggested by others (Leucht et al., 2008). Alternatively, it may be beneficial in future tissue engineering strategies to manipulate regional *Hox* gene function for specific differentiation strategies. To this end, it will also be of interest to explore how to change *Hox* expression status in various *in vitro* organ and tissue differentiation strategies to develop desired differentiation outcomes that are relevant for transplantation *in vivo*.

Future Directions

We have identified adult *Hox11*-expressing cells as a mesenchymal stem/stromal cell population present in the periosteum, endosteum and bone marrow of the zeugopod, but many questions remain. As previously mentioned, studies from several groups suggest that adult MSCs arise from the perichondrium/periosteum during embryonic and postnatal stages. Given our collective data that shows *Hoxa11eGFP* is expressed at these times and in these regions, *Hox*-expressing cells represent an attractive origin for adult MSCs. This can be tested by genetic lineage trace studies; an important future pursuit. Our current data suggests that *Hox* may have more than one

function during the fracture healing process, but it is not clear whether the described function in bone remodeling is a primary function of Hox or whether it is secondary to the earlier endochondral ossification phenotype. Related to this, contributions to normal bone maintenance have not been examined. These will be important distinctions for Hox11 function in future studies and can be dissected by the generation of conditional alleles to provide temporal control over loss of function. Finally, despite known functions for MSCs in other contexts, whether *Hox* functions in contexts that are not related to bone maintenance or regeneration have not been explored. As previously mentioned, LepR+ cells (in which *Hox* is differentially expressed) are known to function in the HSC niche. Studies aimed at exploring functions for Hox in this context may add critical knowledge to inform homing and maintenance functions of the HSC niche as well as possible regional differences in this context as well. Finally, the Wellik lab has previously demonstrated critical roles for *Hox11* genes in muscle patterning. *Hox11* expression and function in adult skeletal muscle remains to be explored.

To study the contribution of *Hox11*-expressing cells in various contexts an inducible *Cre* (*CreERt2*) was successfully engineered in the endogenous *Hoxa11* locus for lineage tracing studies from *Hox11*-expressing cells. This will be an extremely powerful tool for future studies, not only in the embryo, but also for understanding the contribution of *Hox11*-expressing cells in the adult. First, we will be able to definitively show that *Hox11*-expressing cells *in vivo* do indeed give rise to osteoblasts and chondrocytes following fracture injury. A specific context of interest is whether embryonic *Hox11*-expressing cells give rise to adult *Hox11*-expressing MSCs. Using this lineage-tracing strategy, we can begin tracing during embryonic stages and follow

into late adult stages. In addition, lineage-tracing starting in adult stages will allow us to demonstrate whether Hox11+ cells are quiescent like *Lepr*-*Cre*-expressing cells. In line with other studies of postnatal and adult MSC populations, this inducible *Cre* model will be critical to defining the *in vivo* contributions of *Hox11*-expressing MSCs.

All of the *in vivo* functional analyses performed in this thesis work were done with adult *Hox11* compound mutant animals. Three of the four *Hox11* alleles expressed in the forelimb are mutant, but a single wild-type *Hoxa11* allele remains. While the defects observed in these adult animals have provided critical new insight into functions for *Hox11* in the adult, it remains unclear how extensive would be in the context of a full mutant. Thus, it is important to also study adult Hox11 function in the context of full loss of function as has been done for embryonic development. To do this, conditional floxed alleles are required to provide temporal control over the loss of Hox11 function, bypassing defects that arise during embryonic development. To this end, a conditional allele has recently generated in the lab. Flox sites were engineered to flank the second exon of *Hoxd11* such that, when crossed to a genetically engineered mouse carrying a Cre, this exon may be removed and Hoxd11 function lost. After crossing these animals to the traditional loss-of-function allele for *Hoxa11* and an inducible *Cre*, *Hoxd11* may be excised at any point conferring temporal control over full loss of Hox11 function in adult animals.

A specific question raised in the fracture work with *Hox11* compound mutants is: Is the bone remodeling defect a direct result of the loss of *Hox11* or is it a secondary defect due to the loss of endochondral ossification earlier in the healing process? Inducing loss of *Hox11* function after endochondral ossification has occurred in the

healing process will allow examination of this question. With the new *Hoxd11* floxed allele, loss of function may be induced at specific stages during fracture repair: first in the early stages to more carefully define its function in endochondral ossification and, second, after endochondral ossification has occurred to understand its role in bone remodeling. In addition, data presented in Chapter 3 suggests that Hox11 functions in normal bone remodeling (Figure 3.6). Compound mutant animals display disorganized bone matrix. With temporal control over loss of function specifically in the adult, a possible role for *Hox11* in the context in normal bone turnover may also be elucidated.

Previous work in the lab has shown that, beyond its specific role in skeletal development, Hox11 functions for proper patterning of the entire musculoskeletal system in the zeugopod region of the limb (Swinehart et al., 2013). In this context, *Hox11* expression is absent from the muscle cells, but co-expresses with *TCF4*, a transcription factor that is expressed in muscle connective tissue fibroblasts and is critical for muscle development (Mathew et al., 2011). Work from Gabriel Kardon and colleagues shows that *TCF4* is maintained in adult skeletal muscle and is critical for repair following muscle injury with Barium Chloride ($BaCl_2$), an injectable drug that induces the destruction of myofibers while preserving the basil lamina (Harris, 2003; Murphy et al., 2011). Mesenchymal progenitors (not Pax7+ muscle stem cells) express cell-surface markers PDGFRα and Sca1 and have been shown to facilitate in regeneration following muscle injury (Joe et al., 2010; Judson et al., 2013). Given the critical role that *Hox11* plays during embryonic muscle patterning it is an attractive hypothesis that it is also expressed in adult muscle and functions during regeneration.

In a preliminary study not previously described in this thesis work, we tested the requirement of *Hox11* in adult skeletal muscle. We find that *Hox11*-expressing cells may be identified in adult skeletal muscle, they co-express PDFGRα and Sca1 (Figure 4.1B), and they expand following injury with $BaCl_2$ (Figure 4.1C). These preliminary data suggest that *Hox11*-expressing cells in adult skeletal muscle represent a mesenchymal progenitor population that functions in muscle regeneration following injury. The recently generated *Hoxa11-CreERt2* and *Hoxd11* conditional alleles will be beneficial to understand how *Hox11*-expressing cells contribute to muscle regeneration.

Collectively, our results demonstrate that *Hox* gene expression and function is broadly maintained in the adult skeleton and, importantly, maintains the regional restriction that is established during embryonic development. The work described in this thesis provides the first direct evidence that *Hox* genes do function in the adult skeleton as a mesenchyme stem/stromal cells population and are an integral part of the mechanisms that govern the overall fracture healing process. With the new genetic mouse models described above, studies can be conducted to provide a deeper understanding of the *Hox* genes in adult musculoskeletal maintenance and repair as well as in other important contexts described for MSCs.

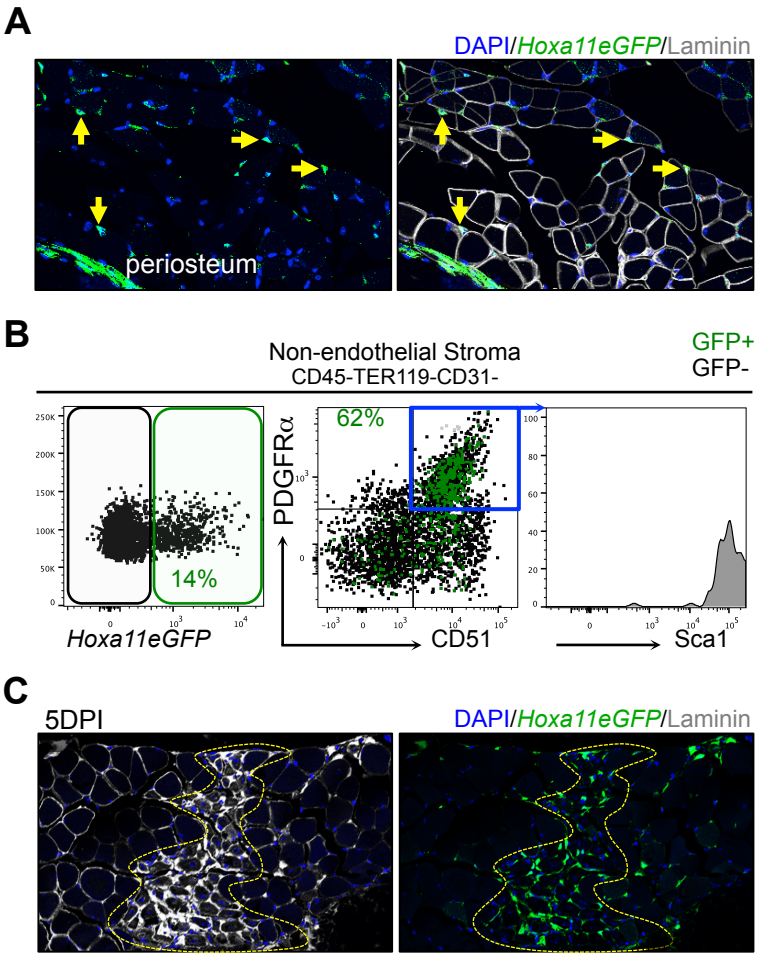

Figure 4.1. *Hoxa11eGFP* is expressed in adult skeletal muscle and expands during regeneration following injury.
(A) *Hoxa11eGFP*-expressing cells are visualized in skeletal muscle, but excluded from the muscle fibers. (B) FACS analysis shows *Hoxa11eGFP*+ cells in non-endothelial stroma of muscle and co-express muscle connective tissue markers PDGFRα and Sca1. (C) *Hoxa11eGFP*-expressing cells expand at the site of $BaCl_2$ muscle injury.

APPENDIX: PUBLICATIONS AND MANUSCRIPTS

Chapter 2 is based on a manuscript in revision titled “Regionally Restricted *Hox11* function in Adult Bone Marrow-Multi-potent Mesenchymal Stem/Stromal Cells.” with authors listed as Danielle R. Rux, Jane Y. Song, Ilea T. Swinehart, Kyriel M. Pineault, Aleesa J. Schlientz, Kelsey G. Trulik, Steve A. Goldstein, Ken M. Kozloff, Daniel Lucas, and Deneen M. Wellik

Chapter 3 is based on a manuscript in submission titled “*Hox11* Function is Required for Region-Specific Fracture Repair.” with authors listed as Danielle R. Rux, Ilea T. Swinehart, Aleesa J. Schlientz, Kayla N. Garthus, Steve A. Goldstein, Ken M. Kozloff, and Deneen M. Wellik

References

Ackema, K.B., and Charite, J. (2008). Mesenchymal stem cells from different organs are characterized by distinct topographic Hox codes. Stem cells and development *17*, 979-991.

Adams, G.B., Martin, R.P., Alley, I.R., Chabner, K.T., Cohen, K.S., Calvi, L.M., Kronenberg, H.M., and Scadden, D.T. (2007). Therapeutic targeting of a stem cell niche. Nature biotechnology *25*, 238-243.

Bais, M., McLean, J., Sebastiani, P., Young, M., Wigner, N., Smith, T., Kotton, D.N., Einhorn, T.A., and Gerstenfeld, L.C. (2009). Transcriptional analysis of fracture healing and the induction of embryonic stem cell-related genes. PloS one *4*, e5393.

Banerjee, S., and Li, D. (1991). Interpreting Multicomponent Infrared Spectra by Derivative Minimization. Appl Spectrosc *45*, 1047-1049.

Bateson (1909). Discussion on the Influence of Heredity on Disease, with special Reference to Tuberculosis, Cancer, and Diseases of the Nervous System: Introductory Address. Proceedings of the Royal Society of Medicine *2*, 22-30.

Becker, A.J., Mc, C.E., and Till, J.E. (1963). Cytological demonstration of the clonal nature of spleen colonies derived from transplanted mouse marrow cells. Nature *197*, 452-454.

Beresford, J.N., Bennett, J.H., Devlin, C., Leboy, P.S., and Owen, M.E. (1992). Evidence for an inverse relationship between the differentiation of adipocytic and osteogenic cells in rat marrow stromal cell cultures. Journal of cell science *102 (Pt 2)*, 341-351.

Bianco, P., Cao, X., Frenette, P.S., Mao, J.J., Robey, P.G., Simmons, P.J., and Wang, C.Y. (2013). The meaning, the sense and the significance: translating the science of mesenchymal stem cells into medicine. Nature medicine *19*, 35-42.

Bolander, M.E. (1992). Regulation of fracture repair by growth factors. Proceedings of the Society for Experimental Biology and Medicine Society for Experimental Biology and Medicine *200*, 165-170.

Bonnarens, F., and Einhorn, T.A. (1984). Production of a standard closed fracture in laboratory animal bone. Journal of orthopaedic research : official publication of the Orthopaedic Research Society *2*, 97-101.

Boulet, A.M., and Capecchi, M.R. (2004). Multiple roles of Hoxa11 and Hoxd11 in the formation of the mammalian forelimb zeugopod. Development *131*, 299-309.

Boulet, A.M., Moon, A.M., Arenkiel, B.R., and Capecchi, M.R. (2004). The roles of Fgf4 and Fgf8 in limb bud initiation and outgrowth. Developmental biology *273*, 361-372.

Calvi, L.M., Adams, G.B., Weibrecht, K.W., Weber, J.M., Olson, D.P., Knight, M.C., Martin, R.P., Schipani, E., Divieti, P., Bringhurst, F.R.*, et al.* (2003). Osteoblastic cells regulate the haematopoietic stem cell niche. Nature *425*, 841-846.

Canalis, E., Parker, K., and Zanotti, S. (2012). Gremlin1 is required for skeletal development and postnatal skeletal homeostasis. Journal of cellular physiology *227*, 269-277.

Cao, A., Pandya, A.K., Serhatkulu, G.K., Weber, R.E., Dai, H., Thakur, J.S., Naik, V.M., Naik, R., Auner, G.W., Rabah, R.*, et al.* (2007). A robust method for automated background subtraction of tissue fluorescence. Journal of Raman Spectroscopy *38*, 1199-1205.

Caplan, A.I. (1991). Mesenchymal stem cells. Journal of orthopaedic research : official publication of the Orthopaedic Research Society *9*, 641-650.

Chan, C.K., Chen, C.C., Luppen, C.A., Kim, J.B., DeBoer, A.T., Wei, K., Helms, J.A., Kuo, C.J., Kraft, D.L., and Weissman, I.L. (2009). Endochondral ossification is required for haematopoietic stem-cell niche formation. Nature *457*, 490-494.

Chan, C.K., Lindau, P., Jiang, W., Chen, J.Y., Zhang, L.F., Chen, C.C., Seita, J., Sahoo, D., Kim, J.B., Lee, A.*, et al.* (2013). Clonal precursor of bone, cartilage, and hematopoietic niche stromal cells. Proceedings of the National Academy of Sciences of the United States of America *110*, 12643-12648.

Chan, C.K., Seo, E.Y., Chen, J.Y., Lo, D., McArdle, A., Sinha, R., Tevlin, R., Seita, J., Vincent-Tompkins, J., Wearda, T.*, et al.* (2015). Identification and specification of the mouse skeletal stem cell. Cell *160*, 285-298.

Chang, H.Y., Chi, J.T., Dudoit, S., Bondre, C., van de Rijn, M., Botstein, D., and Brown, P.O. (2002). Diversity, topographic differentiation, and positional memory in human fibroblasts. Proceedings of the National Academy of Sciences of the United States of America *99*, 12877-12882.

Colnot, C. (2009). Skeletal cell fate decisions within periosteum and bone marrow during bone regeneration. Journal of bone and mineral research : the official journal of the American Society for Bone and Mineral Research *24*, 274-282.

Colnot, C., Huang, S., and Helms, J. (2006). Analyzing the cellular contribution of bone marrow to fracture healing using bone marrow transplantation in mice. Biochemical and biophysical research communications *350*, 557-561.

Condie, B.G., and Capecchi, M.R. (1994). Mice with targeted disruptions in the paralogous genes hoxa-3 and hoxd-3 reveal synergistic interactions. Nature *370*, 304-307.

da Silva Meirelles, L., Chagastelles, P.C., and Nardi, N.B. (2006). Mesenchymal stem cells reside in virtually all post-natal organs and tissues. Journal of cell science *119*, 2204-2213.

Danscher, G. (1983). A silver method for counterstaining plastic embedded tissue. Stain technology *58*, 365-372.

Davis, A.P., Witte, D.P., Hsieh-Li, H.M., Potter, S.S., and Capecchi, M.R. (1995). Absence of radius and ulna in mice lacking hoxa-11 and hoxd-11. Nature *375*, 791-795.

DeFalco, J., Tomishima, M., Liu, H., Zhao, C., Cai, X., Marth, J.D., Enquist, L., and Friedman, J.M. (2001). Virus-assisted mapping of neural inputs to a feeding center in the hypothalamus. Science *291*, 2608-2613.

Ding, L., and Morrison, S.J. (2013). Haematopoietic stem cells and early lymphoid progenitors occupy distinct bone marrow niches. Nature *495*, 231-235.

Ding, L., Saunders, T.L., Enikolopov, G., and Morrison, S.J. (2012). Endothelial and perivascular cells maintain haematopoietic stem cells. Nature *481*, 457-462.

Dominici, M., Le Blanc, K., Mueller, I., Slaper-Cortenbach, I., Marini, F., Krause, D., Deans, R., Keating, A., Prockop, D., and Horwitz, E. (2006). Minimal criteria for defining

multipotent mesenchymal stromal cells. The International Society for Cellular Therapy position statement. Cytotherapy *8*, 315-317.

Dressler, G.R., and Gruss, P. (1989). Anterior boundaries of Hox gene expression in mesoderm-derived structures correlate with the linear gene order along the chromosome. Differentiation; research in biological diversity *41*, 193-201.

Duboule, D. (1994). Temporal colinearity and the phylotypic progression: a basis for the stability of a vertebrate Bauplan and the evolution of morphologies through heterochrony. Dev Suppl, 135-142.

Duboule, D., and Dolle, P. (1989). The structural and functional organization of the murine HOX gene family resembles that of Drosophila homeotic genes. The EMBO journal *8*, 1497-1505.

Einhorn, T.A. (1998). The cell and molecular biology of fracture healing. Clinical orthopaedics and related research, S7-21.

Einhorn, T.A., and Gerstenfeld, L.C. (2015). Fracture healing: mechanisms and interventions. Nature reviews Rheumatology *11*, 45-54.

Evans, M.J., and Kaufman, M.H. (1981). Establishment in culture of pluripotential cells from mouse embryos. Nature *292*, 154-156.

Ferguson, C., Alpern, E., Miclau, T., and Helms, J.A. (1999). Does adult fracture repair recapitulate embryonic skeletal formation? Mechanisms of development *87*, 57-66.

Frenette, P.S., Pinho, S., Lucas, D., and Scheiermann, C. (2013). Mesenchymal stem cell: keystone of the hematopoietic stem cell niche and a stepping-stone for regenerative medicine. Annual review of immunology *31*, 285-316.

Friedenstein, A.J., Chailakhjan, R.K., and Lalykina, K.S. (1970). The development of fibroblast colonies in monolayer cultures of guinea-pig bone marrow and spleen cells. Cell and tissue kinetics *3*, 393-403.

Friedenstein, A.J., Chailakhyan, R.K., and Gerasimov, U.V. (1987). Bone marrow osteogenic stem cells: in vitro cultivation and transplantation in diffusion chambers. Cell and tissue kinetics *20*, 263-272.

Friedenstein, A.J., Chailakhyan, R.K., Latsinik, N.V., Panasyuk, A.F., and Keiliss-Borok, I.V. (1974). Stromal cells responsible for transferring the microenvironment of the hemopoietic tissues. Cloning in vitro and retransplantation in vivo. Transplantation *17*, 331-340.

Friedenstein, A.J., Gorskaja, J.F., and Kulagina, N.N. (1976). Fibroblast precursors in normal and irradiated mouse hematopoietic organs. Experimental hematology *4*, 267-274.

Friedenstein, A.J., Latzinik, N.W., Grosheva, A.G., and Gorskaya, U.F. (1982). Marrow microenvironment transfer by heterotopic transplantation of freshly isolated and cultured cells in porous sponges. Experimental hematology *10*, 217-227.

Friedenstein, A.J., Petrakova, K.V., Kurolesova, A.I., and Frolova, G.P. (1968). Heterotopic of bone marrow. Analysis of precursor cells for osteogenic and hematopoietic tissues. Transplantation *6*, 230-247.

Fromental-Ramain, C., Warot, X., Lakkaraju, S., Favier, B., Haack, H., Birling, C., Dierich, A., Doll e, P., and Chambon, P. (1996a). Specific and redundant functions of the paralogous Hoxa-9 and Hoxd-9 genes in forelimb and axial skeleton patterning. Development *122*, 461-472.

Fromental-Ramain, C., Warot, X., Messadecq, N., LeMeur, M., Dolle, P., and Chambon, P. (1996b). Hoxa-13 and Hoxd-13 play a crucial role in the patterning of the limb autopod. Development *122*, 2997-3011.

Garcia-Fernandez, J. (2005). The genesis and evolution of homeobox gene clusters. Nature reviews Genetics *6*, 881-892.

Gaunt, S.J. (1991). Expression patterns of mouse Hox genes: clues to an understanding of developmental and evolutionary strategies. BioEssays : news and reviews in molecular, cellular and developmental biology *13*, 505-513.

Gaunt, S.J., and Strachan, L. (1996). Temporal colinearity in expression of anterior Hox genes in developing chick embryos. Developmental dynamics : an official publication of the American Association of Anatomists *207*, 270-280.

Gersch, R.P., Lombardo, F., McGovern, S.C., and Hadjiargyrou, M. (2005). Reactivation of Hox gene expression during bone regeneration. Journal of orthopaedic research : official publication of the Orthopaedic Research Society *23*, 882-890.

Gerstenfeld, L.C., Cullinane, D.M., Barnes, G.L., Graves, D.T., and Einhorn, T.A. (2003). Fracture healing as a post-natal developmental process: molecular, spatial, and temporal aspects of its regulation. Journal of cellular biochemistry *88*, 873-884.

Graham, A., Papalopulu, N., and Krumlauf, R. (1989). The murine and Drosophila homeobox gene complexes have common features of organization and expression. Cell *57*, 367-378.

Gross, S., Krause, Y., Wuelling, M., and Vortkamp, A. (2012). Hoxa11 and Hoxd11 regulate chondrocyte differentiation upstream of Runx2 and Shox2 in mice. PloS one *7*, e43553.

Haack, H., and Gruss, P. (1993). The establishment of murine Hox-1 expression domains during patterning of the limb. Developmental biology *157*, 410-422.

Harris, J.B. (2003). Myotoxic phospholipases A2 and the regeneration of skeletal muscles. Toxicon : official journal of the International Society on Toxinology *42*, 933-945.

Hess, R., Pino, A.M., Rios, S., Fernandez, M., and Rodriguez, J.P. (2005). High affinity leptin receptors are present in human mesenchymal stem cells (MSCs) derived from control and osteoporotic donors. Journal of cellular biochemistry *94*, 50-57.

Hiltunen, A., Vuorio, E., and Aro, H.T. (1993). A standardized experimental fracture in the mouse tibia. Journal of orthopaedic research : official publication of the Orthopaedic Research Society *11*, 305-312.

Horan, G.S., Ramirez-Solis, R., Featherstone, M.S., Wolgemuth, D.J., Bradley, A., and Behringer, R.R. (1995). Compound mutants for the paralogous hoxa-4, hoxb-4, and hoxd-4 genes show more complete homeotic transformations and a dose-dependent increase in the number of vertebrae transformed. Genes & development *9*, 1667-1677.

Howlett, C.R., Cave, J., Williamson, M., Farmer, J., Ali, S.Y., Bab, I., and Owen, M.E. (1986). Mineralization in in vitro cultures of rabbit marrow stromal cells. Clinical orthopaedics and related research, 251-263.

Hsieh-Li, H.M., Witte, D.P., Weinstein, M., Branford, W., Li, H., Small, K., and Potter, S.S. (1995). Hoxa 11 structure, extensive antisense transcription, and function in male and female fertility. Development *121*, 1373-1385.

Iimura, T., and Pourquie, O. (2006). Collinear activation of Hoxb genes during gastrulation is linked to mesoderm cell ingression. Nature *442*, 568-571.

Izpisua-Belmonte, J.C., and Duboule, D. (1992). Homeobox genes and pattern formation in the vertebrate limb. Developmental biology *152*, 26-36.

Izpisua-Belmonte, J.C., Falkenstein, H., Dolle, P., Renucci, A., and Duboule, D. (1991). Murine genes related to the Drosophila AbdB homeotic genes are sequentially expressed during development of the posterior part of the body. The EMBO journal *10*, 2279-2289.

Joe, A.W., Yi, L., Natarajan, A., Le Grand, F., So, L., Wang, J., Rudnicki, M.A., and Rossi, F.M. (2010). Muscle injury activates resident fibro/adipogenic progenitors that facilitate myogenesis. Nature cell biology *12*, 153-163.

Judson, R.N., Zhang, R.H., and Rossi, F.M. (2013). Tissue-resident mesenchymal stem/progenitor cells in skeletal muscle: collaborators or saboteurs? The FEBS journal *280*, 4100-4108.

Kahveci, Z., Minbay, F.Z., and Cavusoglu, L. (2000). Safranin O staining using a microwave oven. Biotechnic & histochemistry : official publication of the Biological Stain Commission *75*, 264-268.

Karsenty, G., and Wagner, E.F. (2002). Reaching a genetic and molecular understanding of skeletal development. Developmental cell *2*, 389-406.

Kaufman, T.C., Seeger, M.A., and Olsen, G. (1990). Molecular and genetic organization of the antennapedia gene complex of Drosophila melanogaster. Advances in genetics *27*, 309-362.

Kfoury, Y., and Scadden, D.T. (2015). Mesenchymal cell contributions to the stem cell niche. Cell stem cell *16*, 239-253.

Kmita, M., Tarchini, B., Zakany, J., Logan, M., Tabin, C.J., and Duboule, D. (2005). Early developmental arrest of mammalian limbs lacking HoxA/HoxD gene function. Nature *435*, 1113-1116.

Kostic, D., and Capecchi, M.R. (1994). Targeted disruptions of the murine Hoxa-4 and Hoxa-6 genes result in homeotic transformations of components of the vertebral column. Mechanisms of development *46*, 231-247.

Kronenberg, H.M. (2003). Developmental regulation of the growth plate. Nature *423*, 332-336.

Krumlauf, R. (1994). Hox genes in vertebrate development. Cell *78*, 191-201.

Kunisaki, Y., Bruns, I., Scheiermann, C., Ahmed, J., Pinho, S., Zhang, D., Mizoguchi, T., Wei, Q., Lucas, D., Ito, K.*, et al.* (2013). Arteriolar niches maintain haematopoietic stem cell quiescence. Nature *502*, 637-643.

Kuznetsov, S.A., Krebsbach, P.H., Satomura, K., Kerr, J., Riminucci, M., Benayahu, D., and Robey, P.G. (1997). Single-colony derived strains of human marrow stromal fibroblasts form bone after transplantation in vivo. Journal of bone and mineral research : the official journal of the American Society for Bone and Mineral Research *12*, 1335-1347.

Leucht, P., Kim, J.B., Amasha, R., James, A.W., Girod, S., and Helms, J.A. (2008). Embryonic origin and Hox status determine progenitor cell fate during adult bone regeneration. Development *135*, 2845-2854.

Lewandoski, M., Sun, X., and Martin, G.R. (2000). Fgf8 signalling from the AER is essential for normal limb development. Nature genetics *26*, 460-463.

Lewis, E.B. (1951). Pseudoallelism and gene evolution. Cold Spring Harbor symposia on quantitative biology *16*, 159-174.

Lewis, E.B. (1978). A gene complex controlling segmentation in Drosophila. Nature *276*, 565-570.

Liedtke, S., Buchheiser, A., Bosch, J., Bosse, F., Kruse, F., Zhao, X., Santourlidis, S., and Kogler, G. (2010). The HOX Code as a "biological fingerprint" to distinguish functionally distinct stem cell populations derived from cord blood. Stem cell research *5*, 40-50.

Lonfat, N., and Duboule, D. (2015). Structure, function and evolution of topologically associating domains (TADs) at HOX loci. FEBS letters *589*, 2869-2876.

Madisen, L., Zwingman, T.A., Sunkin, S.M., Oh, S.W., Zariwala, H.A., Gu, H., Ng, L.L., Palmiter, R.D., Hawrylycz, M.J., Jones, A.R.*, et al.* (2010). A robust and high-throughput Cre reporting and characterization system for the whole mouse brain. Nature neuroscience *13*, 133-140.

Maeda, R.K., and Karch, F. (2009). The bithorax complex of Drosophila an exceptional Hox cluster. Current topics in developmental biology *88*, 1-33.

Maes, C., Kobayashi, T., Selig, M.K., Torrekens, S., Roth, S.I., Mackem, S., Carmeliet, G., and Kronenberg, H.M. (2010). Osteoblast precursors, but not mature osteoblasts, move into developing and fractured bones along with invading blood vessels. Developmental cell *19*, 329-344.

Mallo, M., Wellik, D.M., and Deschamps, J. (2010). Hox genes and regional patterning of the vertebrate body plan. Developmental biology *344*, 7-15.

Mandair, G.S., and Morris, M.D. (2015). Contributions of Raman spectroscopy to the understanding of bone strength. BoneKEy reports *4*, 620.

Mardon, H.J., Bee, J., von der Mark, K., and Owen, M.E. (1987). Development of osteogenic tissue in diffusion chambers from early precursor cells in bone marrow of adult rats. Cell and tissue research *250*, 157-165.

Martin, G.R. (1981). Isolation of a pluripotent cell line from early mouse embryos cultured in medium conditioned by teratocarcinoma stem cells. Proceedings of the National Academy of Sciences of the United States of America *78*, 7634-7638.

Mathew, S.J., Hansen, J.M., Merrell, A.J., Murphy, M.M., Lawson, J.A., Hutcheson, D.A., Hansen, M.S., Angus-Hill, M., and Kardon, G. (2011). Connective tissue fibroblasts and Tcf4 regulate myogenesis. Development *138*, 371-384.

McCulloch, E.A., and Till, J.E. (1960). The radiation sensitivity of normal mouse bone marrow cells, determined by quantitative marrow transplantation into irradiated mice. Radiation research *13*, 115-125.

McIntyre, D.C., Rakshit, S., Yallowitz, A.R., Loken, L., Jeannotte, L., Capecchi, M.R., and Wellik, D.M. (2007). Hox patterning of the vertebrate rib cage. Development *134*, 2981-2989.

Mendez-Ferrer, S., Michurina, T.V., Ferraro, F., Mazloom, A.R., Macarthur, B.D., Lira, S.A., Scadden, D.T., Ma'ayan, A., Enikolopov, G.N., and Frenette, P.S. (2010). Mesenchymal and haematopoietic stem cells form a unique bone marrow niche. Nature *466*, 829-834.

Mignone, J.L., Kukekov, V., Chiang, A.S., Steindler, D., and Enikolopov, G. (2004). Neural stem and progenitor cells in nestin-GFP transgenic mice. The Journal of comparative neurology *469*, 311-324.

Mizoguchi, T., Pinho, S., Ahmed, J., Kunisaki, Y., Hanoun, M., Mendelson, A., Ono, N., Kronenberg, H.M., and Frenette, P.S. (2014). Osterix marks distinct waves of primitive and definitive stromal progenitors during bone marrow development. Developmental cell *29*, 340-349.

Montavon, T., and Duboule, D. (2013). Chromatin organization and global regulation of Hox gene clusters. Philosophical transactions of the Royal Society of London Series B, Biological sciences *368*, 20120367.

Morikawa, S., Mabuchi, Y., Kubota, Y., Nagai, Y., Niibe, K., Hiratsu, E., Suzuki, S., Miyauchi-Hara, C., Nagoshi, N., Sunabori, T.*, et al.* (2009). Prospective identification, isolation, and systemic transplantation of multipotent mesenchymal stem cells in murine bone marrow. The Journal of experimental medicine *206*, 2483-2496.

Murphy, M.M., Lawson, J.A., Mathew, S.J., Hutcheson, D.A., and Kardon, G. (2011). Satellite cells, connective tissue fibroblasts and their interactions are crucial for muscle regeneration. Development *138*, 3625-3637.

Nakahara, H., Bruder, S.P., Goldberg, V.M., and Caplan, A.I. (1990). In vivo osteochondrogenic potential of cultured cells derived from the periosteum. Clinical orthopaedics and related research, 223-232.

Nelson, L.T., Rakshit, S., Sun, H., and Wellik, D.M. (2008). Generation and expression of a Hoxa11eGFP targeted allele in mice. Developmental dynamics : an official publication of the American Association of Anatomists *237*, 3410-3416.

Niswander, L., Jeffrey, S., Martin, G.R., and Tickle, C. (1994). A positive feedback loop coordinates growth and patterning in the vertebrate limb. Nature *371*, 609-612.

Oguro, H., Ding, L., and Morrison, S.J. (2013). SLAM family markers resolve functionally distinct subpopulations of hematopoietic stem cells and multipotent progenitors. Cell stem cell *13*, 102-116.

Omatsu, Y., Sugiyama, T., Kohara, H., Kondoh, G., Fujii, N., Kohno, K., and Nagasawa, T. (2010). The essential functions of adipo-osteogenic progenitors as the hematopoietic stem and progenitor cell niche. Immunity *33*, 387-399.

Ono, N., Ono, W., Nagasawa, T., and Kronenberg, H.M. (2014). A subset of chondrogenic cells provides early mesenchymal progenitors in growing bones. Nature cell biology *16*, 1157-1167.

Osawa, M., Hanada, K., Hamada, H., and Nakauchi, H. (1996). Long-term lymphohematopoietic reconstitution by a single CD34-low/negative hematopoietic stem cell. Science *273*, 242-245.

Owen, M., and Friedenstein, A.J. (1988). Stromal stem cells: marrow-derived osteogenic precursors. Ciba Foundation symposium *136*, 42-60.

Park, D., Spencer, J.A., Koh, B.I., Kobayashi, T., Fujisaki, J., Clemens, T.L., Lin, C.P., Kronenberg, H.M., and Scadden, D.T. (2012). Endogenous bone marrow MSCs are dynamic, fate-restricted participants in bone maintenance and regeneration. Cell stem cell *10*, 259-272.

Payumo, A.Y., McQuade, L.E., Walker, W.J., Yamazoe, S., and Chen, J.K. (2016). Tbx16 regulates hox gene activation in mesodermal progenitor cells. Nature chemical biology.

Peichel, C.L., Prabhakaran, B., and Vogt, T.F. (1997). The mouse Ulnaless mutation deregulates posterior HoxD gene expression and alters appendicular patterning. Development *124*, 3481-3492.

Pineault, K.M., Swinehart, I.T., Garthus, K.N., Ho, E., Yao, Q., Schipani, E., Kozloff, K.M., and Wellik, D.M. (2015). Hox11 genes regulate postnatal longitudinal bone growth and growth plate proliferation. Biology open *4*, 1538-1548.

Pinho, S., Lacombe, J., Hanoun, M., Mizoguchi, T., Bruns, I., Kunisaki, Y., and Frenette, P.S. (2013). PDGFRalpha and CD51 mark human nestin+ sphere-forming mesenchymal stem cells capable of hematopoietic progenitor cell expansion. The Journal of experimental medicine *210*, 1351-1367.

Pittenger, M.F., Mackay, A.M., Beck, S.C., Jaiswal, R.K., Douglas, R., Mosca, J.D., Moorman, M.A., Simonetti, D.W., Craig, S., and Marshak, D.R. (1999). Multilineage potential of adult human mesenchymal stem cells. Science *284*, 143-147.

Qian, H., Le Blanc, K., and Sigvardsson, M. (2012). Primary mesenchymal stem and progenitor cells from bone marrow lack expression of CD44 protein. The Journal of biological chemistry *287*, 25795-25807.

Riddle, R.D., Johnson, R.L., Laufer, E., and Tabin, C. (1993). Sonic hedgehog mediates the polarizing activity of the ZPA. Cell *75*, 1401-1416.

Rinn, J.L., Bondre, C., Gladstone, H.B., Brown, P.O., and Chang, H.Y. (2006). Anatomic demarcation by positional variation in fibroblast gene expression programs. PLoS genetics *2*, e119.

Rinn, J.L., Wang, J.K., Allen, N., Brugmann, S.A., Mikels, A.J., Liu, H., Ridky, T.W., Stadler, H.S., Nusse, R., Helms, J.A.*, et al.* (2008). A dermal HOX transcriptional program regulates site-specific epidermal fate. Genes & development *22*, 303-307.

Schindeler, A., McDonald, M.M., Bokko, P., and Little, D.G. (2008). Bone remodeling during fracture repair: The cellular picture. Seminars in cell & developmental biology *19*, 459-466.

Schneuwly, S., Klemenz, R., and Gehring, W.J. (1987). Redesigning the body plan of Drosophila by ectopic expression of the homoeotic gene Antennapedia. Nature *325*, 816-818.

Scott, M.P. (1992). Vertebrate homeobox gene nomenclature. Cell *71*, 551-553.

Shapiro, F. (2008). Bone development and its relation to fracture repair. The role of mesenchymal osteoblasts and surface osteoblasts. European cells & materials *15*, 53-76.

Sinder, B.P., Lloyd, W.R., Salemi, J.D., Marini, J.C., Caird, M.S., Morris, M.D., and Kozloff, K.M. (2016). Effect of anti-sclerostin therapy and osteogenesis imperfecta on tissue-level properties in growing and adult mice while controlling for tissue age. Bone *84*, 222-229.

Small, K.M., and Potter, S.S. (1993). Homeotic transformations and limb defects in Hox A11 mutant mice. Genes & development *7*, 2318-2328.

Smith, L., Bigelow, E.M., and Jepsen, K.J. (2013). Systematic evaluation of skeletal mechanical function. Current protocols in mouse biology *3*, 39-67.

Sugiyama, T., Kohara, H., Noda, M., and Nagasawa, T. (2006). Maintenance of the hematopoietic stem cell pool by CXCL12-CXCR4 chemokine signaling in bone marrow stromal cell niches. Immunity *25*, 977-988.

Sun, X., Mariani, F.V., and Martin, G.R. (2002). Functions of FGF signalling from the apical ectodermal ridge in limb development. Nature *418*, 501-508.

Suzuki, M., and Kuroiwa, A. (2002). Transition of Hox expression during limb cartilage development. Mechanisms of development *118*, 241-245.

Swinehart, I.T., Schlientz, A.J., Quintanilla, C.A., Mortlock, D.P., and Wellik, D.M. (2013). Hox11 genes are required for regional patterning and integration of muscle, tendon and bone. Development *140*, 4574-4582.

Takahashi, K., and Yamanaka, S. (2006). Induction of pluripotent stem cells from mouse embryonic and adult fibroblast cultures by defined factors. Cell *126*, 663-676.

Takahashi, Y., Hamada, J., Murakawa, K., Takada, M., Tada, M., Nogami, I., Hayashi, N., Nakamori, S., Monden, M., Miyamoto, M.*, et al.* (2004). Expression profiles of 39 HOX genes in normal human adult organs and anaplastic thyroid cancer cell lines by quantitative real-time RT-PCR system. Experimental cell research *293*, 144-153.

Taylor, D.K., Meganck, J.A., Terkhorn, S., Rajani, R., Naik, A., O'Keefe, R.J., Goldstein, S.A., and Hankenson, K.D. (2009). Thrombospondin-2 influences the proportion of cartilage and bone during fracture healing. Journal of bone and mineral research : the official journal of the American Society for Bone and Mineral Research *24*, 1043-1054.

Till, J.E., and Mc, C.E. (1961). A direct measurement of the radiation sensitivity of normal mouse bone marrow cells. Radiation research *14*, 213-222.

Tran, D., Golick, M., Rabinovitz, H., Rivlin, D., Elgart, G., and Nordlow, B. (2000). Hematoxylin and safranin O staining of frozen sections. Dermatologic surgery : official publication for American Society for Dermatologic Surgery [et al] *26*, 197-199.

van den Akker, E., Fromental-Ramain, C., de Graaff, W., Le Mouellic, H., Brulet, P., Chambon, P., and Deschamps, J. (2001). Axial skeletal patterning in mice lacking all paralogous group 8 Hox genes. Development *128*, 1911-1921.

Vortkamp, A., Pathi, S., Peretti, G.M., Caruso, E.M., Zaleske, D.J., and Tabin, C.J. (1998). Recapitulation of signals regulating embryonic bone formation during postnatal growth and in fracture repair. Mechanisms of development *71*, 65-76.

Wakitani, S., Saito, T., and Caplan, A.I. (1995). Myogenic cells derived from rat bone marrow mesenchymal stem cells exposed to 5-azacytidine. Muscle & nerve *18*, 1417-1426.

Wang, K.C., Helms, J.A., and Chang, H.Y. (2009). Regeneration, repair and remembering identity: the three Rs of Hox gene expression. Trends in cell biology *19*, 268-275.

Wellik, D.M. (2009). Hox genes and vertebrate axial pattern. Current topics in developmental biology *88*, 257-278.

Wellik, D.M., and Capecchi, M.R. (2003). Hox10 and Hox11 genes are required to globally pattern the mammalian skeleton. Science *301*, 363-367.

Worthley, D.L., Churchill, M., Compton, J.T., Tailor, Y., Rao, M., Si, Y., Levin, D., Schwartz, M.G., Uygur, A., Hayakawa, Y.*, et al.* (2015). Gremlin 1 identifies a skeletal stem cell with bone, cartilage, and reticular stromal potential. Cell *160*, 269-284.

Xu, B., Hrycaj, S.M., McIntyre, D.C., Baker, N.C., Takeuchi, J.K., Jeannotte, L., Gaber, Z.B., Novitch, B.G., and Wellik, D.M. (2013). Hox5 interacts with Plzf to restrict Shh expression in the developing forelimb. Proceedings of the National Academy of Sciences of the United States of America *110*, 19438-19443.

Xu, B., and Wellik, D.M. (2011). Axial Hox9 activity establishes the posterior field in the developing forelimb. Proceedings of the National Academy of Sciences of the United States of America *108*, 4888-4891.

Zakany, J., and Duboule, D. (2007). The role of Hox genes during vertebrate limb development. Current opinion in genetics & development *17*, 359-366.

Zakany, J., Gerard, M., Favier, B., and Duboule, D. (1997). Deletion of a HoxD enhancer induces transcriptional heterochrony leading to transposition of the sacrum. The EMBO journal *16*, 4393-4402.

Zakany, J., Kmita, M., and Duboule, D. (2004). A dual role for Hox genes in limb anterior-posterior asymmetry. Science *304*, 1669-1672.

Zakany, J., Zacchetti, G., and Duboule, D. (2007). Interactions between HOXD and Gli3 genes control the limb apical ectodermal ridge via Fgf10. Developmental biology *306*, 883-893.

Zhang, J., Niu, C., Ye, L., Huang, H., He, X., Tong, W.G., Ross, J., Haug, J., Johnson, T., Feng, J.Q.*, et al.* (2003). Identification of the haematopoietic stem cell niche and control of the niche size. Nature *425*, 836-841.

Zhou, B.O., Ding, L., and Morrison, S.J. (2015). Hematopoietic stem and progenitor cells regulate the regeneration of their niche by secreting Angiopoietin-1. eLife *4*, e05521.

Zhou, B.O., Yue, R., Murphy, M.M., Peyer, J.G., and Morrison, S.J. (2014). Leptin-receptor-expressing mesenchymal stromal cells represent the main source of bone formed by adult bone marrow. Cell stem cell *15*, 154-168.